Biomechanical study of foot with Hallux Valgus deformity

A thesis Submitted for the

Degree of Doctor of Philosophy

by

Saba Eshraghi

School of Engineering and Design and physical sciences

Brunel University

September 2014

Abstract

***Background*:** Hallux valgus (HV) is one of the most common foot deformities. Considering the fact that 23% of adults develop such condition during their lifetime, understanding HV is badly needed. Plantar pressure technologies are used widely for determination of biomechanical changes in foot during walking. There are already published claims relating to the pressure distribution of HV condition. Association of HV to sole pressure widely presented as a means of identifying such condition.

***Methods*:** plantar pressure patterns can be linked to the deformity progression or existence, extracting some patterns out of force measurements can be beneficial in recognizing the patients with and without deformity. The dynamic changes of the forces that applied to the fore-foot in volunteers with and without HV when they walked at self-selected and fast speeds were examined. Furthermore, Markovian chain transfer matrices were used to obtain the transfer coefficient of the force among five metatarsals. Another method was to measure the lateral flexibility of the 1^{st} metatarsal joint as an indication of HV deformity by Motion Capture cameras. Finally, two 3D feet models of HV and non-HV volunteers were made in Mimics software and then in FEA (finite element analysis) the stress distribution under the foot was validated with the experiments.

***Results*:** The higher forces were observed under the 2^{nd}, 3^{rd} and 1^{st} metatarsal heads in both speeds but the results obtained were significantly different among groups and in fast speed and under 3^{rd} and 1^{st} metatarsals in self-selected speed. In this study the use of Markovian transfer matrices as a means of characterising the gait pattern is new and novel. It was intended that highest coefficients of the matrix would indicate the existence of HV, however studies showed that the biggest difference between HV and non HV patients was the scatter of the coefficients which shown to give very strong indication of the existence of HV.

It was shown by kinematic studies and also it was found that the 1^{st} metatarsal joint was significantly more flexible in HV patients compared to non–HV individuals.

Finally FEA studies has shown that in the 3D feet models of both volunteers (with and without HV), the highest stress was under the heal area and then transfers towards fore-foot area. In patient with HV the higher force were seen under the 1^{st} to

3rd metatarsal heads compare to non-HV individual and each model was validated its related experiments.

***Conclusion*:** it was observed that there was a significant variability of pressure distribution of the same individual from one trial to another indicating that getting consistent pressure pattern is an important hurdle to overcome in our studies, raised loading is observed on Metatarsal 2, 3 and 1 in HV patients and it was possible to give statistical significance to these findings. In this thesis, it was intended to obtain early diagnostics of HV condition and much work was put in this, however outcome was not conclusive. However it was possible to distinguish HV form non-HV volunteers from the scatter characteristics of the transfer pattern. Investigation of the 1st metatarsal joint laxity of non-HV and HV patients revealed that HV individuals were significantly higher compared to non–HV volunteers and this can be used as an indication of HV existence. Finally, the 3D models show that FEA is a reliable tool as the FEA study showed good correlation with the experimental results.

List of original publications were used in this study

Eshraghi,S., Esat.I (2013), 'Biomechanical study of foot force pattern in relation to Hallux Valgus progression. ', *Rescon*, Brunel University, London, June 20-24.

Eshraghi.S., Esat.I (2012), 'Finite element of foot with Hallux Vlgus deformity',*Rescon* ,Brunel University, London ,June 20-24.

Eshraghi.S, Esat.I (2014), 'Biomechanical study of foot force pattern in HalluxValgus (HV) patients', *Human computer- Interaction***.** Crete, July 21-24.Springer, 332-339.

Eshraghi.S., Vanat,Q., Yazdifar,M., Eshraghi, M., Saveh,A., Esat,I., Chizari,M. (2012), '3D investigation of a foot with Hallux Valgus deformity using finite element analysis' , *Society for Design and Process Science*. Germany. June 10-14

Eshraghi, S., Esat, I., Rahmanivahid, P., Yazdifar, M., Eshraghi, M., Mohaghegh, A. and Horne.S (2013) 'Study on relationship between foot pressure pattern and Hallux Valgus progression.', *Human-Computer Interaction. Applications and Services.* Las Vegas, 21/07/2013. Springer, 76-83.

Eshraghi, S., Esat, I.,Mohagheghi,A.(2015) 'Relationship between Hallux Valgus and plantar force transformation among metatarsal regions'., Submitted to *Footwear science Journal.*

Acknowledgements

First I would like to take this opportunity to express my gratitude to my supervisor, Professor Ibrahim Esat, for his enthusiastic scientific support, insightful guidance, and patience throughout the course of this research.

I would like to thank Dr. Amir Mohagheghi for his support, assistance and constructive suggestions in this research project.

I thank the project consortium for providing me the opportunity to carry out this work and the many individuals who organised it. In particular, Gopal Jeyasundra and Sara Horne and Dr, Mahmoud Chizari for their kindness and Help.

Despite the hardship moments of I have been fortunate to have had around many individuals that helped in so many different ways in the process of doing my experiments and to whom I am greatly indebted. Thank you to Dr.Sanaz Shamshirsaz, Dr.Pooyan RahmaniVahid, Torang Tehrani, who provided help when needed and with whom I had the opportunity to share good moments outside the lab. Also I should thank to Mr, Hosseini in Erfan hospital and surgeons: Mr, Paul Hamilton and Miss Andrea Sott in Epsom hospital.

Special thanks go to Dr.Mahshid Yazdifar and Dr.Samira Sayad Saravi for their support. Their friendship and encouragement have been a strong wind that helped leading this boat safely to the harbour.

Finally, a big thank you to my family: my parents, sisters, brother, for their support, and Dr. Pejman Fathollahi who helped me during this process from the beginning to the end.

Abbreviations

CT	Computed tomography
FEA	Finite element analysis
MRI	Magnetic resonance imaging
3D	Three dimensional
HV	Hallux Valgus

Notations

e	Time
$\boldsymbol{x}$	Force
SI	International system of units
2D	Two dimensional
T	Transfer matrix
A	The first matrix obtained from the force data
B	The second matrix obtained from the force data with one shift from matrix A
P	Statistical significance value
$\lvert \boldsymbol{x}_2 - \boldsymbol{x}_1 \rvert$	Distance measured between two markers
r	Ratio measured between two markers

Contents

List of Figures

List of Tables

Introduction on foot Biomechanical issues

1.1 Introduction

The Foot is one the most complex segments of the human body, it contains 26 bones and more than 100 ligaments and all joints, ligaments and bones help the body for propulsion.

Analysing human motion becomes one of the major issues in many research fields such as sport injuries and also injuries that occur in the elderly. Any joints and bones deformities, can affect the people's daily life. In order to help patients to be treated and those going under a rehabilitation process, analysing human motion is becoming one of the advanced ways to recognise structural problems of bones.

This chapter is focused on foot anatomy and the reason for the existence of the fore-foot deformity in particular Hallux Valgus (HV) condition, which is the big toe deformity. Then motivation, aims and objectives, and finally, the summary of chapters will be presented.

1.2 Need for biomechanical study of big toe deformity

Foot is one of the most complex structures of human body so understanding the biomechanical issues related to foot disorders seems essential. If any deformity or injury occurs to the foot, or if foot becomes dysfunction as a result, it will affect other parts of the body such as back and nerves. The pain which exist in patients with severe HV can disrupt the daily life of patients.

One of the most common diseases of the foot is HV which is a great toe deformity and it happens when the 1st metatarsal head rotates 15 degrees or more from its original location. Figure1.1 shows the deformity.

The most common known bone deformity is HV that 35.7% of elderly people develop during their lives and 23% of adults affected by this condition (Nix et al., 2012).

There are some ideas about the initiation of this deformity, researchers and surgeons believe that the causes are both congenital and the habit of wearing narrow-toe box and high heel shoes. The prevalence of HV is 2 to 1 women to men because women wear more fashionable shoes that leads to limitation of the toe movements inside the shoe and following that, the mechanical changes occurs especially in fore-foot region. But in men with flat feet, the occurrence is higher compared to men without flat feet (Nguyen et al., 2010)

HV disease can be seen in women in their forties and fifties (Lowery & Wukich, 2009). This deformity is associated with the risk of falling and abnormal pressure distribution (Drake et al., 2005).

People with HV complain of either the bad shape of their foot or discomfort and pain that they feel in the location of the deformity. The condition can be aggravated by wearing unsuitable shoes as the bump of the bone rubs inside the shoe. In both cases when the situation worsens, the need of surgery seems essential. The condition is associated with the gait impairment and the poor balance. Once the condition happens, it cannot be reversed; wearing narrow toe box shoes and high heels worsen this deformity. The progression in the early stages of initiation can be treated by conventional solutions (Vidal et al., 2007).

In recent years, many researches are focused on gait analysis of the patients with different kinds of pressure measurement devices, in order to investigate any existing foot problems. Furthermore, to design proper foot wears, analysing plantar pressure distribution of the foot is necessary in order to prevent possible injuries in early stages of recognition.

Floor based pressure measurement devices are technologies in measuring pressure pattern that have been widely using in recent years. These devices can help the surgeons to assist the patients, to correct their gait based on the style of walking and abnormal pressure distribution under the foot. There are difficulties relating to agreement of results in plantar (under foot) pressure measurements. So controversies

can be seen in previous published researches relating to which areas of foot bearing the higher force while doing different activities but the effect of individuals' speed and walking characteristics on pressure distribution pattern have been missed from previous published works.

Figure1.1: Foot with Hallux Valgus deformity (Rucosm, 2012)

1.3 Significance of the study

This work contributes to both the basic science of designing ways of measuring first metatarsal joint movement and analysis of the force pattern under the foot for the clinical applications of diagnosing foot deformities e.g: designing insoles for patients to re-distribute the pressure under the highly load area .

Two methods were developed: the first method involves, the measurement of the transferred force transfer coefficient from one region of the foot to the other, and the second method to measure the laxity of the 1st metatarsal head's joint in patients with HV disease.

This study first presents the foot anatomy and the biomechanical changes in foot with HV condition to find out the reasons of dislocation of the big toe. Second, the force pattern in volunteers with and without HV is obtained by using the RSscan device. Then the Motion capture cameras were used to get the motion of the 1st metatarsal joint relative to the 2nd metatarsal heads' joint to find out the laxity of the big toe in patients.

Third, the modelling of the foot with and without HV obtained with Mimics, 3Matic and Abaqus software for the comparison of applied force in static position by the help of CT scan images of both groups.

This study of HV involved the measurement of the force distribution under the fore-foot which contains four distal phalanxes, four middle phalanxes, five proximal phalanxes and five metatarsal heads.

In this study the causes of HV were discussed and analysed. Hence, the force distribution pattern under the fore-foot, in the area that HV occurred was analysed.

The force distribution under fore-foot region was analysed and the relationship between high peak force under metatarsal heads in HV and control group were investigated.

1.4 Background

Since humans started covering their feet, many bones deformities happened to the foot. Human started wearing shoes about 40000 years ago (Baker, 2008). Wearing shoe changes the way that the human walk and how their bodies distribute weight change. Those changes end up affecting the bones and ligaments (Baker, 2008).

However, covering the feet is essential in order to prevent some possible injuries that occur while feet have a contact with outside environment, but it has some negative effects on the foot which reduces the real functionality of it. Depending on the shoe type, injuries that happen to the feet varies, some of the them appears as skin disorders, some of them as bone deformities such as joint's dislocation and the others are related to reduction of feet functionality in the long-term usage.

1.5 Foot Anatomy

Foot structure consists of 26 bones, 107 ligaments, 33 joints and 19 muscles. Twenty five percent of the human body bones is located in the foot (Qiu et al., 2011). Each of them has a specific function in relation to each other that helps the body to move forward and to stand in the balanced position (Dawe & Davis, 2011). Foot bones can be categorised in three types:

1) The tarsal bones, which consists of seven bones that make the ankle.

2) Metatarsal 1 to 5 which are the bones of the metatarsus.

3) The phalanges, which are the bones of the toes, each toe has three phalanges except for the great toe which has two (Drake et al., 2005).

4) Leg consists of two bones**:** Tibia and Fibula (Drake et al., 2005).

The mechanical structure of the foot along with soft tissues plays an essential role in the functioning of the lower extremity and this function is controlled by muscles. The whole mechanical structure of the foot stabilise body while walking and standing (Abboud, 2002).

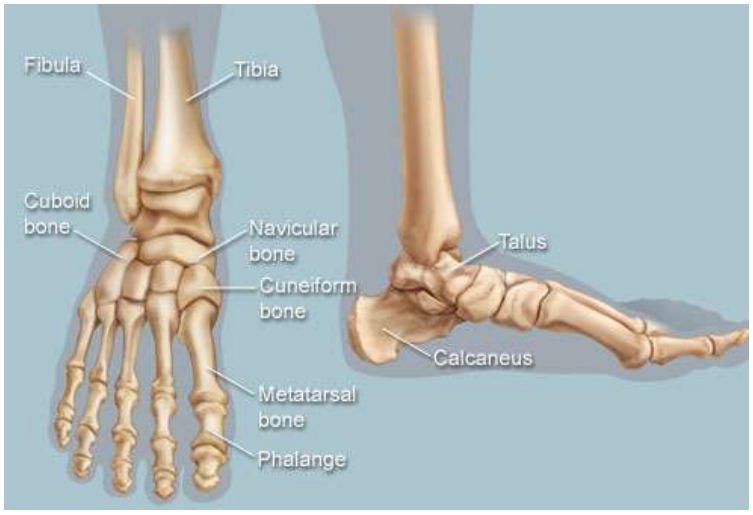

Figure1.2: Foot bones (WebMD, 2010)

1.5.1 Foot arches

As shown in Figure 1.3, foot contains three arches, medial, lateral and transverse. (Further information about the arches and their function is available in Chapter two).

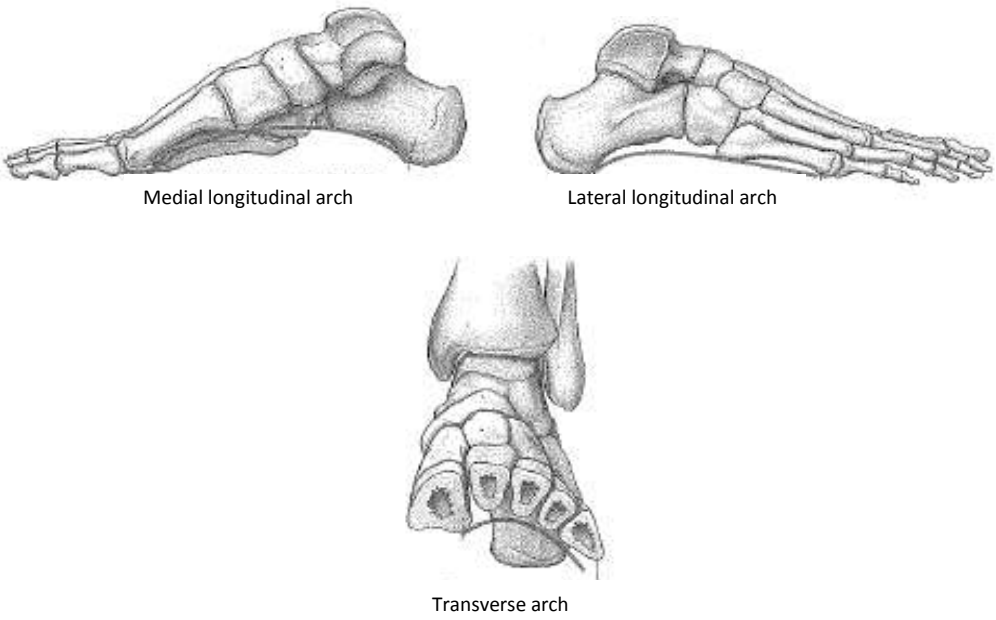

Figure1.3: Foot Arches (Drake et al., 2005)

1.6 Foot movements

There are different foot related movements as shown in Figure1.4 (Abboud, 2002),(McDonald &Tavener, 1999).

Extension: bending the foot or toes upwards, it is also called dorsiflexion.

Flexion: bending the foot or toes downwards, it is also called plantar flexion.

Abduction: spreading the toes apart and the movement of the fingers are extensive.

Adduction: when the toes move toward each other.

Inversion: turning the foot that the sole faces more inwards.

Supination: is the twisting movement of a foot. Inward movements of the sole of the foot when it is off the ground.

Pronation: is untwisting movement of the foot (McDonald 1999).

The movements of the foot are presented in Figure1.4.

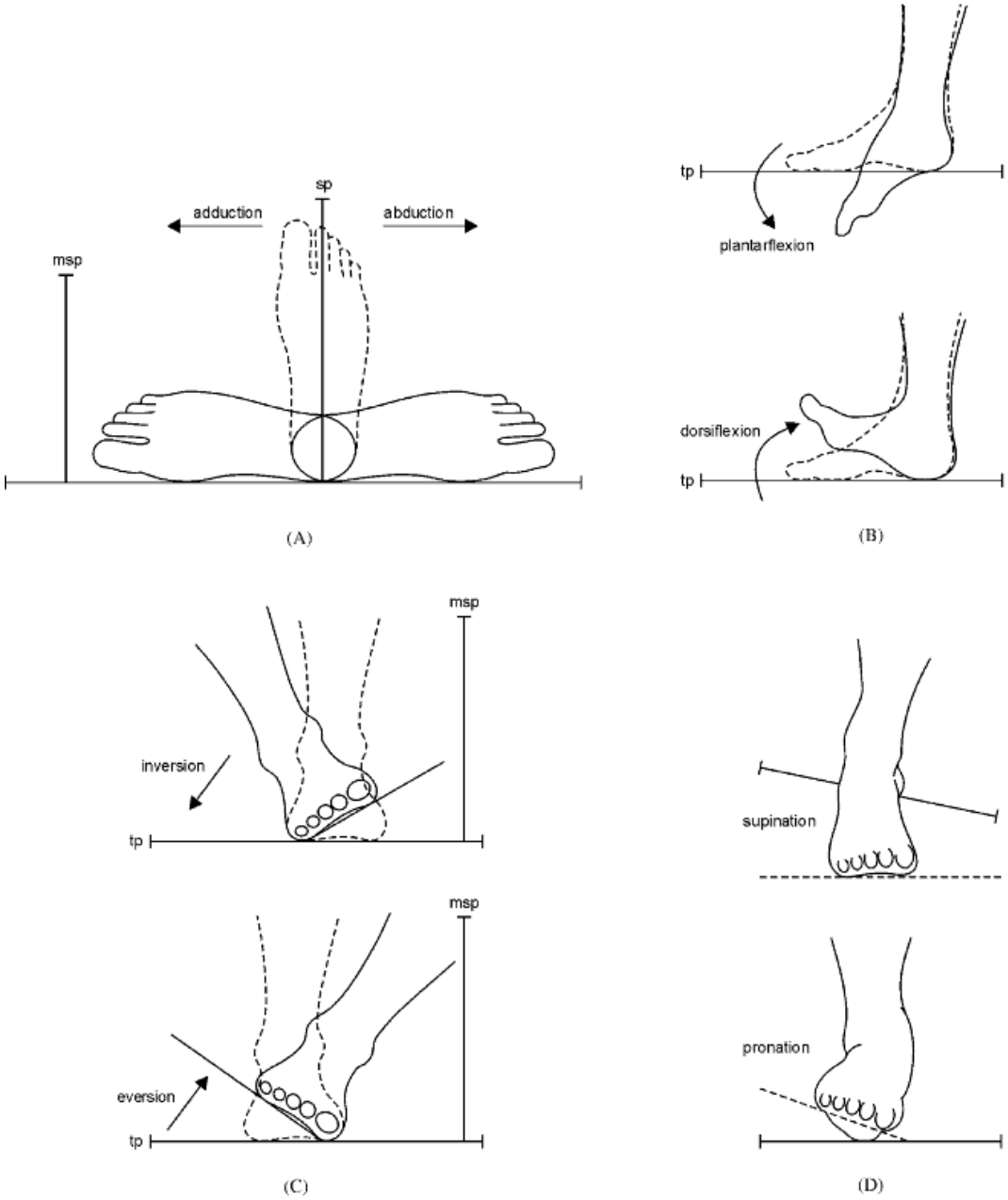

Figure1.4: Foot movements (Abboud, 2002)

The two movements of the foot, including supination and pronation help the joint to be stable and also it decreases the amount of body forces applied to the foot (Donatelli, 1985).

1.7 Function of the foot

The stable function of the foot is because of existence of bones, joints and ligaments, they bring flexibility to the foot and they can be adjustable with uneven surfaces during phase of gait (Briggs, 2005).

The muscles control the joints movements and provide motion function of the foot (Abboud, 2002).

1.7.1 Fore-foot function

In fore-foot region except 2nd and 3rd metatarsals, the rest have more abilities in extension, abduction and flexion movements in the direction of lateral sides of fore-foot region (Briggs, 2005).
There are two little bones under 1st metatarsal head called sesamoids that have the capability of supporting 1st metatarsal head in extension of the hallux, also the bones bear the pressure applies under 1st metatarsal region and finally these two bones improve the mechanism properties of the intrinsic muscles (Glasoe et al., 1999).

1.7.2 Mid-foot function

The mid-foot includes navicular, cuneiforms and cuboid (Abboud, 2002). Mid-foot in normal arch foot people does not bear load in the stance phase (Donatelli, 1985).

1.7.3 Hind-foot function

There are two different motion that heel provides which are pronation and supination (Briggs, 2005). The calcaneus and the talus make the hind-foot. The talus has a function of transferring the ground reaction force toward the ankle joint and leg. The structure of the Achilles tendon which is located behind the calcaneus, enables this bone is to bear high tensile, compressive and bending forces (Abboud, 2002). The specific location of the hind-foot, mid-foot and fore-foot are shown in Figure 1.5.

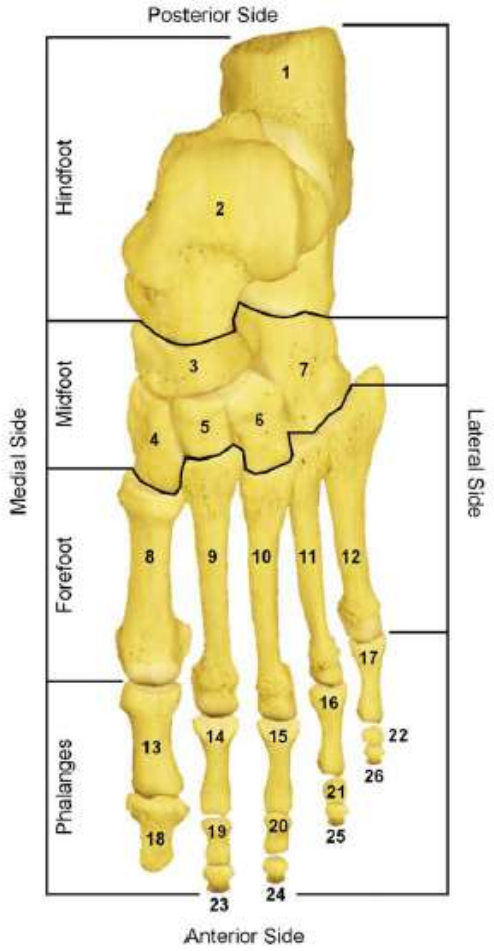

Figure1.5: Foot structure (Abboud, 2002)

1.8 Aim and Objectives

The aim of this study can be classified in two main categories in order to obtain two purposes one is recognising the HV condition. The second one is indication of HV existence among those who are already recognised with the condition to design a proper shoe to redistribute or to reduce the plantar force received from the ground. This would assist the shoe designers to design proper footwears for HV patients.

Category one: establish a new method to measure the transfer force contributions of the metatarsal bones amongst each other.

Category two: the measurement of lateral flexibility of the 1st metatarsal joint where the deformity happens is going to be investigated as an indicator of HV existence.

Category three: constructing the 3D models of feet with and without HV using FEA to validate the stress distribution results with the experimental results.

The objectives of the research are as follows:

- Investigating the plantar force pattern in twenty volunteers with two different speeds (self-selected and fast), ten with and ten without HV and compare the existed differences in both groups.
- Developing the method to measure the transfer force pattern among different fore-foot bones especially five metatarsals as an indicator of HV condition in people who already have this condition.
- Validating the force transfer pattern with finite element analysis in the static condition.
- Developing the method to recognise HV in people who already diagnosed with the condition by measuring the lateral flexibility of the 1st metatarsal bone and HV condition.

1.9 Thesis outline

The research to achieve the stated objective is reported in seven chapters, as follows:

Chapter One: Introduction on foot biomechanical issues.

Introduces the overall view of the project and explains the objectives.

Chapter Two: Literature Review.

Contains a comprehensive review of the literature as the foundation of the research. It covers various methods which were used so far to measure the pressure pattern under the foot in particular.

Chapter Three: Measurements of foot plantar force pattern and joint lateral flexibility.

Illustrates and describes the details of the measurement of foot force pattern in people with and without HV condition. Also in this chapter, the method of measuring lateral flexibility of the 1st metatarsal joint studied.

Chapter Four: Plantar force and joint lateral flexibility measurements' results and discussions.

The mechanism of transferring the force through the forefoot of individuals was analysed, and results was discussed and the relative motion of the 1st metatarsal joint regarding to the 2nd metatarsal joint also was analysed.

Chapter Five: 3D modelling and stress analysis of feet with and without HV.

Describes the modelling process of the volunteers' feet with and without HV, and stress applied to the foot and all boundary conditions explained, then final results compared and the validity of the models analysed.

Chapter Six: Conclusion And Future work would be presented and discussed.

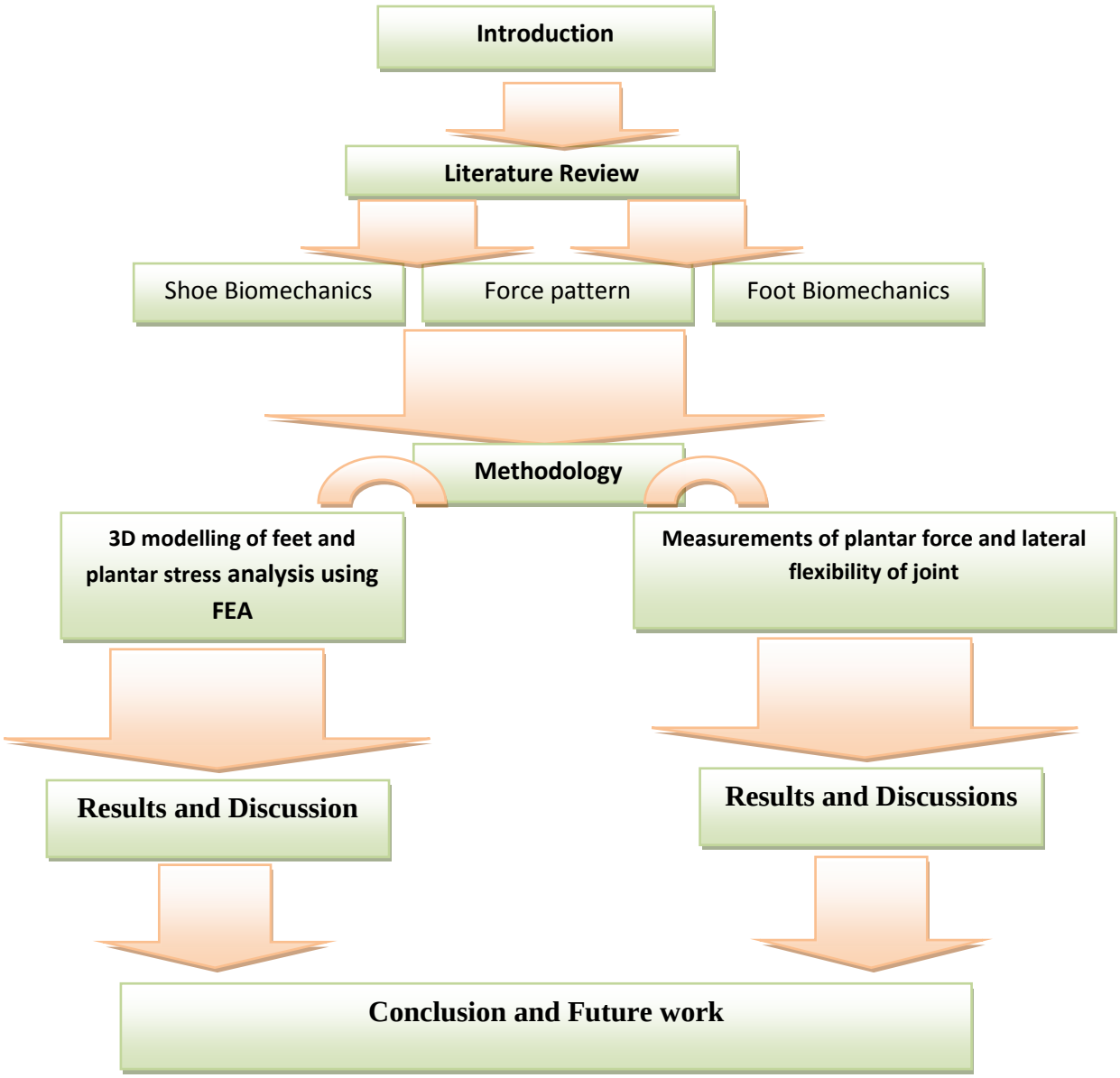

Figure1.6: Thesis outline

Literature Review

2.1 Introduction

In this chapter the causes of Hallux Valgus deformity and the prevalence of this condition in people are discussed. Moreover, foot biomechanical issues such as force distribution pattern under the foot are explained. Shoe related biomechanics which is another subject related to initiation of the deformity, is also studied.

2.2 Foot Biomechanics

2.2.1 Arches of the foot

The people with flat feet feel more pain while walking compared to people with high arch feet. When the arch of the foot is higher, the stability would increase and less energy would consume. In people with flat feet the consumption of energy is higher and also there is a lack of stability compared to high arch foot individuals (Fan et al., 2011). According to Cavanagh, higher arch increases the probability of overuse injuries (Cavanagh et al., 1997). Arches of the foot are shown in Figure 1.3.

Shock absorption properties is one of the major characteristics of foot arches when the arch is higher or less than normal shape. The load transfer differs and significant changes can be seen in plantar pressure distribution under specific regions. The adaptability of distributing force in normal arch foot is higher in comparison to low and high arch foot individuals (Rosenbaum et al., 1994)

2.2.2 Longitudinal arch

The plantar fascia which is located under the foot is one of the strongest ligaments and its function is to stabilize foot structure. When the stiffness of this ligament weakens, the shock absorption property will reduce (Cheung, et al., 2004)

2.2.3 Transverse arch

Transverse arch of the foot is located under metatarsal heads which joins the big toe and little toe to each other. While standing, the body weight rests on the three points where the arches intersects (Vass & Molnar, 1999)

2.2.4 Medial arch

Medial arch is consisting of calcaneus, talus, navicular, three cuneiforms and the 1st ,2nd ,and 3rd metatarsals with the function of energy absorption (Qian et al.,2010).
The navicular bone located in the medial arch and it has vertical displacement and responsible for the deformation of this arch (Qian et al., 2010). The study has been done by Imaizumi who investigated that people with flat feet bear less pressure under the hind and fore-foot area comparing to people with normal arch, also he found out that people with high arch bear less pressure on the mid-foot but the pressure is higher under their fore-foot and hind-foot (Imaizumi et al., 2011).
Flat feet are associated with higher pressure under 1st metatarsal joint. Furthermore, people with flat feet have less flexible feet compared to normal and high-arch footed people. They showed to have 30% increasing pressure under hallux bones compared to high-arch foot people. This study investigated that people with flat feet has tendency to get some deformities such as hallux valgus, hammer toes as shown in Figure2.3, diabetes mellitus and peripheral neuropathy as they have higher load under the hallux compared to people with high arch and normal arch feet (Rao et al., 2011).

2.3 Foot Stability

Stability is related to risk of falling. As explained in the section on the arches of the foot, people with high arches feet have more stability in balance and walking condition compared to individuals with flat feet.

Other causes of instability of the foot, are dislocation of the base of the proximal phalanx over metatarsal heads which causes pain in this area. Furthermore, hyper extending or hyper flexing injuries that cause damage to ligaments will increase the range of motion (Suero et al., 2012).

The mechanical structure of the foot which includes bones, ligaments and arches provides the stability of the foot that leads to maintain balance while standing and also helps feet to have proper propulsion. Also the joints provide flexibility and muscles and tendons helps the body to have movement control (Abboud, 2002).

2.3.1 Under the foot force distribution

When the heel makes a contact with the ground, the high force applies which sometimes is equal to the body weight (Qian, et al., 2010). When the heel deforms as a result of shock absorbing, the rest of the pressure moves towards the metatarsal heads (Glasoe et al., 1999). Bruening found that when the heel unloaded, forces on the hallux increased and force on the lesser toes was less in comparison with the hallux (Bruening et al., 2010). Donatelli highlighted that in the static position, the ligaments under the foot, which called plantar aponeurosis, bear 60% of the body weight and the metatarsals bear about 25% (Donatelli, 1985).

Another study that has been done by Trinkaus established that while walking, three times body weight is applied to the foot. Also he found that the pressure under the hallux is higher compared to metatarsal heads. Furthermore, the pressure under the toes is about one-third to one-half of the pressure applied to the hallux (Trinkaus, 2005).

Many factors are contributing to underfoot pressure distribution such as age, body mass, the skeletal structure of the foot, the shape of the arch, the hallux characteristics and also the lateral side of the foot.

Also the effect of pressure distribution under the foot in men and women investigated and showed the differences existed between genders. Men were shown to bear more pressure in the hind-foot compared to women. In women, the mid and lateral foot shown to bear more peak pressure compared to men. Also the larger contacts of men's feet make additional differences and the maximum pressure ratio was shown to be higher under the hind-foot in men (Periyasamy et al., 2011).

One of the main parts of the foot which is the ball is located in the fore-foot area (under the 1st metatarsal) plays an essential role in bearing body weight during locomotion. Metatarsal heads bear the highest ground reaction force along with the

fat pad located under the heel region which has a major role in push-off (Chen et al., 2010)

Randolph confirms that the higher ground reaction force is applying to the fore-foot area (Randolph et al., 2000). In another study done by Bryant, also there is a confirmation of increasing the pressure under the 1st metatarsal heads when the skin thickness under this region is reduced. Also he found that a short 2nd metatarsal head has the effect of increasing the pressure under the 1st metatarsal bone. Reducing soft tissue mass under the heel increases the applied pressure in this part of the foot (Bryant et al., 2000). Hamill, found that the pressure that comes from the ground, first applies to the lateral part of the heel, and then transfers towards the cuboid,1st and 2nd metatarsal heads. The longest support time is used up by fore-foot especially, the 1st and 2nd metatarsal bones (Hamill, 1995).

2.4 Effect of walking speed on plantar pressure patterns

Hughes established that the load under 1st,2nd and 3rd metatarsal regions increased by increasing the walking speed and found that the highest pressure was under the 2nd and 3rd metatarsal regions (Hughes et al., 1991).

Human speed has a major effect on pressure distribution, when the speed increases, the body force that applies to the foot increases. While running 2-2.5 times body weight applies to the foot. But in walking, the applied force is a little more than body weight (Mc Lester & Pierre, 2008).

Rosenbaum et al.,1994, measured the pressure distribution under the foot of 30 healthy subjects, they were asked to walk with three different speeds slow, self-selected and fast, he found that with increasing the speed the load was shifted towards the medial parts of the fore-foot. The medial part of the fore-foot consists of 2nd and the 3rd metatarsal heads. Furthermore, they found that while increasing the speed the heel has higher eversion movement compared to other speeds.

By increasing the speed both hind-foot and fore-foot bear higher load compare to slow and self-selected speeds (Rosenbaum et al., 1994).

2.5 Shoe related biomechanics

The good design of the shoe has two requirements which is suitability and comfortability. It should reduce the energy consumption and musculoskeletal injuries and also should increase the quality of the performance (Lam et al., 2011).

Shoe hardness and geometry have an effect on ground reaction forces applied to the foot (Wit et al., 2000). In healthy people, 36% of body weight applies to the toes and 43% of the body weight applies to the heel in balance standing. In the shoe with the rigid sole, the peak pressure and the contact times have been affected. The metatarsals contact time with the ground increases by increasing the level of rigidity, because the movement of the centre of pressure towards the fore-foot area will be faster (Soames, 1985). Also in another study done by Ly, he found that peak pressure applied to the foot has a direct relation with the flexibility of the shoe sole (Ly et al., 2010).

In shod condition, where the arches of the foot are in contact with the shoe, the pressure increases compared to the unshod condition where there is no contact of the arch and the ground. Furthermore, wearing shoes applies pressure to the dorsal part of the foot while in unshod condition the applied pressure is less (Chevalier et al., 2010).

There is also pressure that applies to the foot, from the upper part of the shoe to the dorsal area. Shoe lacing system also causes the increase of the movement of the foot inside the shoe and higher pressure applies under fore-foot area (Fiedler et al., 2011).

Zwaard discussed the effect of wearing high heels on increasing the pressure under the foot. He also established that the increasing plantar pressure has direct effect of increasing the risk of falling and changing the gait characteristics Moreover, he stated that there is a relationship between ill fitting shoes and the lesser toe deformities, corn and ulceration and HV (Zwaard et al., 2014).

Ye found that the effect of wearing high heels initiates an unnatural pressure distribution pattern. Furthermore, he confirms Zwaard findings including HV, fore-

foot pain, corns and calluses and ankle sprain are caused by wearing high heels (Ye et al., 2008).

During the weight bearing, the sole of the shoe supports the transverse and longitudinal arches of the foot so the movement of the foot and the adaptability of arches with different movements restricted inside the shoe especially when wearing narrow-toe box shoes (Kadambande et al., 2006).

When the pressure increase under the 1st metatarsal bone, this bone will move medial-dorsally. Also the stress in the soft tissue located in the upper part of the 1st metatarsal joint will be increased as a result of wearing high heels. People with high heels had twice larger joint reaction force compared to bare feet people while walking. (Yu et al., 2008).

The study done by Speksnijder on pressure analysis in healthy women wearing High-heel found that the pressure on the central and medial fore-foot and also on the hallux is higher compared to women who wear lower heel shoes. He established that by increasing the height of the heel, the maximum pressure that applies to these regions is also increased (Speksnijder et al., 2005).

According to the study done by Kadamabande, the women and the men who wear shoe in the population under the study had stiffer feet compared to unshod population. Also he found that shoe can restrict the transverse arch movement of the fore-foot and also the natural position of the longitudinal arch would be disrupted and this has an effect on the force distribution pattern (Kadambande et al., 2006).

Wearing the shoe narrower than the foot causes HV and foot pain but wearing shorter shoe size leads to the lesser toe deformities and if the heel height exceeds of 25 mm then it leads to HV and calluses on the plantar surface of the foot. Lesser toe deformities are shown in Figure 2.3 (Menz & Morris, 2005).

2.6 Fore-foot disorders

When any individual feels pain in the fore-foot area, the symptoms and its location should be considered very carefully by surgeons, for if there is no sign of callus under the forefoot region, misalignments is invariably due to joint or soft tissue abnormalities. Some fore-foot disorders include: lesser toe deformities, the hallux rigidus, sesamoidities and HV with the last three being first ray deformities (Coughlin, 2000).

2.6.1 Hallux Reigidus

After HV, this is the most common deformity of the fore-foot. It is a deformity of the big toe whereby the joint becomes stiff and movements related to this, especially in the dorsiflexion direction are difficult. The report published by Brantigham shows that Hallux Rigidus is prevalent in people aged between 31 and 69 years old in 345 individuals who took part in the experiments.

As the 1st metatarsal joint becomes stiff, pain reduces and increasingly transfers to the other parts of the foot with the pain being caused by the unnatural weight bearing. One result of this deformity is loss of motion (Brantingham & Wood, 2002). Figure 2.1, shows the location of the hallux rigidus deformity.

Figure2.1: Hallux rigidus deformity (Brantingham & wood, 2002).

2.6.2 Sesamoiditis

The Sesamoid bones as shown in Figure 2.2, are two little bones located under the 1st metatarsal head. The function is to reduce the friction and it also protects the tendon located under the hallux. Inflammation, swelling and the fracture of these bones is termed sesamoiditis. Fracture mostly happens due to weight bearing as they transmit 50% of body weight (Atiya et al., 2013).

Figure2.2: Sesamoiditis fracture (Crates, 2013)

2.6.3 Lesser toe deformities

These kinds of foot problems happen in old and middle ages because of the muscle imbalance that happens between the extensors and flexors located in the toes (Milner, 2010) As shown in Figure 2.3. Mallet toe, claw toe and hammer toe are lesser toe deformity classifications.

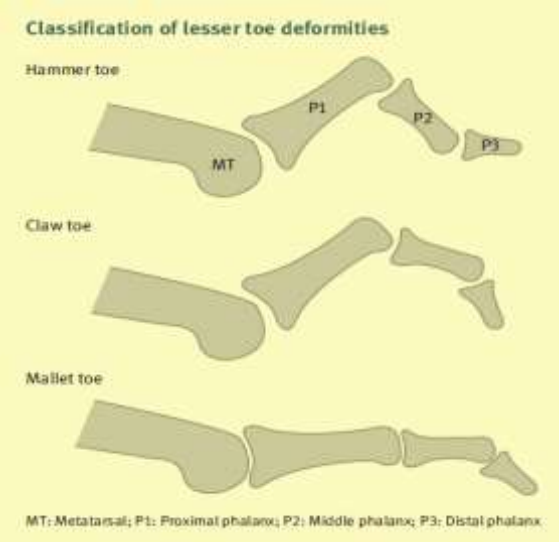

Figure2.3: Lesser toe deformities (Milner, 2010)

2.6.4 Rheumatoid fore-foot disease

Rheumatoid arthritis found in 75% of the population has effect on the metatarsophangeal joints. Regular inflammation of the lining between joints can lead to HV and may also cause the lesser toes become dislocated with pain extending under the metatarsals (Milner, 2010).

2.6.5 Hallux valgus (HV)

The most common foot deformity is HV and many such complaints are presented to surgeons and foot specialists. This deformity is presented in Figure 2.4. (Nix, et al., 2010). It has been pointed out that HV initiation is as a result of osteoarthritis in this joint and in other sites of the foot. The osteoarthritis occurs, after the cartilages are damaged, and more specifically, HV is associated with pain felt in the knee and big toe (Roddy et al., 2008). In another study the factors that associated with HV are identified as poor balance, immobility, risk of falling, and gait injuries all of which have a negative effect on quality of life (Eshraghi et al., 2013).

2.7 Hallux Valgus deformity

The severity of HV is categorised under three conditions, mild, moderate and severe (Martínez et al., 2010).

In addition, its progress is classified as taking four stages, the first stage happens when there is an outward movement of the 1st metatarsal joint and sesamoids begin to dislocate. The second is when the 1st toe presses the 2nd toe and the displacement of the sesamoids becomes visible. With the third stage, the angle between the head of the 1st and 2nd metatarsals increase, and in the final stage, complete dislocation happens at the 1st metatarsal joint and it presses on the lesser toes (Gilheany et al., 2008).

Women are reported as having HV more often than men and it is also associated with the hyper mobility of joint (Milner, 2010).

Figure2.4: Hallux valgus deformity on the 1st metatarsal head (LFAC, 2014)

People with HV presents with distorted loading in their fore-foot because of increasing pressure distribution but there is an argument regarding whether this changes in the plantar pressure distribution happens in the medial, lateral or central metatarsals (Mickle et al., 2011).

Mickle et al., 2011, claimed that peak pressure in HV individuals is on their 1st and 2nd metatarsal heads. Furthermore, Nguyen et al.,(2010), reported some factors

associated with the incidence of HV such as body mass, age, flat feet, foot pain, wearing high heels , and gender (Nguyen et al., 2010).

Another factor associated with having HV is the range of motion between joints which in HV people is higher compared to non-HV individuals when they are observed walking barefoot (Deschamps et al., 2010). In such cases, the deviation that happens in the big toe causes the 1st metatarsal joint to become dislocated and the great toe may move towards the 2nd toe, sometimes causing overlapping which results in a fluid-filled bursa between toes (Draper, 2013).

2.7.1 Prevalence of HV

A study by Mafart on data pertaining to the French population from the 5th to the 17th centuries shows that a genetic explanation for the cause of HV is not correct because he observed that men during the 16th to 17th centuries had significantly higher prevalence of HV compared to women. He attributed this to the fact that they were wearing boots made from stiff leather. It is of note that he found that women during the period lasting from the 11th to 13th century were more prone to HV and that changes to the big toe happened over time and that HV was absent among younger people. It can be concluded that changes in foot wear types is a key factors determining incidence of HV (Mafart, 2007).

In contemporary times, Nix and his colleagues highlighted that in the UK the prevalence of HV in adults is 28.4% while that amongst elderly people can reach up to 74 % (Nix, et al., 2010). However, there are some contradictory claims in reported studies, for while Mann and Coughlin (1993) explained that 33% of people who wear shoes suffer from HV (Mann&Coughlin,1993), in another study the reported population was 38% of women aged between 50 to 70 years old (Dawson et al., 2002).

2.7.2 Pathophysiology

Naturally, the hallux and other toes should remain parallel to the long axis of the foot. In order to keep this function, the extensor and flexor hallucis longus and adductor tendons help the toes to stay parallel. However, joint displacement disrupts this function and tension occurs at the medial part of the joint which leads to the

ligaments being pulled and then the 1st metatarsal bone becoming dislocated (Draper, 2013).

2.7.3 The causes of the disease

Smith and Coughlin asserted that first ray hypermobility happens as a result of HV rather than vice versa (Smith & Coughlin, 2008). But contrary to this claim, work by Lowery and Wukich (2009), contended that hypermobility of the 1st metatarsal joint is one of the causes of HV initiation and, as a result, the range of motion in the first ray is higher in HV individuals (Lowery & Nicholas, 2009).

The study of 600 males and females by Nguyen et al., (2010), showed that 58% of women had the HV condition and 25% of men. Further, it was shown in this study that HV in women is related to having a lower body mass index and for men, having flat feet and a high body mass index were associated with HV. In fact, men with flat feet were two times more likely to get HV than those without. Nguyen et al., (2010), reported that women with higher body mass are less prone to getting HV but inversely, men with higher body mass are more prevalent to HV because it is thought that overweight women were less likely to wear high heeled shoes.

These scholars commented that metatarsal length, first ray hypermobility, heel pronation and the shape of the metatarsal head are factors that associated with HV. Although foot pain in some cases is associated with HV, evidence from this study shows that men with foot pain are less likely to get HV studied population compared to men without foot pain. They also highlighted that there are structural bone differences between the genders with men having larger bones and women higher levels of bone movements. As a result, the way that pressure is distributed under the foot differs between the sexes (Nguyen et al., 2010).

Moreover, according to the investigations carried out by Dereymaeker et al., (2011) it was reported that the differences between the sexes have an influence on the initiation of foot deformities. They found that women's bones have more potential to move in the adduction direction as compared to men's. In addition, anatomical differences such as the size of 1st metatarsal and the shape of it can play an essential

role in HV deformity (Dereymaeker et al., 2011). Wen et al., (2012), investigated how the collapse of the transverse arch in the standing position accompanies HV incidence (Wen et al., 2012)

2.7.4 Foot plantar pressure in patients with HV

The 1st metatarsal joint and the hallux play an essential role in transferring the body's weight during locomotion (Mickle et al., 2011). A number of researchers have investigated the pattern of pressure distribution under the foot in HV patients. One study confirmed higher peak pressure occurred under the medial metatarsal heads (Hughes et al., 1991). In another study, scholars claimed that maximum force is higher in the medial part of the metatarsals in the fore-foot region (Nyska et al., 1998).

In his work, Plank (1995), examined volunteers with and without HV and found that in the non-HV group members the highest pressure was on 3rd,2nd , 4th and 1st metatarsals heads and 5th metatarsal head bears the lowest pressure. However in the HV group the maximum pressure observed was on the 3rd, 2nd, 1st, 4th and 5th (Plank, 1995).

In contrast to Plank's (1995), findings, Bryant and colleagues found lower pressure under the big toe and the second toe, and higher pressure under the 3rd to 5th metatarsal heads in HV patients (Bryant, et al., 1999). Moreover, Yavuz et al., (2009), confirmed that the whole pressure under the foot transfers to the 2nd and the 3rd metatarsal areas and that shear stress appears on the lateral sides of the metatarsal heads. Further, the pressure under the hallux in people with mild HV appears to be increased compared to non-HV individuals (Nova et al., 2010). In a study carried out by Rao and colleagues, it was reported that people with a low arch bear more pressure under the hallux and the 2nd metatarsal accompanied with the decreasing of dorsiflexion movement in the 1st metatarsal joint (Rao et al., 2011).

Mickle et al., (2011), elicited that people with HV bear higher peak pressure under the hallux. Also it is found that there is no relationship between the increasing angle of the 1st metatarsal bone and the peak pressure under the hallux as compared to individuals without any foot deformities, that is, the pressure pattern under the hallux

was found to be similar in HV and non-HV groups. There are studies on plantar pressure pattern in HV patients reported that higher pressure was under the 1st to 3rd metatarsals and other studies highlighted that the higher pressure was under the lateral and central metatarsals. Individuals with severe HV condition showed a significant increased pressure under the 1st and the 2nd metatarsals (Mickle et al., 2011).

2.7.5 Gait analysis

Understanding the foot structures which have an effect on normal gait can help to diagnose any foot dysfunction. The functioning of muscles is to control the centre of gravity for propulsion movement by their becoming shortened and lengthened (Dawe & Davis, 2011). Foot bones and the ankle joint together transfer the force which applies from the ground towards the leg and all together, these push the body forward (Boonpratatong & Ren, 2010). Figure 2.5, shows the eight steps of one complete gait cycle.

The gait phase is categorised as having two parts: 60% of gait comprises the stance phase and the remainder is the swing phase. These two phases are further divided into eight steps as shown in Figure 2.5. Each walking cycle contains two separate stages that are supported with double limbs, i.e. the initial and terminal swings. This support happens at the point of heel strike and they make up 20% of the gait. The foot can adapt to uneven surfaces because, while walking, in the first 15% of the gait, the lower limb rotates inward internally, then the foot pronates and this helps it to become more flexible and match a variety of surfaces (Dawe & Davis, 2011).

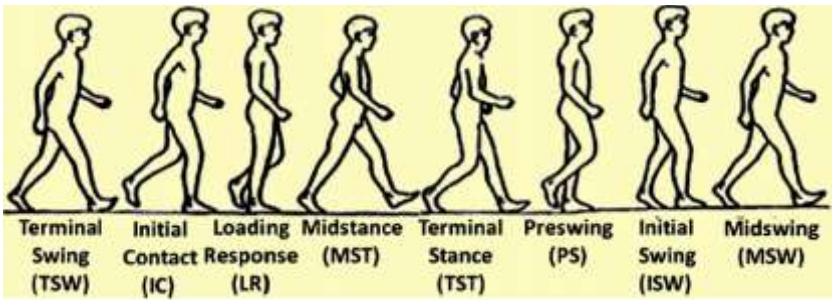

Figure2.5: Eight steps of the complete gait (Dawe &Davis, 2011)

In the beginning of the stance phase, first, the heel makes contact with the ground laterally with the ankle joint and then the centre of the body weight is placed near the 1st metatarsal joint (Qian et al., 2010). As Mickle et al., (2010), reported, the gait pattern in HV and non-HV individuals appears to be similar in the stance and swing phases of gait. The plantar flexion motion in the hallux is reduced in HV patients in the terminal stance and they have elevated heel eversion in the same stance, further, as the loading pattern changes in elderly patients with HV, there are structural changes to the bone and the soft tissue under the head of the metatarsal bones becomes increasingly painful and causes discomfort while walking. This brings instability in elderly individuals, especially when going up and down stairs and when changing direction (Mickle et al., 2011).

2.8 Soft tissue affected by HV formation

Soft tissue includes ligaments and tendons which have elasticity and pressure distributing abilities, as well as the capacity to absorb shock. However, when soft tissues become deformed these properties reduce and their functions are negatively affected, especially under the metatarsal heads. It is of note that the soft tissue under the foot will lose its function due to ageing and it becomes thickened, especially in locations where high levels of pressure apply, such as at the heel and metatarsal heads.

Moreover, the heel and metatarsals have a cushioning ability when body weight is applied, but this function changes with increasing age. Thus, when the structure of the foot gradually changes, the range of movement, strength and sensation will decrease and the prevalence of the foot deformities can be expected to increase with ageing. With age, soft tissue becomes stiff and this may lead to metatarsalgia which refers to when patients feel pain under the metatarsals as a result of soft tissue dysfunction. At the same time, the adaptability of soft tissue to cope with sudden and continual stress reduces (Kwan et al., 2010).

Proximal phalanxes are kept together with plantar fascia, one of the strongest ligaments in the foot. It may lose its function when deformity happens to the foot and, as a result, the longitudinal arch collapses (Stainsby, 1997).

2.8.1 Joint Instability caused by HV formation

One of the causes of pain in the fore-foot and initiation of deformity is the instability of metatarsophalangeal joints. This instability occurs when the plantar plate is disrupted as the task of the plantar plate is to stabilize the metatarsophalangeal joints. There are different factors associated with the metatarsophalangeal joints instability, such as HV deformity, joint hypermobility and there being a long metatarsal bone (Gregg et al., 2007). The first ray has an important function of stabilising the body while under propulsion, standing or walking. This is owing to the fact that about two-thirds of body weight appears to be under the first ray (Wong et al., 2014).

2.9 Techniques to measure under foot force distribution pattern

Under foot pressure measurement systems have been used widely for the recognition of foot deformities, to analyse gait problems and to observe biomechanical changes under the foot in the walking phase. Another usage of these techniques is to design ergonomic footwear that can be matched with patients' gait difficulties for the relief of their problems. There are three types of plantar pressure measurement systems: pressure platforms, in-shoe systems and imaging systems (Podoscope). These are shown in Figure 2.6. Sensitivity, calibration, sampling frequency and accuracy of these systems are important factors that need to be considered when measuring plantar pressure (Abdul Razak et al., 2012).

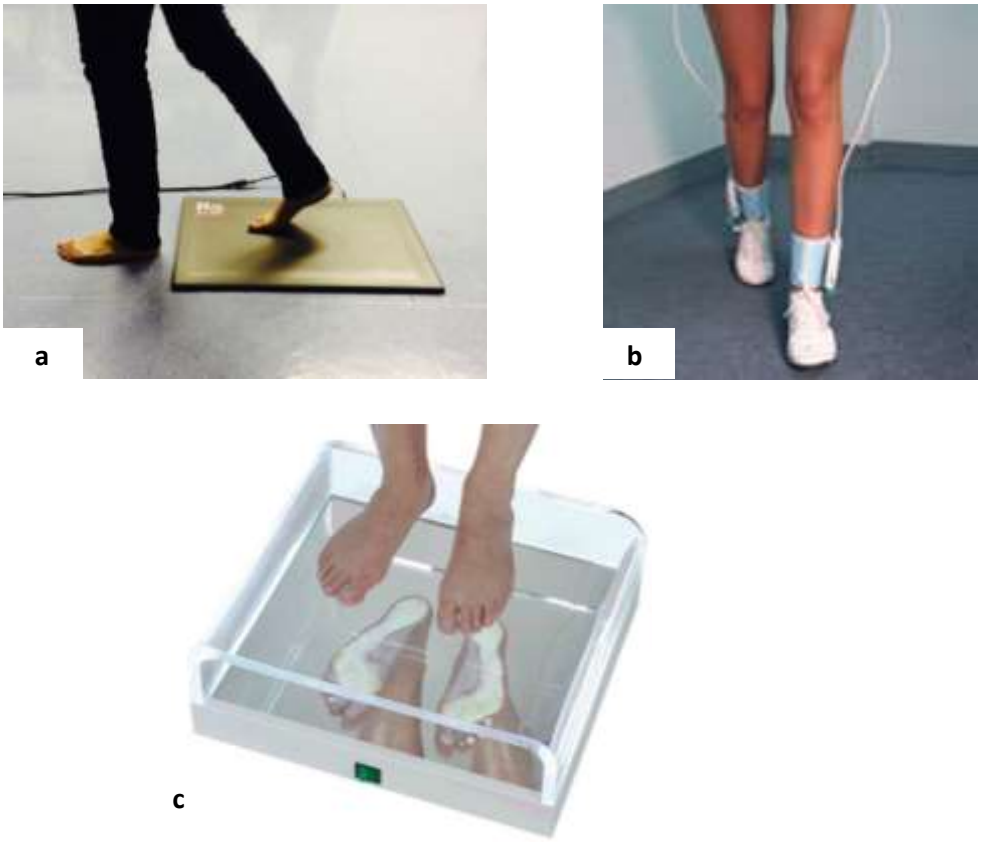

Figure2.6: Foot pressure measurement systems (a) platform (b) In-shoe system(c) Podoscope (MedicalExpo, 2014)

2.9.1 Platform Systems

There are several advantages of using platforms. Firstly, they are easy to use and the calibration process is not time consuming. Both feet cannot have contact while walking but in a standing position, it is possible to have both touching the mat. The problem with using platforms is that they require familiarisation in order to achieve the patient's natural gait (Abdul Razak et al., 2012).

2.9.2 In-shoe system

This system contains sensors which are placed inside the shoe. Although the system is portable, it can restrict movement inside the shoe and the sensors move inside the shoe while in contact with the foot. Another disadvantage is having fewer sensors as compared to pressure platforms and this may result in obtaining lower spatial resolution in the recorded data (Abdul Razak et al., 2012).

2.9.3 Imaging technique (Podoscope)

This device does not provide temporal and spatial data. It simply shows the regions that are under maximum pressure and thus does not have the facility for analysing the duration of contact time of pressure across the foot (Gefen, 2007).

2.10 Techniques to measure foot segments motion in 3D space

One technique used to measure foot motion in 3D space is by deploying Motion Capture cameras which have been widely adopted to analyse gait characteristics in this study,12- camera infrared motion analysis system (Qualisys, Sweden) were used to analyse the foot behaviour during locomotion (Qian et al., 2013). In one experiment the Motion Analysis Corporation's Santa Rosa system was used by deploying six cameras to analyse the internal rotation of the tibia by placing 14 markers on the rear-foot, fore-foot and tibia (Eslami et al., 2007).

Motion Capture cameras are used to investigate the fore-foot and hind-foot ranges of motion by using rigid clusters with a base of polyurethane carbon-fiber stalks (Jenkyn & Nicol, 2007). In the study done by Stebbins et al., (2006), the range of motion for the hind-foot, fore-foot and tibia investigated. They were focussed on the variability of their results by repeating the trials and used the Body Builder function of the Vicon program in order to build the data in the case of marker loss with Vicon 612 system (Stebbins et al., 2006).

Deschamps et al.,2010 applied a technique using Vicon cameras in their study to reveal that dorsiflexion of the hallux is higher in HV patients in the stance phase of gait compared to a control group. Moreover, the eversion of the hind-foot was reported to be higher in HV patients (Deschamps et al., 2010).

Hwang et al., (2005), investigated multi segments of the foot with HV patients. To this end, 19 markers were placed on the right foot of HV volunteers and six Vicon cameras were used to capture the motion of the hallux. They found that the movement in this region in the terminal stance is limited for these individuals as compared to non-HV individuals. The outcomes of other studies have reported that the hypermobility of the first ray, which includes the first metatarsal and first

cuneiform bones, is one of the factors that are associated with HV deformity. The higher degree of movement of the first ray in the saggital plane in HV patients was shown to have an effect on the HV plantar force pattern. According to Hwang and his colleagues, some of the foot segments appeared to have restricted motion, such as external rotation of the heel, in HV patients when compared to non-HV ones. However, HV individuals were shown to have higher heel internal rotation as compared to non-HV participants (Hwang et al., 2005).

Although a number of studies have been presented above regarding investigations in 3D space, in these reports none of the researchers explained their method for attaching the reflective markers on the surface of the skin of their subjects. How these are attached is important because this can restrict marker movement over the skin and hence negatively impact on the reliability of the data being collected.

2.11 The experimental methods on measuring plantar pressure done by different authors

The dynamic pedobarograph system was used in the study done by Hughes et al., 1991, and three trials were obtained from each volunteer and the mean value of each trial was obtained and compared. They found that 2nd and 3rd metatarsal heads bear the highest pressure in the fore-foot region (Hughes, 1991).

In another study done by Wen et al., 2012, RSscan device was used to get the pressure distribution under the 679 volunteer with and without HV,92% of them were females who felt pain in their fore-foot region especially, in 2nd and 3rd metatarsal heads areas. They found that volunteers with HV had significantly higher load in metatarsals 2 and 3 and significantly lower load under the 1st metatarsal head comparing to volunteers without HV (Wen, 2012).

Gurney et al., (2008), studied the plantar pressure distribution in nine volunteers using (EMED AT, Novel GmbH) pressure measurement system and collected three trials to analyse the coefficient of variation between trials. Volunteers walked with self-selected speed. Peak pressure, maximum force and contact time were obtained. The mean of the collected trials was obtained by SPSS software (as explained in

chapter three) and found that medial hind-foot and fore-foot were highly loaded (Gurney, 2008).

In the study done by Nova et al., (2010), the in-shoe system (Biofoot, IBV, Valencia, Spain) was used to get the pressure distribution of 79 volunteers with mild HV. Regression analysis was used to predict mean pressure under the five metatarsal regions and SPSS software was used to achieve the mean. The results show the increase load under the hallux (Nova, et al., 2010).

2.12 Finite element analysis of foot with HV deformity

Cheung et al., (2005), simulated a 3D foot model with the foot's 72 ligaments and defined the contact surfaces between bones in order to have relative movement between them. The relationship between the soft tissue stiffening and stress distribution under the foot in the standing position was investigated (Cheung et al., 2005). Similarly, in another study a 3D model of the foot was made with the Achilles tendon and plantar fascia in CAD. As part of their study, the researchers, Antunes et al.,(2008) included cartilages by using CAD, to investigate the biomechanical behaviour of the foot for the optimization of shoe design (Antunes et al., 2008).

A complete model of the foot was made including the plantar fascia and 70 ligaments by using CAD in a study by Qiu and his colleagues (Qiu et al., 2011). The body force that applied as a ground reaction force was validated through reference to previously published papers to confirm that most loads were on the hind and fore-foot areas. Ye et al., (2008), worked on modelling the wearing of high heeled shoes in a standing position with an elevated heel wedge. The study outcomes revealed an increase in Von Mises stresses at the 1st metatarsal joint and that the displacement of the hallux in the outward direction was not noticeable (Yu et al., 2008).

2.13 Conclusion

It is claimed by previous literatures that collapsing the longitudinal arch is one of the causes of progressing HV deformity and it occurs as a result of the weakening of the major ligament of the foot, the plantar fascia. When the arch of the foot collapses, the

shock absorption function of the foot weakens and the major load applies under the metatarsal heads, especially the 1st, 2nd and 3rd metatarsal heads. The higher force under these regions in long term causes pain and other problems under the foot such as corns and calluses. Recognising HV according to their pressure distribution pattern under the foot can help to design proper insoles to redistribute the pressure under the highly loaded area. Once the deformity happens it cannot be prevented but the progression can be reduced so in order to prevent the pain and other diseases associated with HV, plantar force measurement seems necessary in order to reduce patients' gait impairments.

Furthermore, as previous published papers women have more hyper mobile joints compared to men, so measuring the joints flexibility in the area that HV happens can help to recognise this condition in early stages of the initiation to prevent progression of the deformity.

Hence, to recognise the HV deformity by pressure distribution pattern, many authors worked on 3D foot models of patients with this condition such as Antunes et al.,2008 and Ye et al.,2008. They analysed the pressure distribution under the foot which is necessary when designing the footwear for people with different foot problems.

Measurements of Foot plantar force pattern and Joint lateral flexibility.

3.1 Introduction

In this chapter, under the foot (plantar) force pattern applied to the foot of HV and non-HV volunteers is investigated. Analysis of force pattern under the foot is fundamental for developing a clear understanding of the reasons behind the initiation of HV and it is important for finding treatments for these patients. This knowledge assists clinicians when making decisions regarding offering their patients conventional treatments. The precise causes of HV are unknown but it appears that the wearing of narrow toe box shoes and high heels aggravates the condition. When people started wearing such shoes, the free movement of toes inside the shoes became restricted and some historical evidence suggests that this has had an effect on exacerbating the formation of foot bone deformities (Baker, 2008). The aim in this thesis is to investigate the application of the plantar force pattern as an indicator for recognising the HV condition. To this end, a range of different devices have previously been reported in published papers with regards to the plantar force pattern. In addition, to assess whether movements of the foot joints have an effect on progressing the condition or not, these movements are studied. This method are investigated because according to previous published papers women have more hyper mobile joints compared to men so as the prevalence of HV is twice in women compared to men, the flexibility of the foot joint is studied.

In this chapter, the focus is on measuring the plantar force pattern under the right foot of individuals, ten people with HV and ten without (12 female and 8 males) were recruited to the investigation during which the force pattern for each volunteer were tested while she/he walked at a self-selected and fast speed. The average age of HV volunteers was 39.4 with average weight of 66 in which for non-HV individuals the average age was 30.2 with average weight of 59.9.

The force plantar pattern is recorded by using an RSscan which is a pressure platform which records the load magnitude when it is compressed. Another device used to diagnose vulnerability to the HV condition is the Motion Capture system and in this study this was used for analysing the volunteers' joints movements. In this

experiment, the lateral laxity of the 1st metatarsal bone in the two groups of volunteers was measured and the differences between them were identified in order to diagnose. As the biomechanics laboratory of Brunel University is equipped with the RSscan device, this was used for measuring plantar force of volunteers' right feet.

3.2 Experiments

In this projects two experiments were carried out using, 1) Foot scan device and 2) Motion capture system.

3.3 Experimental setup of RSscan pressure platform

The test was performed at the biomechanics laboratory in Brunel University and the procedure for it was approved by the ethics committee.

Plantar pressure measurement provides useful information for clinicians and researchers regarding: the structure and function of the foot, the general mechanics of gait, and is a helpful tool for evaluating patients with foot complaints (Keijsers et al., 2009). The RSscan (International NV, Belgium) device is used for clinical and scientific purposes and its dimensions are: 578mm × 418mm × 12mm (length×width×height), number of sensors 4096(arranged in a 64× 64 matrix),the sensor dimension was 7.62 mm×5.08mm,the weight is 4.2 kg and the resolution is 8 bits. It works by recording the pressure and the data on forces that apply while the foot is in contact with the platform as shown in Figure 3.1(a). In this way an evaluation of any existing abnormalities is made possible through an analysis of the force pattern recorded.

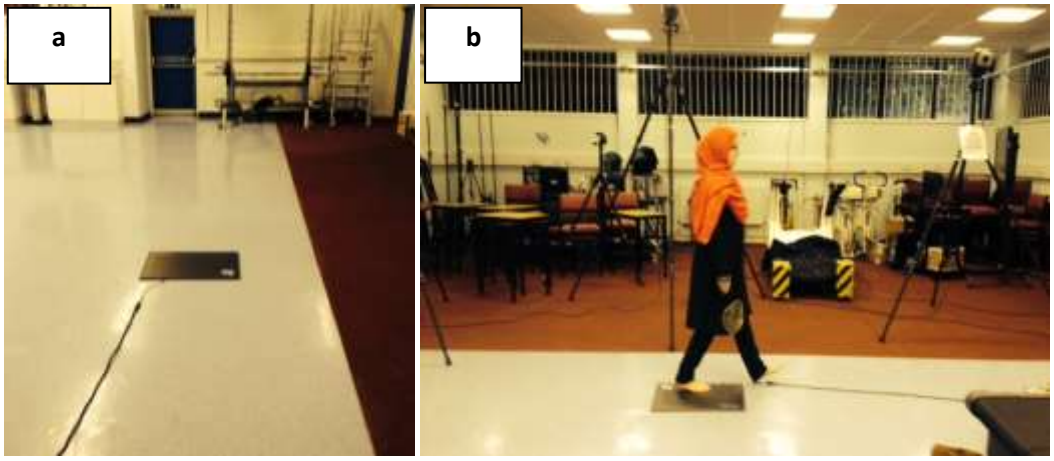

Figure3.1: (a) the lab environment, (b) the process of stepping on the mat

A six meter long track was set up in the laboratory and the RSscan mat positioned in the middle of it as shown in Figure 3.1(b). In order to familiarise the volunteers with the process of stepping on the pressure mat, in one go making full contact with their right foot, the volunteers were asked make three trial walks. This was to prevent them attempting to make any adaptations to their natural walking style when trying to achieve full contact with the mat. On occasions, the location of the device was changed because it was better to adapt the mat's location to the individuals' style of walking, rather than they adapt their walking with the location of the mat. After the volunteers were familiarised with the test process, they were ready to commence the actual test. They were expected to say "start" when they started from the start point and say "stop" when passing the end point. This was necessary because the time of walking needed be recorded in order to have consistency in their walking speed.

3.3.1 Calibration

3.3.2 Static Calibration

To achieve accurate results with the least number of errors, the very first action is measuring each person's weight independently. First the calibration is done in the static condition and then the person's weight is measured when she/he is standing on the mat and this is compared with the software measurement. Under these conditions, the person's weight should be the same as what the software shows in the main screen.

This weight related information is needed in order to normalise the force pattern data. Figure 3.2, shows the calibration of the device in the standing position and presents information for both feet of the volunteer also colour scale on the figure shows the pressure distribution magnitude based on colour scale which blue representing the lowest pressure and red representing the highest pressure. This is termed the weight calibration and the icon for it is also included in the Figure. The foot scan 7.9 Gait 2nd Generation software was used for the test.

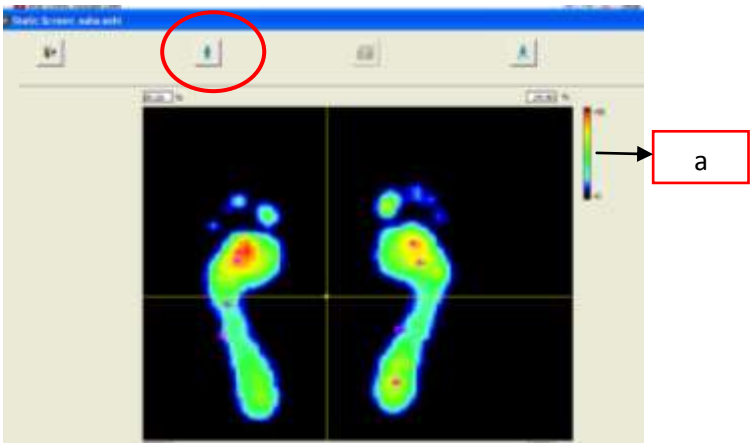

Figure3.2: Force distribution under the foot in the static position, a shows the magnitude of pressure distribution.

3.3.3 Dynamic Calibration

After scanning the foot plantar pressure for calibration, the dynamic test can be started. An individual was asked to pass over the mat five times to activate all the sensors in the active areas of the mat. The person who had done the calibration was not one of the twenty aforementioned volunteers because if the volunteers are asked to walk too many times, they could get tired and their results would not be accurate. They were already expected to walk ten times for the test and three times for familiarisation. In the screen for the dynamic test, an icon for "Measure" is pressed to start recording the forces applied under the foot. As soon as the foot made contact with the mat, the shape of the foot sole accompanied with the forces applied under the foot appeared on the screen. After activating sensors inside the mat and after following this warm-up stage, the system was ready to use for the actual test. In the calibration process, the volunteer was asked to have full contact with the right foot to activate more sensors and to capture the contact data more appropriately. The tests

were held on different days, and so the device was recalibrated according to the manufacturers' instructions in order to achieve accurate results. Figure 3.3, shows the dynamic screen which is divided to three windows, "a" representing the dynamic image of the force during roll-off of the foot, "b" shows the left foot contacting the pressure mat and "c" showing the right foot contacting the pressure mat.

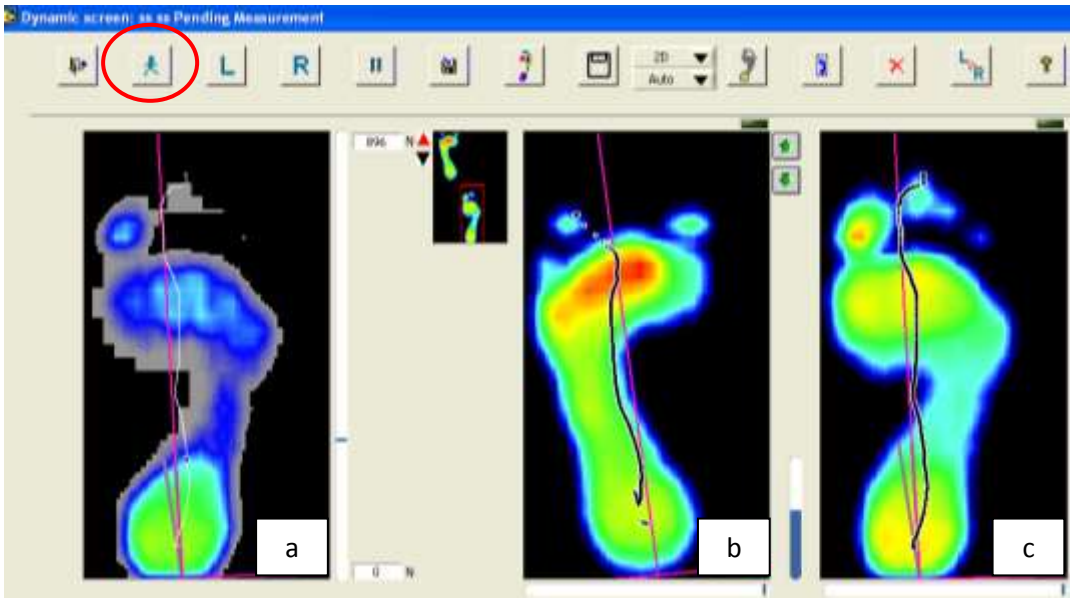

Figure3.3: The right and the left foot touched the mat in one complete gait cycle and the applied force is shown for the different regions of the feet in different colours. a is dynamic image of pressure. b is the left foot force measurement and c is the right foot force measurement.

3.3.4 Recording Applied force Data

3.3.4.1 Static related data

When the static calibration was complete two volunteers one with HV and one without were standing on the pressure mat. Both volunteers were trying to stand in the balance position on the mat while right foot was in contact with the mat. The results will be compared with their FEA modelling results in chapter five.

The pressure that was applied to the ten anatomical regions was recorded and saved the results of plantar pressure distribution is explained in chapter five.

3.3.4.2 Dynamic related data

After the calibration was complete volunteers walked barefoot and naturally, with the right foot stepping onto the mat, so that one complete footprint could be collected. After the foot made contact with the mat, the sensors under the mat started receiving the data related to the forces that applied to the foot and the results indicated the force and pressure distributed under the right foot.

The volunteers in both groups walked at their self-selected and fast speeds. The software divided the foot to the ten anatomical zones including: Toe 1, Toe 2-5, Metatarsal 1, Metatarsal 2, Metatarsal 3, Metatarsal 4, Metatarsal 5, Mid-foot, Heel medial, and Heel lateral. Each groups of sensor inside the mat represent one region of overall 10 as mentioned before the number of sensors is 4096. Figure 3.4 shows these by colour.

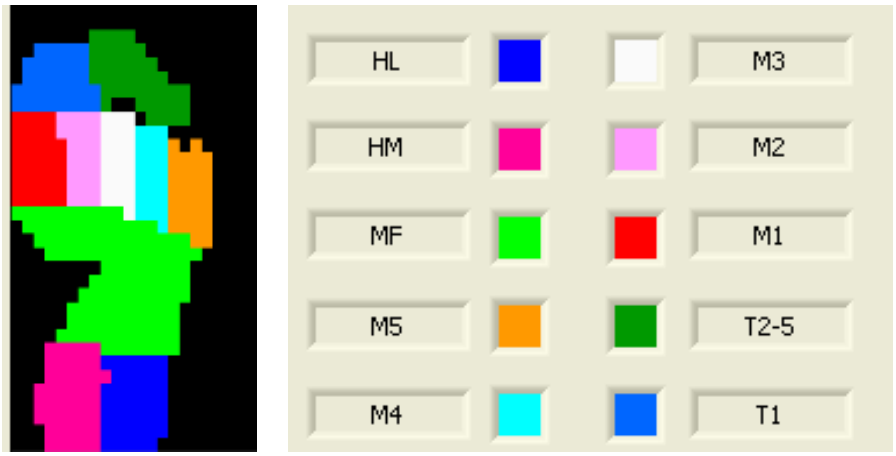

Figure3.4: The zones screen showing the ten anatomical regions in different colours. Key: Toe 1 (T1), Toe 2-5 (T2-5), Metatarsal 1 (M1), Metatarsal 2 (M2), Metatarsal 3 (M3), Metatarsal 4 (M4), Metatarsal 5 (M5), Mid-foot (MF), Heel medial (HM), Heel lateral (HL).

When the right foot of each volunteer made contact with the mat, the data for the forces were obtained by pressing the "Pressure/Forces" button in the zone screen. The graphs obtained indicated the forces and pressures for each anatomical area, recorded in Newton for force and N/cm^2 for pressure as shown in Figures 3.5 and 3.6.

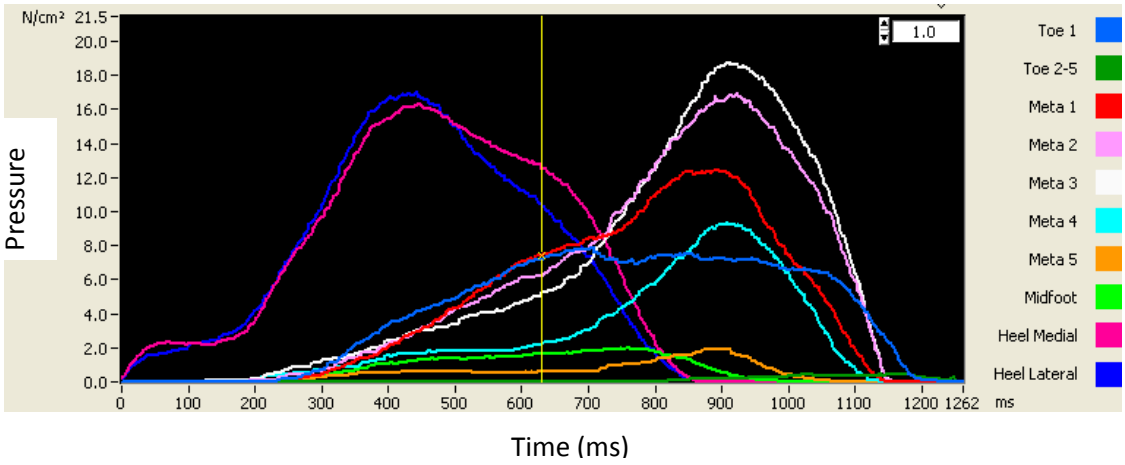

Figure3.5: The pressure distribution under the ten anatomical regions indicated in different colours. The X axis shows the time in ms (milliseconds) and the Y axis presents the pressure (N/cm^2).

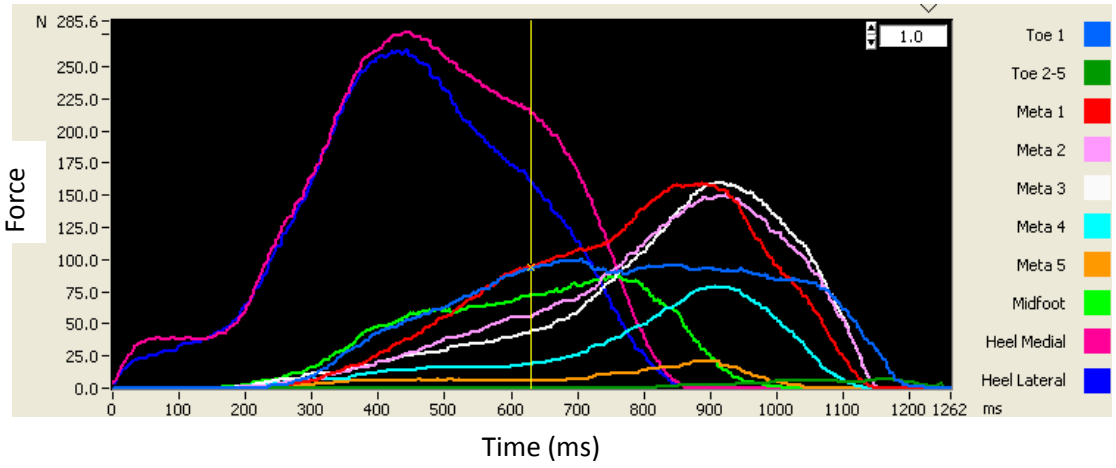

Figure3.6: Force distribution under the ten anatomical regions indicated in different colours. The X axis shows the time in ms (milliseconds) and Y axis presents the force (N).

After recording the force and pressure graphs, the icon directs the user to the "parameter table" that shows all recorded information regarding force. This table covers the following: the "start time" of the contact in milliseconds, the "end time", and the "last contact", i.e the toe-off condition in milliseconds. In addition, the "percentage of contact time", "maximum force", and "pressure" measured, "load rate", which is the speed of loading to the peak value, the "contact area" in cm^2, and lastly, the "max peak" which is the maximum measured pressure.

This software can also measure the heel rotation and foot balance and shows the motion patterns which may be an indication of the patient's low risk regarding injuries (RSscan, 2014).

3.4 Reliability issues of force recorded data

In order to obtain reliable results, a minimum of three trials was needed (Gurney et al., 2008). The variability, consistency and accuracy of the recorded force graphs were important issues that had to be taken into consideration. In order to achieve accurate results, the calibration process for the device was carried out each time before starting the experiment as specified in the company manual. To get similar force graphs for each person the participants were each asked to walk ten times over the pressure mat and each time, their foot had to make contact almost precisely at the centre of the mat. Furthermore, they had to have full contact with the pressure mat while passing over it walking at a steady speed of the foot on pressure mat for about 0.4 - 0.45 milliseconds. Moreover, the same procedure was repeated in faster speed by 20% of their self selected speeds. For instance, if they walked with the range between 0.4 - 0.45 milliseconds in self selected speed, for the fast speed individuals tried to walk with 0.32 – 0.35 milliseconds.

3.5 Methods of analysing force data

In order to diagnose the HV condition by drawing on the force distribution patterns collected from the tests, three methods were employed: comparing the average maximum force in fore-foot region, an Independent sample T-test and Markov Chain Transfer matrices.

These methods of analysis were done for all volunteers and on both speeds.

3.5.1 Comparing the average of maximum force

The average of maximum force that applied to each fore-foot region was calculated. The average of the all trials was obtained, so that for each volunteer, one average number could be used for making a comparison between the two groups to assess whether the average is higher in one group than the other.

This procedure also was done for the fast speed of each volunteer.

3.5.2 Independent Sample T-test

This test is used when comparing the mean scores of two different groups regarding an identified condition. For conducting the test, two variables are needed, one which is categorical and serves as the independent variable (the HV and non-HV groups). The other is the continuous dependent variable, which, in this case, is force. The Independent Sample T-test outcome indicates whether there is a statistically significant difference in the mean profile between the groups (Pallant, 2005). The T-test algorithms can be found in appendix D. When the sample size is small, this method of analysis is an appropriate measure of statistical significance. The probability value is a agreement in statistics in which when two groups of data is going to be compared it can be used. This value is defined as 0.05, if the results of comparison between two groups of data obtain more than this value, groups are not significantly different and if the obtained value is less or equal to 0.05 the groups are significantly different. This number called as "*p*" value showing that there is just a 5% probability of the data being similar and 95% probability that they are significantly different in their mean profiles. To investigate the force magnitude differences under the fore-foot region in both groups, this test was carried out using the software "IBM SPSS statistics DATA Editor". This software package has two views into which data is imported. The first view is labelled the "Data View" and in this all the force related data was imported. The other view is the "Variable View" in which the different variables were defined. (More information on this is given in appendix D).

For comparing the same regions in both groups of volunteers, the "Measure" of the variables were entered under three different categories: scale, nominal and ordinal. Depending on the data that were being compared, one of these categories was chosen. The HV group named as group number 1 and the non-HV as group number 2. In the "Data View" when all the force data relating to both groups were imported into the first column, the group numbers entered in the second column. After importing all the data related to both the groups, the Independent Sample T-test was carried out by accessing the "Analyse" tool bar and then the option "Compare

Means". The results of comparison between the groups appeared and presented all the significant differences regarding the areas of the foot. The comparison was made for seven regions of the fore-foot: toe 1, toes 2-5, and metatarsals 1 to 5 for both speeds.

3.5.2.1 Markov Transfer matrix

The force is transferring through the foot while it is in contact with the ground, the force pattern under the foot can be obtained from the pressure measurement devices as shown in Figure 2.6. These devices can measure the amount of forces and pressures that apply to different foot regions and in different time sequences. In order to investigate the effect of different foot regions on each other due to the force transformation, Markovian chain transfer matrices can be used to see whether there is any force transformation between fore-foot regions. As it is shown in Figure 3.1, by looking at the foot force pattern graphs, it is obvious that the peak forces are transferring from heel to the metatarsal regions, therefore it can be concluded that it should be possible to measure this transformation.

When looking at how the peak forces transferring from one region to another in the plantar force distribution graphs, there should be a way to measure these changes.

Time is one of the important issues in measuring force transfer from one state to another in one specific location of the foot.

The dynamic of the human body is changing over the time and the load is decreasing in some regions and increasing in other regions. Figure 3.7, shows that the centre of pressure is moving from the heel towards the big toe which means the maximum load moves from the heel towards big toe under one path as shown in the same figure. It should be considered that the centre of force trajectory does not move in just one path as shown in Figure 3.7, because the maximum loads under the fore-foot bear by 2^{nd}, 3^{rd} and 1^{st} metatarsal heads which means the force is transferring from that path to other fore-foot regions where the maximum force received by those metatarsals. Regarding the fore-foot position the amount of force receives by metatarsals differs in different time steps in the last stance phase so while the 2^{nd} and 3^{rd} metatarsals receiving the higher ground reaction force the rest of metatarsals

receiving less force as another time steps because of the foot dynamics. This can be explained as transformation of the maximum force through metatarsal regions in different time steps.

Force is transferring along the foot when the foot makes a first contact with the ground and then it transfers from the heel and then mid-foot and finally to the fore-foot. When the heel is unloaded the load moves forward and fore-foot bears the highest load. Time is the factor that is engaged with the transfer of maximum force from the initial contact to the toe-off position. The force would not remain unchanged under the foot while walking. The idea of using Markov Chain transfer matrices came from the centre of force trajectory under the foot when the dynamic of the foot is changing through the time sequences.

Figure 3.7, shows the schematic of the maximum force trajectory that moves from the heel region towards the toes, the red circles on the foot presents each metatarsal and the black line in the middle of them shows that the force is going to be measured in the same line but in different time steps. When the force moves from the heel towards the toes, it changes through the time. When the position of the foot changes, the force moves from one region towards another and the magnitude may decrease or increase.

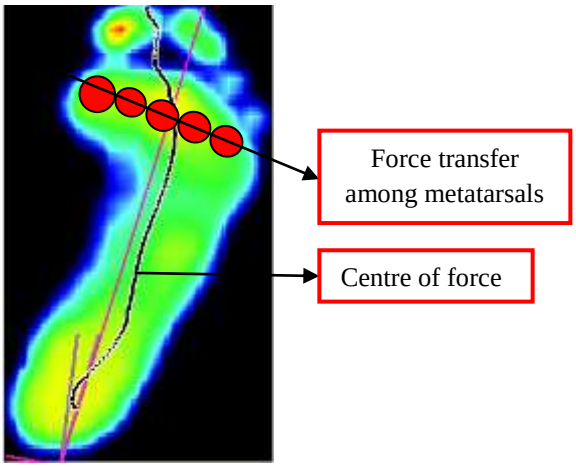

Figure3.7: Schematic of the metatarsals' locations and the centre of force which is moving along the foot.

Markov chain shows the changes of the state of the system which are called transitions, and the probabilities associated with various state-changes are called

transition probabilities. The set of all states and transition probabilities completely characterises a Markov chain (Dodge, 2003).

The foot plantar force distribution pattern was measured in all volunteers from the force recorded raw data in five regions of the foot from metatarsal 1 to 5.

The force data were normalised against weight of each volunteer. More information regarding Markov Chain transition matrices is given in chapter four.

3.6 The Motion Capture system

During walking cycle in barefoot condition the toes spreading away especially, when the metatarsals are in contact with the ground in mid-stance condition. This condition is shown in Figure 2.5. While wearing shoes the movements of the toes would be restricted depending on the shoe type if it is flexible or rigid. There is a cyclic separation between metatarsals while walking and the shoe can restrict this cyclic separation but in bare foot walking they can separate naturally. In people who have HV the lateral deviation of the 1^{st} metatarsal head is larger compared to non-HV people. It means that the distance between the 1^{st} and 2^{nd} metatarsal heads is bigger in HV group compared to non-HV individuals. Furthermore, HV is associated with hypermobility of joint especially in women, it means that the movement of the foot joints in females is higher compared to men. Moreover, HV people have higher range of motion in the 1^{st} ray compared to men. Joint hypermobility is one of the causes of HV according to Lower & Wukish, (2009). Also the foot bones in women have more potential to move in adduction direction . This gives the idea of measuring the flexibility of the 1^{st} metatarsal joint in people as an indicator of HV existence.

In order to investigate whether the separation between these two joints can be used as an indicator of HV's existence, the Motion Capture experiment was carried out.

To measure the lateral flexibility of the 1^{st} metatarsal joint, the Motion Capture system was used to see whether HV patients have more movements in this location compared to the non-HV individuals. The aim of the experiment was to establish lateral flexibility as an indication of HV.

Motion Capture is the process of recording the movement of the volunteers who walked in front of seven cameras with markers stuck on the 1st and 2nd metatarsal heads of their right foot as shown in Figure 3.13. When using the system, each time calibration was very important before starting the test because the distance between the two markers was very small and rigorous calibration helped the cameras to capture the movement with minimal error.

3.7 Experimental set up for measurement of joint lateral flexibility by the Motion Capture cameras

The test was set up in the Motion Capture laboratory in Brunel University and the procedure for executing it was approved by the ethics committee. To measure the related movements between the 1st and 2nd metatarsal joints, the facilities in the laboratory comprising the seven Vicon cameras (model 141RC Manfrotto), and the software Vicon Bladder 1.7 were used. The setup for this test involved calibrating the cameras to capture the movement and preparing the volunteers to walk naturally at their own self-selected speed. The goal of calibration is to minimise any measurement uncertainty by ensuring the accuracy of cameras. Calibration quantifies and controls errors or uncertainties within measurement processes to an acceptable level.

The environment of the Motion Capture lab is presented in Figure 3.8, also the way that volunteers walk between defined points on the floor is also presented in the same figure.

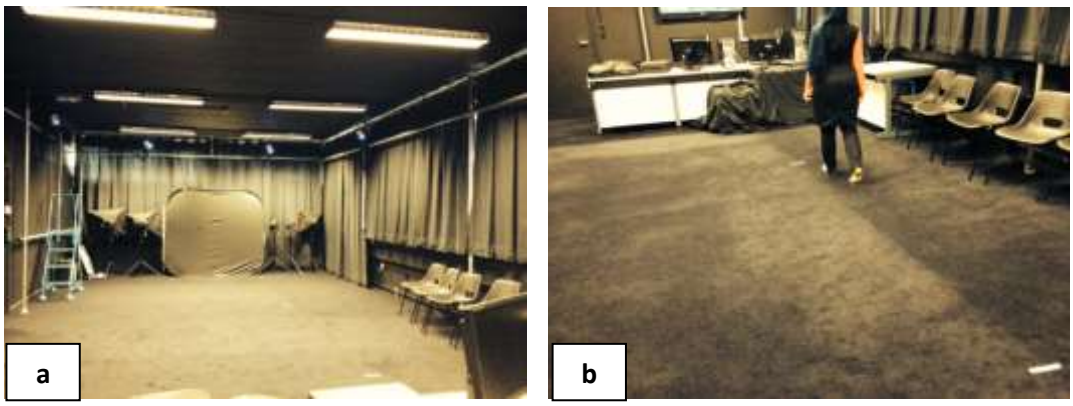

Figure3.8: (a) The Motion Capture lab environment, (b) the walking procedure with the markers stuck on the right foot between the defined points on the floor

Each participant's walking movements were captured through the seven Vicon cameras available in the laboratory, the locations of which are shown in Figure 3.8(a), and 3.10.

3.8 Calibration

In the calibration process, the first action is to switch on the device and then launch the "Vicon blade" software. By clicking on the "Connect" all cameras were switched on as shown in Figure3.9.

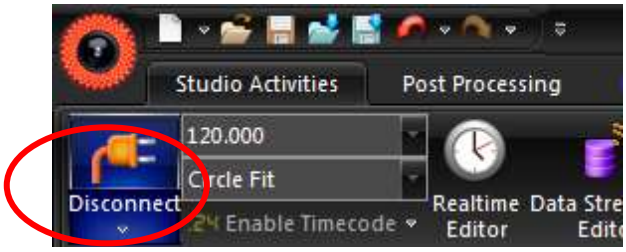

Figure3.9: The connect option after it is clicked and turned to the Disconnect position

3.8.1 Camera hardware reset

Figure 3.10, shows that the seven cameras were connected to the computer and all appear on the main page of the software.

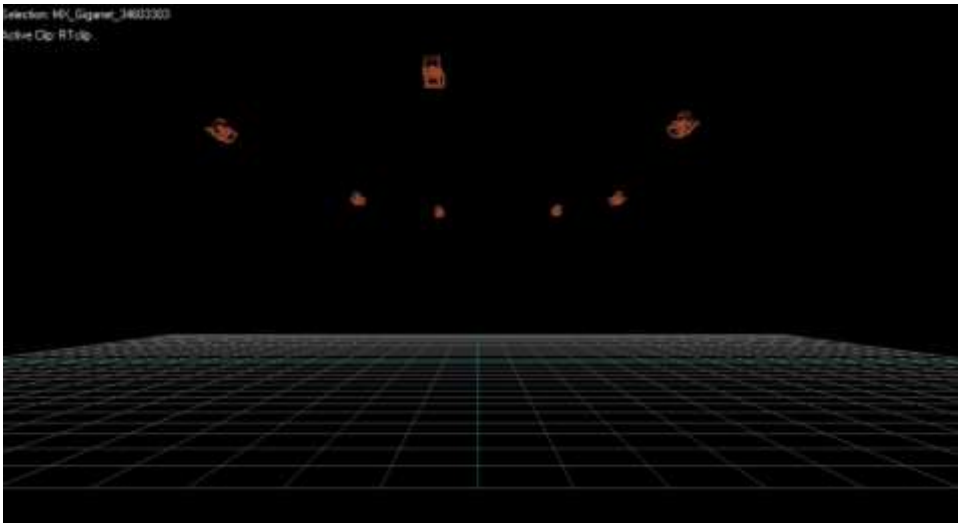

Figure3.10: All cameras present in the 3D space and located in their original positions

Next the “Hardware” icon on the main toolbar was clicked to let the cameras have a better view of the markers in the space and to improve the quality of the recorded data by having a minimum of noise in the space. In order to achieve the best recording quality, the “Camera Setting Attributes” need to be implemented according to the software manual, see table 3-1. These values should be checked before each test because they may affect camera sensitivity levels.

Table3-1: Good default ranges for the camera hardware settings and their related colours

Strobe Intensity (red)	1
Threshold (yellow)	0.2-0.5
Gain (white)	1
Circularity (green)	0.4-0.5

These defaults are defined as the best for the camera setting hardware by the manufacturer with Figure 3.11, showing the location of the hardware setting for cameras with each presented by a different colour.

Figure3.11: The views of the seven cameras. The bar graphs beside each camera represent the hardware setting attributes. Key: red represents strobe intensity, yellow shows threshold, gain shows white and circularity shows green.

3.8.2 3D space calibration

The next step is the 3D space calibration process which is performed with the five marker T-shaped wand. To achieve this, the wand was moved in all directions in front of all cameras and as the wand was waved up and down it defined the maximum 3D space area. This was shown in the view of each camera and when each view was filled with colours, it meant that the cameras could capture all the movements of the wand in the space, as shown in Figure 3.12.

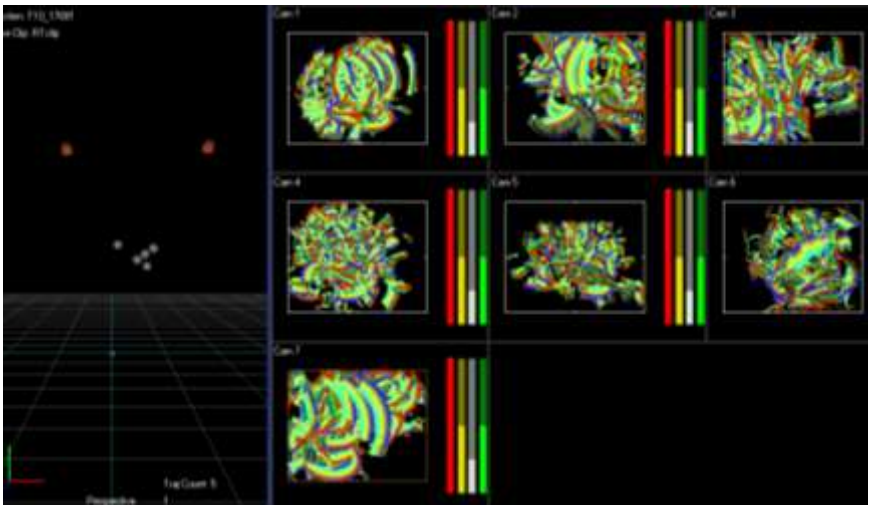

Figure3.12: 3D space definition achieved by moving the wand around in the space

As shown in Figure 3.12, all the views of cameras were filled with colours. Thus, it could be taken that the cameras could capture every wand movement in any direction. In the same figure, (left hand side) the five markers over the wand are shown in the room space. After the researcher moved around the room with the wand and pressed "Stop Wand Wave" the software presented the calibration status, as "bad", "good", "excellent", or "awesome". For this project, the status of the calibration for every test was recorded as "awesome".

3.8.3 Origin calibration

The wand was located in the middle of the room on the floor to define the floor and at this stage, all the cameras were shown as being above the floor as they were located in their original locations.

3.8.4 Floor plan calibration

Five markers were placed over the wand. These markers had to touch the floor plan on the screen in order to define the floor.

3.8.5 Saving calibration

After floor plan calibration, the calibration parameters should be "saved" in case the software crashes.

3.9 Markers size selection

After calibration, suitable markers had to be chosen. There were three available sizes: diameters of 3mm, 6.35mm and 9.5mm (Vicon, 2014). As the markers were to be located on the head of metatarsal joints 1 and 2, each was very close to the other, and so the 6.35mm diameter ones were chosen for this test because of the availability of this size of the markers in the laboratory.

3.10 Preparation for capturing the motion

The volunteers (those with and without HV) participating in this experiment had two markers stuck on the heads of their metatarsals 1 and 2, as shown in Figure 3.13. All the data that was going to be captured was expected to be logged in the "Data Management" file available in the program's main tool bar. Before capturing the motion of the markers this file had to be made.

Figure3.13: Positions of markers on the right foot.

The markers were attached to the bare skin of the individuals by a blue tag in order not to create any movement restrictions while walking. The uses of adhesives such as cello tape are therefore not suitable for fixing the markers to the skin. The volunteers were asked to walk three metres to become familiar with the test process before the actual test. They undertook this three times, walking between the defined start and end points.

3.11 Capturing 1st and the 2nd metatarsal joints motion

Individuals were asked to stop and wait behind the start point. They were requested to say "start" when they began walking, and say "stop" when passing the end point. Thus, the start button of the capture menu was pressed and released according to the volunteer's prompts.

For the experiment, two points were defined on the floor for participants to walk between. The distance that they walked was three metres. The cameras could capture the motion with the least errors in this part of the room and they had the best view of the markers. When the participants were ready to walk, the "Start" button had to be pressed to start recording the related movement data. The "Start" button was pressed when the participant said "start" and when they passed the end point, as marked on the floor, he/she said "stop" and the "Stop" button on the screen was pressed by the operator. This process was carried out in this way because the room was so dark that the operator could not see the marked points on the floor and so could not press the buttons at the appropriate times. Successful trials were achieved from each volunteer, with ten HV patients and ten without HV participants. In all cases, the relative movement between the two markers stuck on the right foot of each person was analysed. The data sheet exported from the software contained the following information: the first column was for the frame count, the second column was for the time from the start of the walking phase to the end. In addition, the following three sets of columns x, y, z contained the coordinate data for each marker. The row data relating to the x, y, and z coordinates is presented in Appendix C.

Volunteers walked at their self-selected speed between the defined distance, barefoot, and the cameras captured the relative movements between 1st and 2nd metatarsal joints. Each participant walked ten times between the defined points, and for each, ten trials were recorded. The total of ten, trials was selected from each individual for further analysis regarding comparing the control and HV groups.

During the walking procedure, the researcher who was controlling the view of the markers on the computer screen had constantly to look out for the markers, as view of the markers could be lost while one foot was blocking the other, or when the markers were flashing. When markers disappeared or were flashing, it meant that there was no collection of the data taking place at that moment. When this happened, the volunteers were asked to walk again so that all the data was recorded. This procedure was repeated as necessary because a complete walking phase without any missing data was required for a robust trial.

3.12 Saving and exporting data

After capturing the movements, the data was exported to a spreadsheet. To see the movement of the markers in the 3D space, it is necessary to construct the data by multiple trials (ten trials were taken for each person), otherwise they are not readable by the Excel software. To save the data, under the "Data Management" toolbar, first the "Raw Data" is clicked. Then the "Pipeline" icon selected and then "Reconstruct" button chosen. Through this procedure the whole movement of the markers, frame by frame in the 3D space, became visible.

The raw data showed two markers with the coordinates of x, y, z for each one. Hence the number of frames is dependent on walking speed. It was noted that the number of frames, trial to trial and across the individual participants were different. The saved data were exported as a "trc" file that could be opened in Excel as a spreadsheet. When "trc" file was copied and pasted to the Excel sheet, the data was translated in the form of x, y, z coordinates for each marker. Then the ratio of changes between markers was obtained from Equation (4.3) and the comparison was made according to the ratio of changes (more explanation in chapter four).

3.13 Methods of measuring joint movement

For investigation of the flexibility between 1st and 2nd metatarsal joints after exporting the data to the Excel sheet, the coordinate (x, y, z) of each marker was gained. When "trc" file was copied and pasted in Excel sheet, the data was translated as x, y, z coordinates for each marker.

The distance between two markers (1 and 2) is obtained from the Euclidean Equation (3.1) and the ratio of changes was measured according to Equation (4.1).

$$|\boldsymbol{x}_2 - \boldsymbol{x}_1| = \sqrt{(x_2 - x_1)^2 + (y_2 - y_1)^2 + (z_2 - z_1)^2} \qquad (3.1)$$

When $|\boldsymbol{x}_2 - \boldsymbol{x}_1|$ presents the distance between the two markers while walking and (x_2, y_2, z_2) presents the location of the marker placed on the 2nd metatarsal head. Also (x_1, y_1, z_1) presents the location of the markers stuck on the 1st metatarsal head.

3.14 Measure of reliability of the results

The volunteers were asked to walk between start and the end points marked on the floor, three times before the actual test so as to become steady while walking the course during the trials. Their walking speed did not have an effect on the results, because the aim of doing this experiment was to measure the distance and the ratio between the two markers that had been stuck to their bare feet. However, the way in which they walked was an issue. To assure the reliability of recorded data, two markers were stuck on the two ends of the 20 cm ruler (18cm between the centres of the markers), and then after the calibration was finished the capturing the motion was started by moving around the room with the ruler.

This was done in order to compare the distance between markers placed on the ruler with the distances obtained from the captured data. After analysing the data and calculating the distance between them on Motion Capture data it was achieved that the distance captured by cameras was 18.104. This can be an indicator of reliability of the captured data.

It should be mentioned that the location of the cameras never changed during the process of experiment in different days after the best location of the room for capturing the markers' motion were recognised.

Another issue was obtaining the consistent graphs that were comparable, so each individual walked ten times between the defined points, and on each occasion, if the markers were lost or were flashing (became invisible), the trial was repeated. This was necessary because each time that the markers were lost or began flashing the data related to that specific time was missed. The distance between the two markers for all the volunteers measure by ruler, when in the standing position to see whether the data was reliable. The distance between the two centres of the markers was obtained by hand and compared with the captured data regarding the x, y, and z coordinates in the standing position. This way it was checked that both numbers, the one measured by ruler and the other captured by camera, were almost the same.

3.15 Error estimation of the devices used in this project

The RSscan device has 10% error estimation according to the company manual. The Motion Capture device reported to have a sub millimetre error. In Motion Capture the lowest distance between the markers was measured not less than 30 mm so sub millimetre error did not have an effect on the final results.

3.16 Conclusion

Previous studies have been studied the pressure pattern distribution under the foot with and without deformities also they tried to find out the changes in pressure distribution when any deformity happens to the foot.

In this study different methods were used to find out the force pattern under the foot with and without HV to see whether the force pattern can be an indication of the HV condition. Furthermore, another method was measuring the fluctuation between metatarsal 1 and 2 joints to recognise HV patients from those without any deformity.

There is a need to examine whether the force transformation under the fore-foot region can be an indicator of the diagnosis of HV.

The methods that are used in this project to analyse force pattern under the foot can help the researchers and surgeons to have better understanding of foot biomechanics. Furthermore, it is first time to use the Markovian chain transfer matrices to measure the transfer coefficient from one region of the foot to another.

Plantar force and joint lateral flexibility measurements' results and discussions

4.1 Introduction

This chapter is going to present the results obtained from the two devices used to establish a pattern out of force data under the foot in people with and without HV deformity. The process of using the devices was explained in chapter three. This experiment was done to establish the pattern of plantar force distribution in HV patients when comparing this with the pattern for non-HV individuals. More specifically, the focus in this chapter is on comparing the force transformation among the five metatarsals to see if the pattern of force transfers among HV patients differs from that in non-HV group and whether this can be an indicator of HV disease. It is expected that the pattern obtained from the transfer matrices results will provide an indicator for recognising the condition.

The second experiment was based on measuring the lateral flexibility of the 1st metatarsal joint to see if the level of flexibility of the joint can be used as an indication of the HV condition. In sum, both experiments (RSscan and Motion Capture) were executed in order to investigate any indication of the existence of HV based on the emergent pattern differences. The methods for the analysis of the plantar force pattern in HV and non-HV individuals were captured for both self-selected and fast speed walking.

4.2 Experiments

As discussed in chapter three, two types of experiments were conducted using:

1) The foot scan device and,

2) The Motion Capture system.

4.3 RSscan device

The comparison of the foot force pattern data collected from using the foot scan device with the HV and non HV groups is presented. The reliability of the force distribution graphs has been checked by analysing this in different trials conducted

for each person. The fore-foot region is the main area for comparing the mean with an Independent Sample T-test carried out to see significant differences in force magnitude in fore-foot region among both groups. Furthermore, a comparison was made of individuals' transfer coefficients among the metatarsal bones using Markovian chain transfer matrices.

Details of the experimental set up were discussed in chapter three.

4.4 Motion Capture system

The data collected by the Motion Capture system is collected according to the distances and the ratio measured between two markers located on the 1st and 2nd metatarsal head joints while the individual is walking.

Fluctuations regarding the ratio are studied as an indicator of lateral laxity of the 1st metatarsal joint. For the HV group, this investigation of the lateral flexibility of the 1st metatarsal joint enables to see if this can be an indication of the disease.

4.5 Methods of Analysis

As explained in chapter three, in this study in order to recognise the HV condition two methods were employed.

- The first method is based on the plantar force pattern.

This was measured using the RSscan. This device collects force for anatomical regions as a function of time. The force measurement can then be calculated in terms of function of time to function of foot length, where the foot length is taken to be 100 units. The contact force is normalised to volunteers' body weight. The normalised force data enables comparison of results collected from different individuals walking at different speeds, even though great care is taken to ensure similar walking speeds.

- The second method is based on measuring metatarsal joint laxity.

Lateral laxity (flexibility), as will be explained later, has not been considered suitable for recognising HV in its early stages whereas the force pattern has been found to be effective in recognising the HV condition. Three methods of analysis were

developed. The first one was to compare averages of maximum force applied on the fore-foot region. The second one was the transition matrix, which is a form of Markov chain transfer matrix. The third was Euclidean distances and the ratio of changes measured between 1st and 2nd metatarsal joints. All the methods were done on both self-selected and fast speed.

1) Comparison of average of maximum force applied in fore-foot region

The maximum force that applied in every region in the fore-foot area in all trials was obtained, then the average of those calculated and the comparison in HV and non-HV groups was done to see whether the HV patients bear the higher force compared to non-HV participants. Then Independent Sample T-test was carried out to see whether the forces that applied on the fore-foot region of both groups of volunteers are significantly different. Self-selected speed results were compared with the fast speed results.

2) Markov Chain / transition matrix

It is assured that force pattern measured at step e+1 is related to force pattern measured at step t. Again it is assured that the transition matrix relating patterns at e+1 is stationary as function of foot force position. The force data used for this analysis was the last 20% of the recorded force readings because there were recorded force readings in metatarsal regions while they were in contact with the pressure mat. This represents the force readings while the fore-foot is in contact and loaded. And that, this pattern can therefore, be used as a feature or at least has potential to be used a feature.

3) Lateral laxity of 1st metatarsal joint measurement

The lateral laxity method is based on measuring the variation of the distance between the two markers placed on the 1st and 2nd metatarsal heads. The motion of the two points and the distance between them is recorded as a function of the walking cycle. The distance between two markers $(x_1, y_{1,} z_1)_e$ and $(x_2, y_{2,} z_2)_e$,this is defined in the equation (3.1).

Where "r" is the ratio of change between the two markers to its initial distance. $|x_2 - x_1|_0$ is the initial distance between the two markers before starting to walk and $|x_2 - x_1|$ describes the movement between the markers while walking. The ratio is given in Equation 4.1.

$$r = \frac{|\boldsymbol{x}_2 - \boldsymbol{x}_1|_{max} - |\boldsymbol{x}_2 - \boldsymbol{x}_1|_{min}}{|\boldsymbol{x}_2 - \boldsymbol{x}_1|_{min}} \tag{4.1}$$

4.6 Results on foot force pattern by RSscan data on self-selected speed

The two methods of analysis as explained before (compare the average of maximum force/ Markov Chain transfer matrix) were used to analyse the plantar force pattern between the two groups of volunteers, with self–selected and fast speed walking subsequently, the comparison of results was carried out between the groups.

4.6.1 Comparing the average of maximum force applied to the fore-foot regions

The RSscan device collected data for each volunteer's full contact of the right foot with the force mat, when they walked at a self-selected speed. The aim of the experiment was to compare the maximum force applied on the fore-foot regions in HV and non-HV volunteers.

In all, the volunteers' force graphs, the total frames recorded while walking were normalized to 100 frames and the force data in the Y axis normalised to that person's body weight. In Figure 4.1, each graph shows dimensionless force in the Y axis against normalized frames in the X axis.

The chosen trials for one individual from the HV group and for one individual from the control group are presented in Figures 4.1, and 4.2. Furthermore, the purpose of selecting three trials all belonging to one individual, with one subject taken from each group, was to assure the similarity of the graphs. In total, 200 trials were obtained, that is, ten trials for each of the twenty volunteers for self-selected speed.

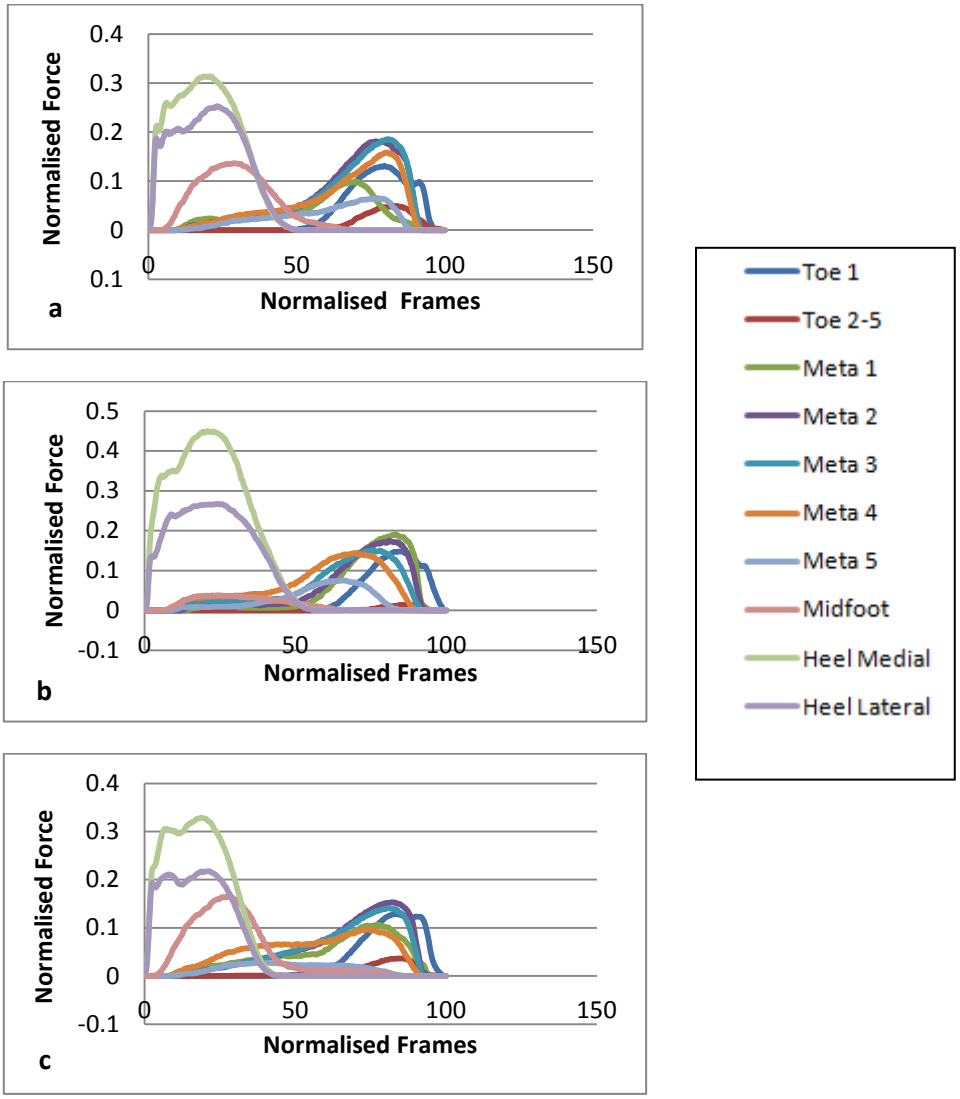

Figure4.1: Three sample trials showing the force in anatomical regions of the foot against normalised frames in a patient with HV. The highest force under the fore-foot is under the 3rd, 2nd metatarsal heads.

In order that the groups were comparable, the validity of the trials was assured by obtaining trials from each volunteer and by comparing the force magnitude in different regions of the foot for all these trials. After familiarisation with the test process, the volunteers gradually became consistent in their walking speed. Additionally, a trial to make sure that there was full valid contact with the pressure mat was required. It was checked that their speed remained unchanged within ±5% in all the trials. By taking these measures, consistency in speed was gained and the comparison between each trial regarding the force magnitude for each person became reliable.

As presented in Figures 4.1, and 4.2, in all the graphs the higher force is under the 3rd and 2nd metatarsal bones. All volunteers had a steady speed while walking and differences in the force graphs can be seen but this does not change the overall results when making the maximum force comparisons between the two groups (HV and non-HV). All the data presented in the graphs in Figure 4.1, was collected from a male volunteer and it can be seen that the highest force is applied on the mid-foot part. According to previously published works, HV is associated with flat feet in men, and this patient develops flat feet as well as HV, because HV causes the collapse of the transverse arch (Nguyen et al., 2010).

In Figures 4.1, and 4.2, it appears in all the graphs that, while the fore-foot area has contact with the mat in the heel off position, there is still distribution of force in the heel region, while the force is transferring towards the fore-foot. This means that even when the fore-foot is in contact with the mat, the force is distributing under the heel.

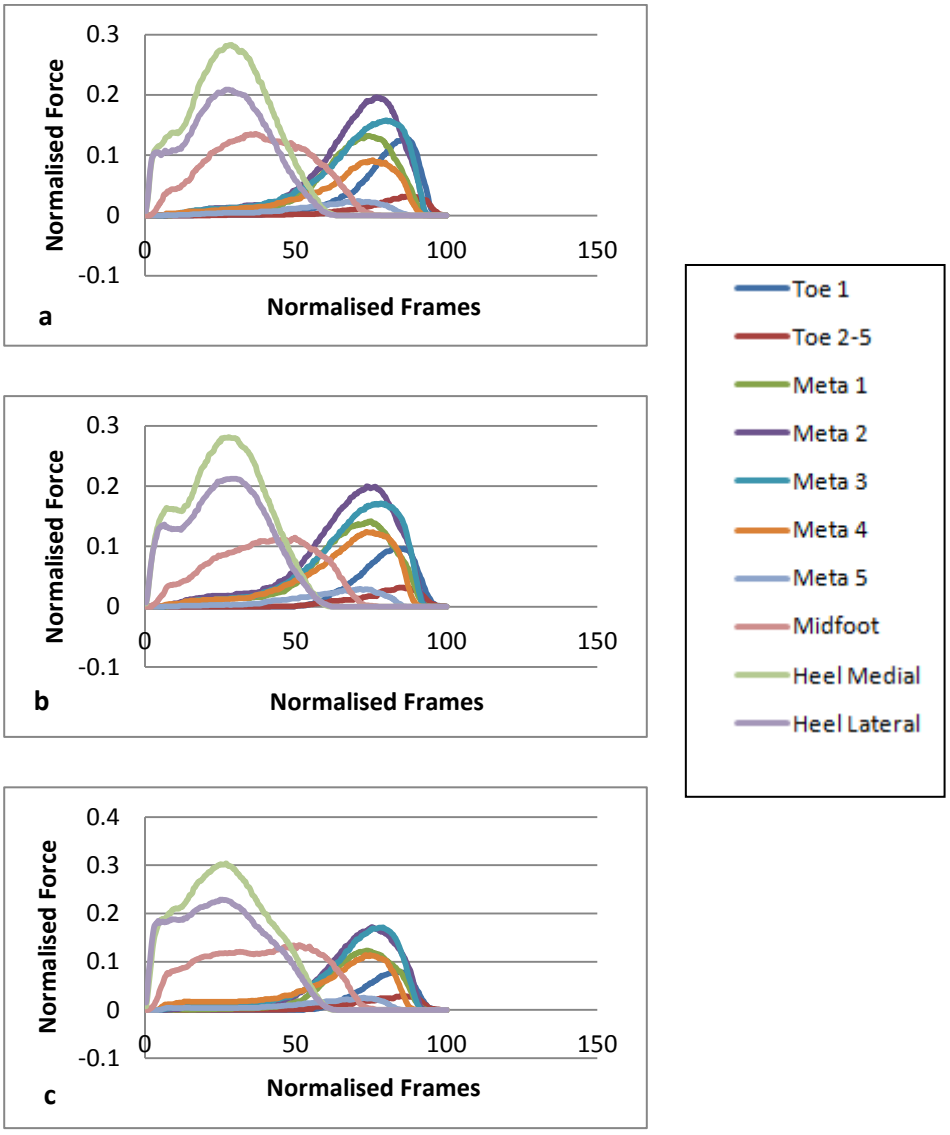

Figure4.2: Three sample trials, force in ten anatomical regions of the foot against normalised frames in a non-HV volunteer shows that the highest force in fore-foot in under metatarsals 2nd , 3rd following by 1st metatarsal heads.

As shown in the Figure 4.2, relating to the non-HV individual, the 2nd and 3rd metatarsals followed by the 1st are bearing the most force in the fore-foot region, ranging from frame 60 to frame 90. Figure 4.3, shows the maximum force distributed in the fore-foot regions of the foot. The force presented is normalised by individuals' body weights. For each region and for each person the maximum normalised force is obtained, and the average of the maximum is calculated, for both HV and non-HV individuals. Figure 4.3, shows the comparison between the groups indicating the averages of the maximum force. After comparing each foot region in the HV and non-HV groups, it emerges that the force under the 1st, 2nd and the 3rd metatarsals in the HV group is higher than that for the control group. Moreover, the

maximum force under the 3rd metatarsal head shows that this is bearing the highest amount of force, as compared to other fore-foot regions, for both groups.

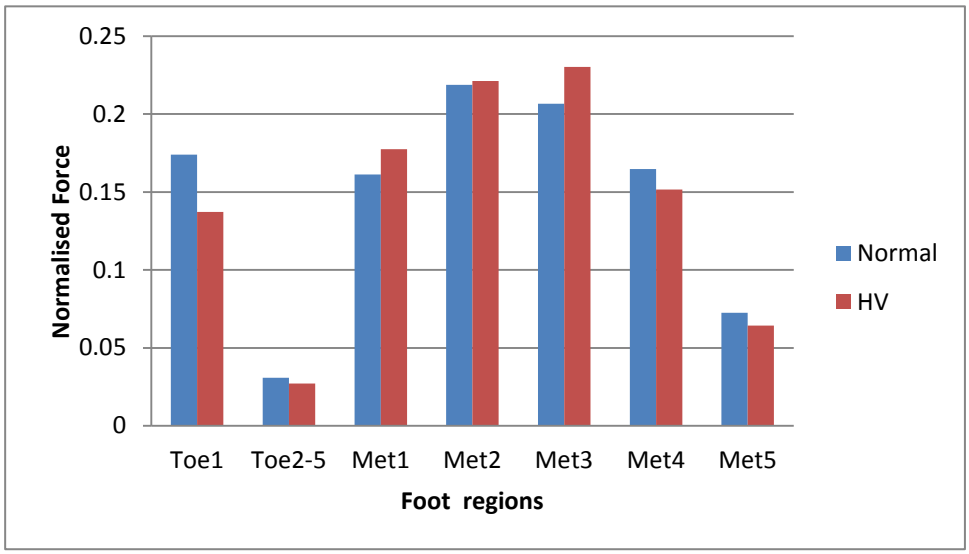

Figure 4.3: Comparison of Average of Maximum force distributed in fore-foot areas in HV and control group, metatarsal 1, 2 and 3 show to bear higher force compared to non-HV individuals in self-selected speed

In the control group, the higher force is under toe 1, toes 2-5, metatarsals 4 and 5. As shown in Figure 4.3, in both groups, toes 2-5 appear to be almost the same in respect of the force bearing condition. The magnitude of the force in this region is precisely less than the other regions in the fore-foot area. This means that metatarsals 1 to 3 are highly loaded in both groups. Following these metatarsals, toe 1 bears a higher load compared to the other regions.

Many published papers have studied the plantar pressure pattern and many of them reported the same results as those obtained in this study. For example, (Wen et al., 2012) discovered that the loading under the 2nd and 3rd metatarsal bones were higher in HV patients compared to subjects without HV. In another study, Plank, 1995, investigated the pressure pattern under the foot in patients with HV and found that the most loading was under the 3rd, 2nd followed by the 1st metatarsal bones. There is some variation among some previous findings, such as those of (Nova et al., 2010), who reported that higher loading was under the big toe, 1st, 3rd and 2nd metatarsal bones in patients with HV and under the 3rd, 2nd and 1st in the control group.

4.6.2 Independent Sample T-test:

The data from the volunteers in each group (HV and non-HV) were compared to see whether their applied forces on the fore-foot area differed. The Independent Sample T-test used in order to achieve mean differences between the groups. When the number of participants is less than thirty, T-test analysis is appropriate for comparing means and for presenting the significant differences between groups. This test can be used when the variables are independent, and in this case, these are two groups of volunteers, those with HV and those without HV, which satisfies this condition.

All the force data relating to one region of the foot was imported and comprised approximately 300 frames for an HV patient. This means that approximately 6000 force data was imported to the first column of the software which was belong to all volunteers HV and non-HV and this was done for each region of the fore-foot. The sample of the "data view" in SPSS is enclosed in appendix D.

After completing the data importing, the analysis was conducted. By accessing the toolbar, the comparing means icon and eventually clicking on the Independent Sample T-test option, the process was completed for all fore-foot regions which covered: Toe1, Toe2-5, Metatarsal 1, Metatarsal 2, Metatarsal 3, Metatarsal 4, and Metatarsal 5. A comparison between the HV and non-HV groups was made to see whether the force pattern was different between them. The results were obtained from the software along with the statistical significance ($p \leq 0.05$). See Table 4-1, below.

Table4-1: Comparison of the mean differences in HV and non-HV groups for self-selected speed achieved by independent sample T-test in which in all regions except toe2-5 and 2nd metatarsal have a significant difference, as $p < 0.05$.

Fore-foot regions	*P* Value
Toe1	0.013
Toe2-5	0.197
Metatarsal 1	0.001
Metatarsal 2	0.142
Metatarsal 3	0.001
Metatarsal 4	0.001
Metatarsal 5	0.001

The results indicate that there is a significant difference in the "equality of means", where $p \leq 0.05$, for all fore-foot regions, except for toe2-5 and the 2nd metatarsal, for which no significant difference was observed. This may be interpreted as indicating that the forces applied on the regions other than these exceptions in the HV group are totally different when compared to the force applied on the same region in the control group.

4.6.3 Comparing transfer force under five metatarsals in self-selected speed

When force is transferring along the foot, from the initial heel contact with the ground to the toe-off position, the ground reaction force is moving alongside. When using the RSscan device, the foot is divided into ten anatomical regions and the force applying to these regions is measured as a function of time, with the results showing the magnitude of the force in each area with respect to time. That is, as time changes, the foot position changes and the force readings differ accordingly.

The force transformation relationship given by Markov matrix, from one region to another in the fore-foot and for all the metatarsals was established by developing a code in Matlab R2010b software. This was then used to investigate the transformation of the force among these regions of the foot in the control and HV groups, when the volunteers walked at self-selected and fast speed and with the foot making full contact with the pressure mat. While walking, the force distributed along the foot and the force state on each area changes with the movement of the foot. In order to find out how much is the effect of one region of the foot on another in different time sequences, Markovian transition matrices are used. To calculate the probability ratio of transferring force along the five metatarsals, the code for the transition matrices was written (The code is available in appendix B).

Subsequently, to gauge how the forces are transferring, two matrices have been made from the normalised forces and frames data for each participant: matrix **A** and matrix **B**. These matrices have been calculated according to following equations.

Vector $\mathbf{x}_e$ represents five force readings at time e, this may be written as:

$$\mathbf{x}_e = \begin{Bmatrix} x_1 \\ x_2 \\ x_3 \\ x_4 \\ x_5 \end{Bmatrix}_e \tag{4.2}$$

Each element of the matrix in Equation (4.3) represents one metatarsal in time step "*e*" and $\boldsymbol{x}$ represents the metatarsals force vector.

The first row of the matrix is the force applying to the five metatarsals in time "e" and the second row shows the force applied to the same region in "e+1", first matrix A was achieved and then the second matrix B was gained by one shift of the time from the matrix A shown in Equation 4.4.

$$\begin{bmatrix} x_1 \\ x_2 \\ x_3 \\ x_4 \\ x_5 \end{bmatrix}_{e+1} = \begin{bmatrix} T_{11} & T_{12} & T_{13} & T_{14} & T_{15} \\ T_{21} & T_{22} & T_{23} & T_{24} & T_{25} \\ T_{31} & T_{32} & T_{33} & T_{34} & T_{35} \\ T_{41} & T_{42} & T_{43} & T_{44} & T_{45} \\ T_{51} & T_{52} & T_{53} & T_{54} & T_{55} \end{bmatrix} \begin{bmatrix} x_1 \\ x_2 \\ x_3 \\ x_4 \\ x_5 \end{bmatrix}_e \tag{4.3}$$

According to equation (4.4), matrix T presents the transition between the forces on metatarsals at state *e* and *e*+1.

To solve the matrix T vector **A** and **B** should become in the matrix form in order to solve the 25 unknown elements of matrix **T.** Then these vectors changed to matrix **A** and **B** as follows:

$$\begin{bmatrix} x_1 \\ x_2 \\ x_3 \\ x_4 \\ x_5 \end{bmatrix}_{e+1} \begin{bmatrix} x_1 \\ x_2 \\ x_3 \\ x_4 \\ x_5 \end{bmatrix}_{e+2} \begin{bmatrix} x_1 \\ x_2 \\ x_3 \\ x_4 \\ x_5 \end{bmatrix}_{e+3} \begin{bmatrix} x_1 \\ x_2 \\ x_3 \\ x_4 \\ x_5 \end{bmatrix}_{e+4} \begin{bmatrix} x_1 \\ x_2 \\ x_3 \\ x_4 \\ x_5 \end{bmatrix}_{e+5} = \begin{bmatrix} T_{11} & T_{12} & T_{13} & T_{14} & T_{15} \\ T_{21} & T_{22} & T_{23} & T_{24} & T_{25} \\ T_{31} & T_{32} & T_{33} & T_{34} & T_{35} \\ T_{41} & T_{42} & T_{43} & T_{44} & T_{45} \\ T_{51} & T_{52} & T_{53} & T_{54} & T_{55} \end{bmatrix} \begin{bmatrix} x_1 \\ x_2 \\ x_3 \\ x_4 \\ x_5 \end{bmatrix}_e \begin{bmatrix} x_1 \\ x_2 \\ x_3 \\ x_4 \\ x_5 \end{bmatrix}_{e+1} \begin{bmatrix} x_1 \\ x_2 \\ x_3 \\ x_4 \\ x_5 \end{bmatrix}_{e+2} \begin{bmatrix} x_1 \\ x_2 \\ x_3 \\ x_4 \\ x_5 \end{bmatrix}_{e+3} \begin{bmatrix} x_1 \\ x_2 \\ x_3 \\ x_4 \\ x_5 \end{bmatrix}_{e+4} \quad (4.4)$$

And:

$$\mathbf{T}= \begin{bmatrix} T_{11} & T_{12} & T_{13} & T_{14} & T_{15} \\ T_{21} & T_{22} & T_{23} & T_{24} & T_{25} \\ T_{31} & T_{32} & T_{33} & T_{34} & T_{35} \\ T_{41} & T_{42} & T_{43} & T_{44} & T_{45} \\ T_{51} & T_{52} & T_{53} & T_{54} & T_{55} \end{bmatrix} \quad (4.5)$$

Equation (4.4), may be written as:

$$\mathbf{T}\mathbf{x}_e = \mathbf{x}_{\mathbf{e+1}} \quad (4.6)$$

Equation (4.6) was done for 5 time steps,

Matrix **A** consists of the force acting on the selected regions of the foot (metatarsals 1 to 5) in a specific time period. As the focal areas of the study were these regions, the matrices have to be five by five, because solving the transfer matrix requires a square matrix relationship. For instance, according to the **A** expression, the five elements of the first row of matrix **A** are the forces applied to the metatarsals in time "*e*". The second row of the same matrix represents the force applied to those areas in time"$e + 1$", which is equal to $\mathbf{T}\mathbf{x}_e$.

Moreover, the final row of matrix **A** is the selection of the force data in time " $e + 4$", which is equal to $\mathbf{T}\mathbf{x}_{\boldsymbol{e4}}$.

So the first matrix has been made by this method of selecting the normalised force data.

The selection of the normalised force data was the same as for matrix **B**, but with the one shift of the data. That is, the first row of matrix **B** is the normalised force data related to metatarsals in time "$e+1$" and for the second row, the force data in time"$e+2$", whilst the last and fifth row is the applied force on the focal regions in time"$e+5$". Thus, the data in matrix **B** have been chosen with one shift from the selection of those in matrix **A,** equations (4-7) and (4-8) presents matrix **A** and **B** elements.

Introducing **A** and **B** matrices where:

$$\mathbf{A} = [\,\mathbf{x}_e \;\; \mathbf{x}_{e+1} \;\; \mathbf{x}_{e+2} \; \mathbf{x}_{e+3} \; \mathbf{x}_{e+4}\,] \tag{4.7}$$

$$\mathbf{B} = [\,\mathbf{x}_{e+1} \;\; \mathbf{x}_{e+2} \;\; \mathbf{x}_{e+3} \;\; \mathbf{x}_{e+4} \, \mathbf{x}_{e+5}] \tag{4.8}$$

T is a function of time that is the same as "*e*" in the equations related to matrices **A** and **B**, whilst "$\boldsymbol{x}$" is the normalised force regarding each participant's body w (4.9)
Matrix **A** and **B** should be selected very carefully because it may give infinity or NaN as the data were so close to each other. That is, because the contact force readings remained unchanged for multiple intervals, this caused a problem in the inversion, which resulted in the matrix being infinity. However, when making a gap between the data matrix **A** and matrix **B** created, whenever any of the toes were in the off the ground position, there were zero forces showing in that region and this led to the problem of the matrix becoming singular. To avoid this, selection of the data for Matrix **A** and **B** was crucial. Table 4-2, shows the selection of the normalised force data from the row data captured by the sensors of the RSscan device. Each row and column shows metatarsal 1 to 5 in time e to e+5. Matrix **T** can be obtained from the Equation (4.11).

$$[\,\mathbf{x}_{e+1} \;\; \mathbf{x}_{e+2} \;\; \mathbf{x}_{e+3} \;\; \mathbf{x}_{e+4} \, \mathbf{x}_{e+5}] = \mathbf{T}[\,\mathbf{x}_e \;\; \mathbf{x}_{e+1} \;\; \mathbf{x}_{e+2} \; \mathbf{x}_{e+3} \; \mathbf{x}_{e+4}\,]$$

Writing Equation (4.9), in matrix form

A is the matrix holding data points as a function of time shifted starting from e, and **B** starting from $e+1$:

$$\mathbf{B} = \mathbf{TA} \tag{4.10}$$

From here the Markovian Chain matrix T can be obtained by post multiplying equation (4.10), with $\mathbf{A}^{-1}$

$$\mathbf{T} = \mathbf{BA}^{-1} \tag{4.11}$$

Table4-2: Matrix (A) of force data of an HV patient

	Metatarsal 1	Metatarsal 2	Metatarsal 3	Metatarsal 4	Metatarsal 5
Time e	0.131769	0.13284	0.132305	0.131233	0.133376
Time e+1	0.160158	0.160694	0.160158	0.160694	0.162837
Time e+2	0.143018	0.142482	0.141946	0.142482	0.142482
Time e+3	0.063206	0.062671	0.061064	0.061599	0.059992
Time e+4	0.009106	0.008035	0.007499	0.007499	0.006428

Table4-3: Matrix (B) of force data with one time step shift from matrix B of an HV patient

	Metatarsal 1	Metatarsal 2	Metatarsal 3	Metatarsal 4	Metatarsal 5
Time e+1	0.13284	0.132305	0.131233	0.133376	0.133376
Time e+2	0.160694	0.160158	0.160694	0.162837	0.162837
Time e+3	0.142482	0.141946	0.142482	0.142482	0.141411
Time e+4	0.062671	0.061064	0.061599	0.059992	0.058921
Time e+5	0.008035	0.007499	0.007499	0.006428	0.006428

Table4-4: Matrix (T) obtained from matrix A and B of an HV patient

	Metatarsal 1	Metatarsal 2	Metatarsal 3	Metatarsal 4	Metatarsal 5
Metatarsal 1	-0.99411	1.342842	0.099189	0.569744	-0.15715
Metatarsal 2	-1.01218	0.101013	2.156856	-0.28224	-1.39898
Metatarsal 3	0.370153	-1.82752	2.959293	-0.39147	-1.32752
Metatarsal 4	1.001016	-1.71675	1.861928	-1.14314	1.283243
Metatarsal 5	0.608935	-0.40741	0.084974	-0.45969	1.092584

Table 4-4, shows the transfer data among different metatarsals related to each other in an HV patient. Negative numbers (considering such values as that at position 4,2 with a value -1.71675 in this table) show that the data transferring to metatarsal 4 have a negative contribution from metatarsal 2. In other words, for this case there is load movement from metatarsal 4 to 2. In summary, the table shows how the load on each metatarsal at a given time step is influenced by load transfers from all the other metatarsals from the previous time step. In table 4-4, the effect of metatarsal 3 on 2 and on itself in HV patient is greater than the effect of other variables on each other.

The procedure and calculations performed for HV patients were repeated for non-HV patients and the set of results are presented in the Table 4-7.

Table4-5: Matrix (A) of force data of a non-HV volunteer

	Metatarsal 1	Metatarsal 2	Metatarsal 3	Metatarsal 4	Metatarsal 5
Time e	0.123447	0.122414	0.119315	0.119315	0.118282
Time e+1	0.235532	0.232432	0.230366	0.229333	0.226751
Time e+2	0.193694	0.193694	0.193177	0.192144	0.191111
Time e+3	0.103166	0.104246	0.103166	0.103166	0.101546
Time e+4	0.022727	0.020661	0.018595	0.017562	0.017045

Table4-6: matrix (B) of force data with one shift from matrix A of a non-HV volunteer

	Metatarsal 1	Metatarsal 2	Metatarsal 3	Metatarsal 4	Metatarsal 5
Time e+1	0.122414	0.119315	0.119315	0.118282	0.116733
Time e+2	0.232432	0.230366	0.229333	0.226751	0.227267
Time e+3	0.193694	0.193177	0.192144	0.191111	0.188529
Time e+4	0.104246	0.103166	0.103166	0.101546	0.101546
Time e+5	0.020661	0.018595	0.017562	0.017045	0.016012

As before, the matrix **A** is derived from the last 20% of the gait and each column presents a different time stage of the fore-foot contact with the pressure mat, such that the first column is the contact of all the metatarsals in time t and column five which shows force for the same regions in time t+5.

Table4-7: Matrix T obtained from matrix A and B of a non-HV person

	Metatarsal 1	Metatarsal 2	Metatarsal 3	Metatarsal 4	Metatarsal 5
Metatarsal 1	-0.62704	1.073456	-0.1242	-0.29183	0.050748
Metatarsal 2	0.297521	-0.41057	2.222719	-1.49033	0.687855
Metatarsal 3	-0.54447	0.481478	0.229601	0.935047	0.288921
Metatarsal 4	-0.33775	-0.11034	1.076373	-0.4871	0.60256
Metatarsal 5	-0.29064	0.514019	-0.47101	0.158172	0.456994

Matrix **T** for the non-HV participant shows that the transition coefficient from metatarsal 3 to 2 with the value of 2.222719 has the greatest value when compared with the interactive effect between the other metatarsals.

In order to compare the spread or dispersion of the transfer data obtained from matrix **T** in both groups, for each person, the effect of these data from one region to another

was extracted from this matrix. That is, transfer data of the same regions relating to ten HV volunteers were gathered from their **T** matrices and likewise for non-HV volunteers. Finally, the data for all twenty participants were presented on graphs shown in Figure 4.4.

As the matrices were 5×5, twenty five graphs regarding the associations between the variables were required. That is, each metatarsal's transfer contributions as obtained from matrix **T** for all volunteers in both groups are presented in a separate graph. The negative numbers in the transfer matrix **T** are changed to positive numbers by taking their absolute values as what is important is to identify cross "communication" between the metatarsals rather than the directionality. The results show there is a significant difference between HV and the control group in the transferring coefficients. Furthermore, the bigger the number in the matrix, the greater the transfer coefficients among all the metatarsals. Three sample graphs are presented in Figure 4.4, (more samples are enclosed in appendix A).

The three graphical examples from the total of twenty five were chosen to show clearly the dispersion of the transfer data. Each red point represents the transfer coefficient from one region on another in each HV volunteer.

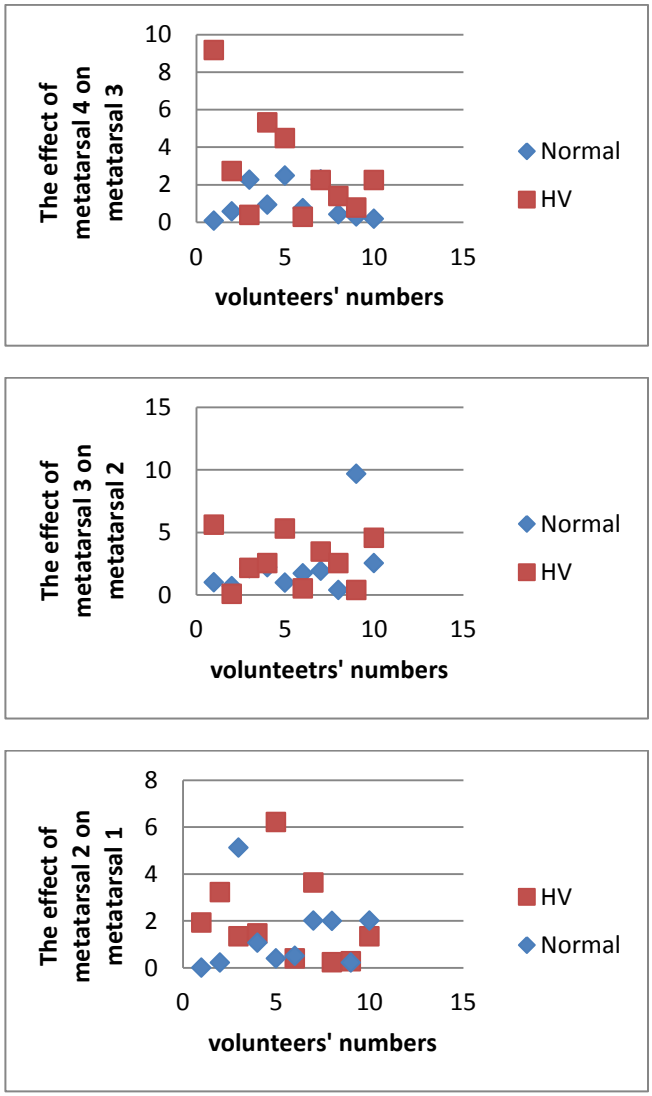

Figure4.4: Three samples of the contribution of data (Matrix T) happen between 2nd metatarsal to 1st metatarsal in all participants. Red points represents HV group and blue points represents non-HV group.

The way of walking has an influence on the gait pattern in that the transferring effects and contributions among metatarsals would be different, because people with deformities when they feel pain try to adapt their gait to overcome it that is why the transfer coefficient among metatarsal heads between HV patients are found to be different than those in control group.

As table 4-7, shows the effect of different metatarsals on each other in the control group is less than the effect found in the HV group. However, both groups show the transfer function in fore-foot but the effect of each metatarsal on the other metatarsals is different amongst volunteers. Standard Deviation can show how much is the dispersion of the data from the mean. To see whether the HV patients transfer

data has larger dispersion from the mean standards deviation of the each region in both groups and in both speeds was obtained.

The results present the higher dispersion of data in HV group compared to non-HV people as shown in Figure 4.5.

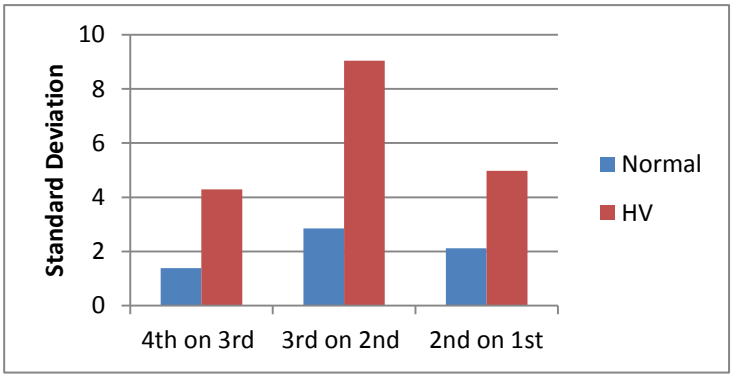

Figure4.5: The comparison of the standard deviations among HV and non-HV group obtained from their transfer matrices coefficients shows the effect of metatarsals 4 on 3, 3 on 2, and 2 on 1.

4.7 Results on foot force pattern by RSscan data on fast speed

All the analysis methods that were carried out on the self-selected speed data which was obtained from all twenty volunteers as well as for the same individuals at a fast speed.

4.7.1 Comparing the average of maximum force applied to the fore-foot region

As explained in chapter three, the same method of collecting data for obtaining the force distribution under the foot was also used to collect the fast speed data of the volunteers. In the experiment procedure, these volunteers were asked to walk 20% faster as compared to their self-selected speed. Three samples of the results of the force distribution pattern under the volunteer's right foot are presented in Figure 4.6.

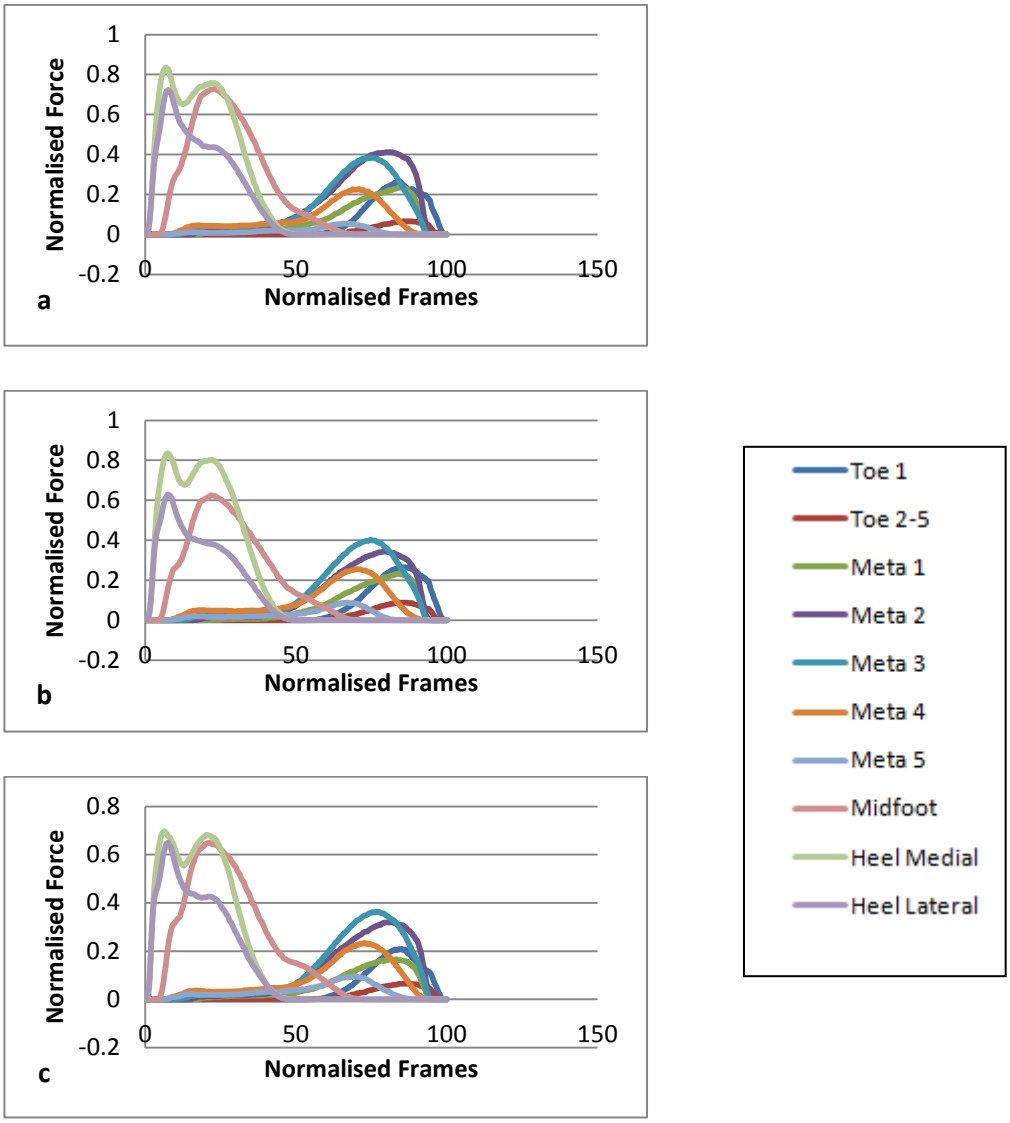

Figure4.6: Three sample trials showing the force distribution under the HV feet agianst notmalised frame. The highest force excluding the heel and the mid foot is under the 3rd,2nd and 4th metatarsal heads.

After volunteers had full contact with the pressure mat for ten trials, the force distribution under their foot was obtained and the maximum force that applied to each fore-foot region in all the trials were gathered, as shown in Figure 4.6. In Figure 4.6, after the heel and mid-foot which bear the highest force, in the fore-foot region the 3rd and 2nd metatarsals bear the highest force.

When compared with the graphs for the self-selected speeds, it is evident that the load is increased in the heel and mid-foot, but in the fore-foot, the level of bearing force did not increase and remains at the same level as found with the self-selected speed. Figure 4.7 shows the plantar force distribution in a non-HV volunteer who is

the same individual who walked at a self-selected speed and for whom the outcomes are shown in Figure 4.2.

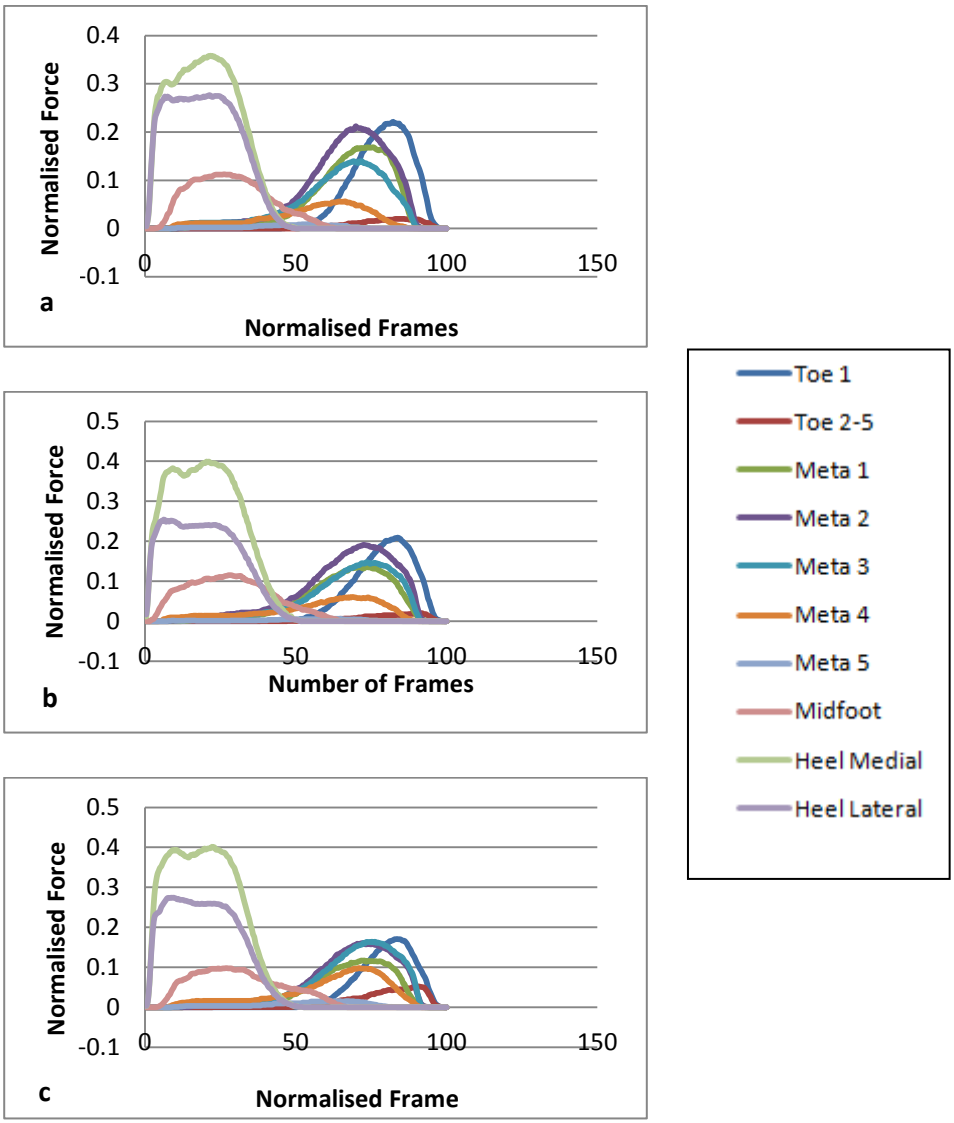

Figure4.7: Three samples trials of plantar force distribution in non-HV individual. The highest force after the heel is on toe1 and 2nd metatarsal head.

As shown in Figure 4.7, the heel bears the highest pressure compared to other foot regions, and then toe 1 and the 2nd metatarsal bear the highest force in the fore-foot area. However, when this is compared with the self-selected speed graphs of the same person, it can be seen that the higher force is applied on the 2nd, 3rd followed by the 1st metatarsal. Further, an increase of the force distribution can be seen in the

fore-foot region regarding the fast speed condition for of the same individual when compared to the self-selected speed.

To compare the average maximum force that applies to each fore-foot region, the same procedure as for testing the self-selected speed was followed so that the maximum normalised force for each region was obtained. Each region is compared with its own data for both groups of individuals and the results of these comparisons are shown in Figure 4.8.

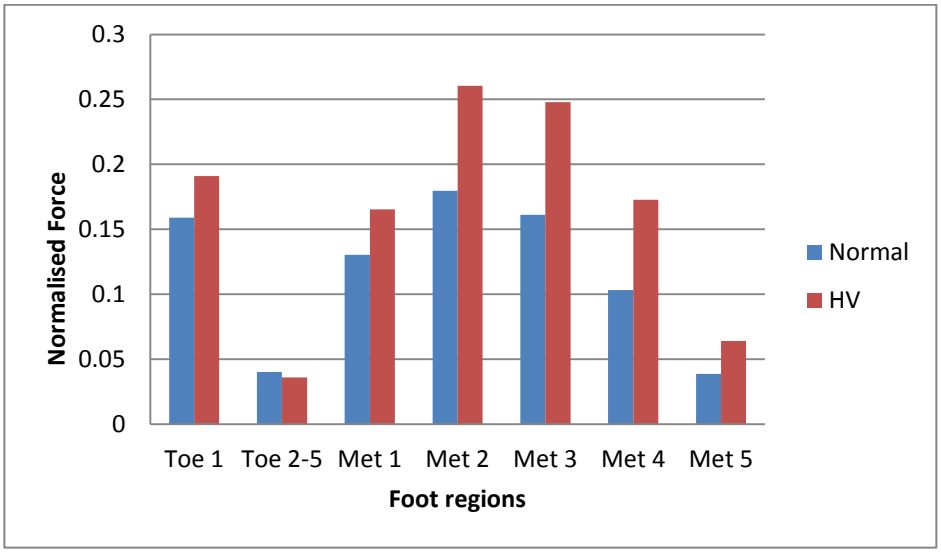

Figure4.8: Average of maximum of normalised force distributed in fore-foot areas in HV and non-HV groups for fast speed

In Figure 4.8, the HV group is shown to bear higher force compared to non-HV individuals in all the fore-foot regions excluding toes 2-5. Furthermore, toe 1 is shown to bear higher force in the HV patients in the case of walking at a fast speed unlike when walking at a self-selected speed the non-HV individuals have higher force under toe 1. Moreover, the 4^{th} and 5^{th} metatarsals and toe1 in non-HV volunteers bears higher force compared to the HV patients in self-selected speed. Toes 2-5 do not present any difference for either speed and in both groups of volunteers. The higher load in the fast speed condition is on the 2^{nd}, 3^{rd} and 4^{th} metatarsals when compared to the self-selected speed.

4.7.2 Independent sample T-test on fast speed

This test was carried out for fast speed force data to see whether there is any significant difference in volunteers' fast speed data. The whole procedure aiming to find out the significant mean differences in among the groups was the same procedure applied for the self-selected speed and the results are presented in Table 4-8.

Table4-8: Comparison of the mean differences in HV and non-HV groups for the fast speed achieved by Independent sample T-test in which in all regions excluding 2-5, the significant differences can be seen where the $p<0.05$

Fore-foot regions	*P* Value
Toe1	0.001
Toe2-5	0.640
Metatarsal 1	0.001
Metatarsal 2	0.001
Metatarsal 3	0.001
Metatarsal 4	0.001
Metatarsal 5	0.001

The results from the T-test indicate that there are significant differences in all metatarsal regions except toes 2-5. Moreover, in the self-selected speed T-test analysis there was no significant difference seen in the 2nd metatarsal.

4.7.3 Comparing Transfer force under five metatarsals in fast speed

The transfer matrices of all HV and non-HV volunteers were obtained according to aforementioned equations for self-selected speed. So the same procedure of getting the transfer matrices was done to get the fast speed related matrices in both groups of volunteers. Table 4-9, shows the obtained matrix **A** from the normalised force

data in each volunteer and with one gap of data matrix **B** was created as shown in Table 4-10. Transfer matrix shows the changes that happen in one region in different time steps as the position of foot changes, T matrix is shown in Table 4-11 which is related to an HV patient.

Table4-9: Matrix (A) obtained from normalised force data from fast speed of an HV patient

	Metatarsal 1	Metatarsal 2	Metatarsal 3	Metatarsal 4	Metatarsal 5
Time e	0.103915	0.158016	0.190155	0.129091	0.02089
Time e+1	0.106058	0.158551	0.187476	0.127484	0.017141
Time e+2	0.106594	0.158016	0.185334	0.122663	0.014462
Time e+3	0.104987	0.159087	0.183727	0.117842	0.013391
Time e+4	0.106594	0.159623	0.181584	0.1157	0.011249

Table4-10: Matrix (B) obtained from normalised force data from fast speed of an HV patient

	Metatarsal 1	Metatarsal 2	Metatarsal 3	Metatarsal 4	Metatarsal 5
Time e+1	0.106058	0.158551	0.187476	0.127484	0.017141
Time e+2	0.106594	0.158016	0.185334	0.122663	0.014462
Time e+3	0.104987	0.159087	0.183727	0.117842	0.013391
Time e+4	0.106594	0.159623	0.181584	0.1157	0.011249
Time e+5	0.107665	0.159623	0.180513	0.112486	0.009642

Table4-11: Matrix (T) obtained from matrix A and B of an HV patient

	Metatarsal 1	Metatarsal 2	Metatarsal 3	Metatarsal 4	Metatarsal 5
Metatarsal 1	0.020974	1.623071	-1.01563	0.193694	0.743435
Metatarsal 2	0.475462	0.004258	0.971539	-0.58639	-0.02749
Metatarsal 3	0.834148	-0.09071	0.688149	-0.22541	0.640196
Metatarsal 4	-0.18394	0.375082	0.129829	0.322932	1.003054
Metatarsal 5	0.48901	-0.77728	0.541399	-0.20112	0.582162

The Table 4-12, shows the **A** matrix related to the non-HV volunteer and Table 4-13 shows the matrix B achieved from one shift of data from matrix **A**.

In matrix **T** of the HV patient the highest contribution of data transfer is between 2^{nd} to 1^{st} and 3^{rd} to 1^{st} and 5^{th} to 4^{th} metatarsals.

Table4-12: Matrix (A) of force data of a non-HV volunteer related to fast speed

	Metatarsal 1	Metatarsal 2	Metatarsal 3	Metatarsal 4	Metatarsal 5
Time e	0.105886	0.254643	0.223652	0.116733	0.011363
Time e+1	0.105369	0.253093	0.224168	0.116733	0.008264
Time e+2	0.104336	0.25206	0.223135	0.112601	0.007748
Time e+3	0.10227	0.255159	0.220036	0.112084	0.007231
Time e+4	0.099171	0.254126	0.220553	0.109502	0.005682

Table4-13: Matrix (B) of force data with one shift from matrix (A) of a non-HV volunteer related to fast speed

	Metatarsal 1	Metatarsal 2	Metatarsal 3	Metatarsal 4	Metatarsal 5
Time e+1	0.105369	0.253093	0.224168	0.116733	0.008264
Time e+2	0.104336	0.25206	0.223135	0.112601	0.007748
Time e+3	0.10227	0.255159	0.220036	0.112084	0.007231
Time e+4	0.099171	0.254126	0.220553	0.109502	0.005682
Time e+5	0.096072	0.255676	0.219003	0.106402	0.006198

Table4-14: Matrix (T) obtained from matrix (A) and (B) of a non-HV person related to fast speed

	Metatarsal 1	Metatarsal 2	Metatarsal 3	Metatarsal 4	Metatarsal 5
Metatarsal 1	0.694081	-0.21153	0.219158	0.27958	0.359946
Metatarsal 2	0.421476	0.622463	0.865355	-1.23933	0.096082
Metatarsal 3	-0.19409	0.440298	0.27178	0.596649	0.19083
Metatarsal 4	0.625619	0.023068	0.272696	-0.26322	1.262979
Metatarsal 5	-0.3247	-0.24376	0.384898	0.12004	0.406816

In Table 4-14, the highest contribution is between the 4^{th} and 2^{nd} metatarsals and also between the 5^{th} and 4^{th} metatarsals but in the self–selected speed, the higher contribution was between the 3^{rd} and 2^{nd} metatarsals. As explained before, the effect of each metatarsal on the other metatarsals among all the volunteers are shown in Figure 4.8. The associations between the metatarsals show that in HV patients, the spread of transfer data is larger compared that for non-HV volunteers.

Twenty five graphs were obtained as the **T** matrix contains twenty five elements comprising contributions of transferring force between the metatarsals and three

samples of the effects of metatarsals on each other are shown in Figure 4.9. Other samples are enclosed in appendix A.

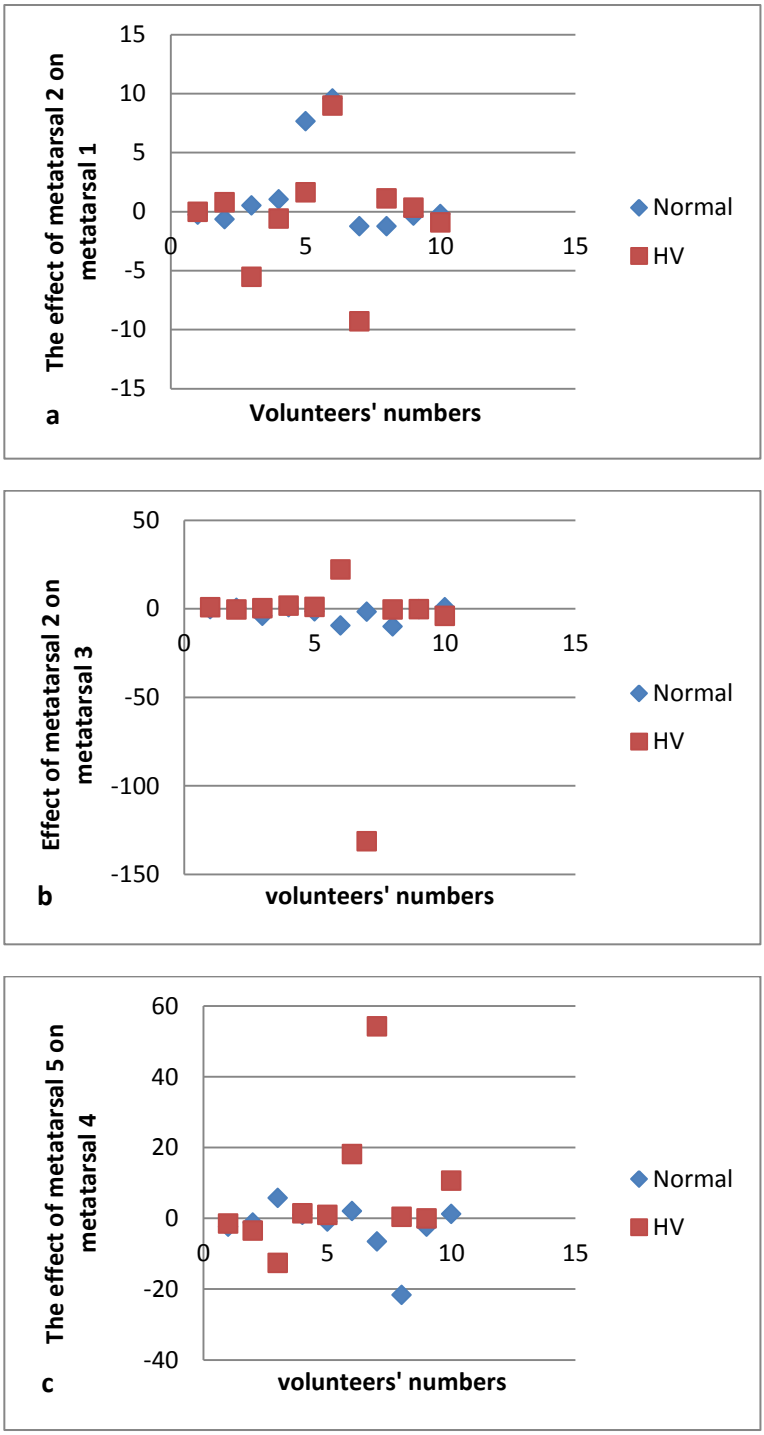

Figure4.9: Three samples of metatarsal contributions on each other in both groups of volunteers. Red points represents HV group and blue points represents non-HV group.(a) shows that effect of metatarsal 2 on 1(b)shows the effect of metatarsal 2 on 1and (c)shows the effect of metatarsal 5 on 4.

The larger spread of data in HV patients shows that the transfer force among the metatarsals is higher in this group as compared to the non-HV individuals. Further,

the SD of the effect of one region on another was obtained for all regions, for all volunteers. The results show that in all regions, the spread of data was higher in the HV patients which show the higher contribution among the metatarsals.

The Standard Deviation of the effect of one region on another was obtained for all regions and in all volunteers. The results show that in all regions the spread of data was higher in HV patients which show the higher contribution among metatarsals. Three samples of comparison of standard deviation in both groups in fast speed was obtained as shown in Figure 4.10.

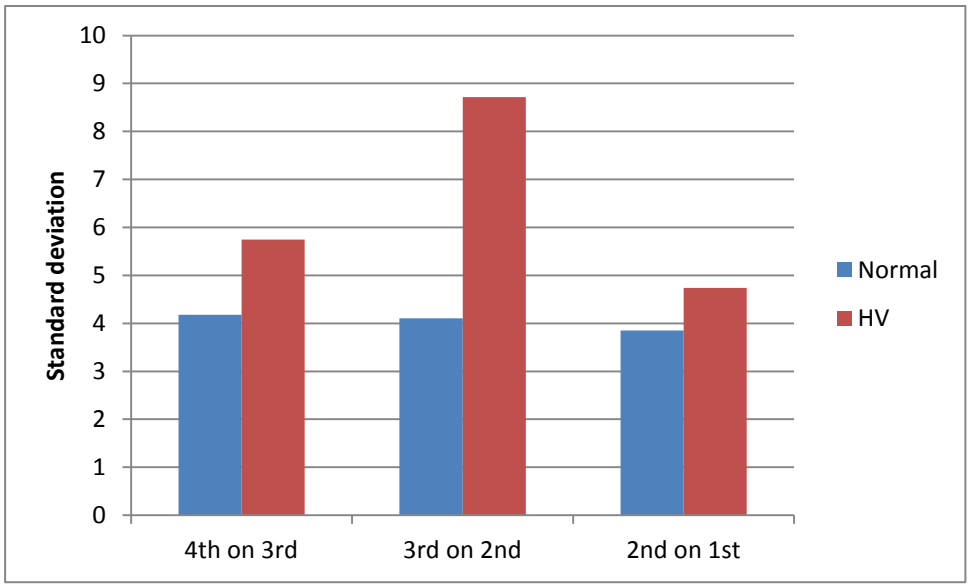

Figure4.10: The comparison of the standard deviations among HV and non-HV group obtained from their transfer matrices coefficients shows the effect of metatarsal 4 on 3, 3 on 2, and 2 on 1.

4.8 Factor affecting the results obtained from RSscan device

The speed of volunteers while stepping on the pressure mat had to be consistent in all the trials in order to do the comparison among groups. Therefore, before the test they were familiarised with the process but nonetheless, it was not possible to get all trials to be the same. To generate matrix **A** and **B**, the most crucial issue was selecting the force data from the raw data obtained from the RSscan device. If the gap chosen between the time steps was too little, then singularity in the **T** matrix would occur. Further, if the gap was too large then the **T** matrix would not show the instantaneous behaviour of the transfer data. Furthermore, the large gap between time steps would record NaN or a singular **T** matrix because of the non-contact force

points in the raw data. Moreover, the large gap between time steps would not show the transfer force from one time step to the next one.

4.9 Results and Discussion of measuring the lateral flexibility of joint using the Motion Capture system

As explained in chapter three, the measurement of the lateral flexibility claims to recognise HV patients by the joint flexibility between the 1st and the 2nd metatarsals and the Motion Capture measurement system has been used to investigate this. All the volunteers who took part in this test were the same as those who participated in the footscan test. The Motion Capture cameras captured the 3D coordinates of these markers so that the distance and the change in distance between them could be calculated. The Euclidean Distance equation (3.2) is used.

Before the start of the experiment, the calibration process, as explained in chapter three, was carried out according to the Motion Capture manual and the system was made ready to capture the motion of the markers. Before the final calibration, through trial and error, the best position in the room that allowed the cameras to capture the motion with the best quality resolution was determined. This was finalised after getting the motion of markers without any flashing or missing data being recorded, as explained in chapter three.

The number of frames differed trial to trial because the walking speeds of volunteers varied, including when the same individual repeated the test. The relative distance for the number of frames in each trial was calculated and the related graphs for trials were obtained. For each person, three graphs are chosen out of the total of ten obtained. The distance between two metatarsals for a non-HV volunteer is shown as graphs in Figure 4.11, where the amplitude between the maximum and minimum points on these graphs is expected to be related to the flexibility between the metatarsals.

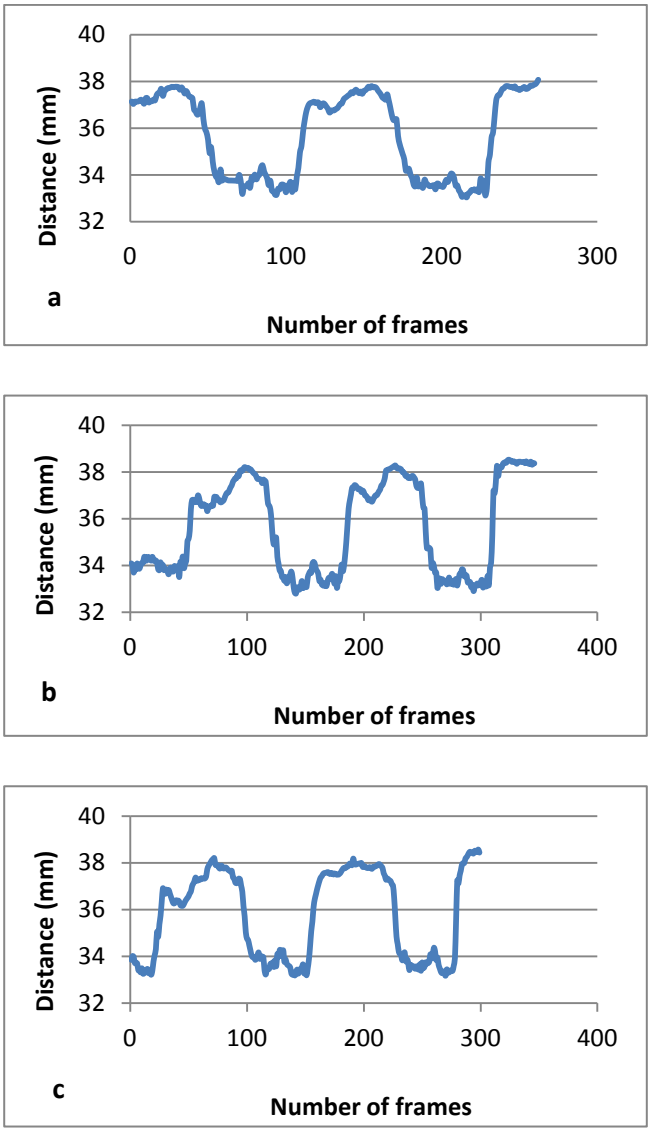

Figure4.11: Three sample trials showing the fluctuations between the markers in a non-HV volunteer

As shown in Figure 4.12, which is for a thirty year old female HV patient, the pattern was completely different in comparison to the non-HV individual's data presented in Figure 4.11. As explained earlier with respect to Figure 4.11, before walking, the distance between the markers did not remain unchanged as the centre of pressure might have been pushing forward or backward and could have had an influence on the distance between the markers before starting walking. In graph (a), Figure 4.12, the distance between the markers in the standing position was 47.49 mm and in (b), the distance was 45.95mm, and it changed once again in (c).

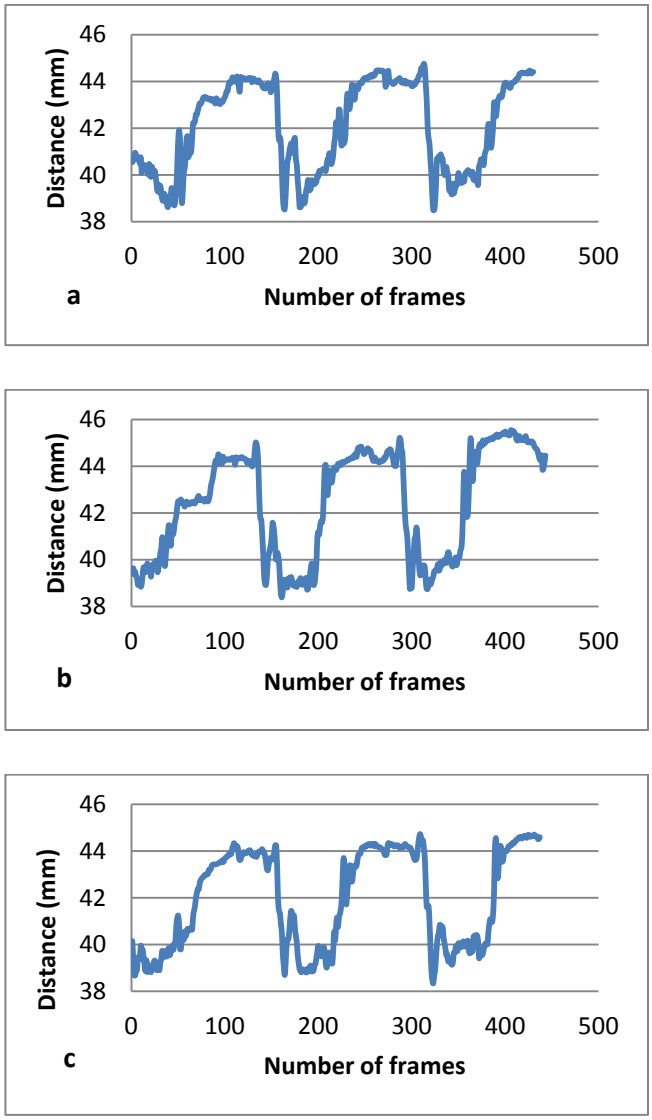

Figure4.12: The distance between the 1st and 2nd metatarsal heads in HV patient. The X vector represents the number of frames and the Y corresponds to the distance (in millimetres).

The fluctuation observed from the HV graphs appears to be higher when compared to that observed for the non-HV individual. Moreover, Figure 4.12, illustrates that the fluctuation of the HV patient is not as constant as the non-HV volunteer and the distance between the two markers is wider in comparison with the non-HV group member. Figure 4.12, shows the relative movement of the1st and 2nd metatarsal heads in the HV patient has bigger fluctuations which means a more flexibility is opening up between these two regions during walking.

The rhythm of walking in those volunteers without the deformity is more constant in comparison to the HV group volunteers and the fluctuation observed in the data is much less than that for HV patients as shown in Figures 4.11 and 4.12. For the

purposes of making a comparison between the HV and non-HV groups, the ratio of fluctuations happening between two metatarsals in all volunteers were obtained according to the equation (4.1).

The changes of distance between metatarsals cannot be compared as the initial distance between the two joints were different in the standing position in each individual compared to the other volunteers. This depends on the size of the foot and the existence of any deformity. That is, the measured initial distance varied person to person and for this reason, doing an independent sample T-test comparing the averages was not possible. But the ratio of changes between these two metatarsals while walking could be measured according to the equation (4.1). The maximum distance that happened between the two markers on each individual was calculated then the maximum distance minus the initial distance divided by initial distance was calculated for each person and for each trial. In the next step, the ratios of all trials regarding the HV and non-HV volunteers were compared.

For comparing the ratio of fluctuations between the groups, the analysis of the means employed to see whether they were significantly different or not. This test can be used when the variables are independent. In this case, there are two groups of volunteers, one with HV and the other without HV, which satisfies this condition. Moreover, the ratio of changes between the two joints are different for each volunteer as compared to the others, so the Independent Sample T-test is the best way of comparing variables among these groups. The Independent Sample T-test is carried out to distinguish whether the differences in their means is equal or less than 0.05. This is an accepted value and where the differences are less or equal to this, the results confirm that the differences between the groups are significant. After making the comparison it could be concluded that the means for both groups (HV and non-HV) were significantly different by 0.012 as shown in table 4-15.

Table4-15: The number of participants and *P* value which shows the statistical significant difference

Number of participants		*P* value
Female	12	0.012
Male	8	

This result illustrates that the 1st metatarsal joint is more flexible in those patients with HV. It should be noted that there are no previously published papers investigating the lateral flexibility of the1st metatarsal joint in HV patients although some researchers have studied the relative movement of other bones while subjects are undertaking various activities.

4.10 The factors affecting the results

Although the start points of all the graphs for an individual should be the same, it appears that they are different which is due to the standing resting position of the individual at the start of the trial. In Figure 4.11 (a), the start point is from 37 mm, which indicates that the distance between the two markers while the volunteer was standing behind the start point was 37 mm. However, regarding graph (b), the distance between the markers is 34 mm showing that the distance between two markers before the individual started walking had decreased for the next trial. The markers had not moved on the skin surface, but the reason for the difference may be because when the body's centre of pressure is towards the fore-foot, the distance between the two markers increased and when towards the heel, the distances between them decreased. The initial distance between the metatarsals are not important as that recorded during the walking cycle, when the distance will oscillate between its minimum and maximum.

Another factor that may have had an impact on the data collection and the results was the way of walking of each volunteer. However, beforehand, they walked three times so as to become familiar with the experiment, but still an error may have happened due to the nature of their motion. The volunteers tried to be consistent in their walking during the experiment. Furthermore, the way of sticking the markers onto the bare skin was an issue because volunteers should be able to walk naturally.

4.11 Conclusion

In this study, two methods were developed: Markovian Chain transfer matrices and measurement of lateral flexibility of the 1st metatarsal joint. When the position of the foot changes, the way that the force is transferring along the foot changes so the centre of maximum force moves from the heel to toes, which means that the force is transferring from one foot region to another. In order to investigate the contribution of transfer coefficient from one region to the other regions, Markov Chain matrices were used to clarify this transfer. The pattern of transfer obtained from this method shows that the higher transformation is happening in the five metatarsal regions of HV patients compared to non-HV volunteers. This pattern was found in self-selected and fast speed testing and the results indicate that in both speeds a higher contribution is happening in HV volunteers.

Furthermore, the results achieved from the comparison between groups regarding plantar force distribution show that the higher force was applied on the 3rd and 2nd followed by the 1st metatarsal heads in the non-HV group and the 3rd, 2nd and the 4th in the HV group for the self-selected speed. In the fast speed case, the higher force was applied to the aforementioned regions in the HV group whereas in the non-HV group, the higher force was applied on toe 1, and the 2nd, 3rd followed by 1st metatarsal heads. The highest force, excluding the heel, was applied under these regions but the groups were significantly different when comparing the maximum force. In the fast speed condition, the force that applied under the metatarsal regions was significantly higher in HV people compared to non-HV individuals as well as when compared to the same individuals when walking at their self-selected speed.

The second method was based on measuring the lateral flexibility of the 1st metatarsal joint and the results show that the lateral flexibility or the movements between the 1st and 2nd metatarsals for the HV volunteers were higher than for those in the control group. The separation between the 1st and 2nd metatarsals is a good indicator of the existence of lateral flexibility of the 1st metatarsal joint, in those with the HV deformity.

3D Modelling and stress analysis of feet with and without HV

5.1 Introduction

Finite element analysis is a useful tool for gauging the biomechanical changes that happen during daily activities. Plantar pressure distribution can be obtained by applying FEA but in order to obtain an accurate stress distribution pattern, ensuring that the foot model is as real as possible can present a challenge. As the foot is a complex structure, obtaining a model that can facilitate accurate analysis of the biomechanical behaviour of the human foot would appear to be essential particularly in the application of shoe design or predicting foot deformities and pathologies. FEA is useful when, for instance, designing insoles that minimise the contact force areas which cause pain and discomfort.

For this current project, two 3D foot models were obtained from CT images taken of the right feet, in the neutral position, of a 38 year old woman with the HV condition and a 24 year old woman without any foot deformity. The two constructed models contained the 28 bones of the foot: the calcaneus, talus, navicular, cuboid, medial cuneiform, intermediate cuneiform, lateral cuneiform, 5 metatarsals, 5 proximal phalanxes, 4 medial phalanxes, and 5 distal phalanxes. For making the 3D models, Mimics 14.0, 3Matic V6.0 and Abaqus v6.11-1 software packages were used. The images of the two individuals were obtained from the radiography section of the Erfan hospital, Iran.

The purpose of modelling the volunteers' feet was to compare the plantar stress distribution pattern in the static position in the fore-foot area in both a HV and a non-HV participant. The stress distribution pattern under the foot in both these volunteers was validated with the static condition pressure distribution pattern to see whether their FEA results were similar to those achieved in the experiments. These two models were made with similar defined boundary conditions so that all interactions between bones in both models were similar to each other. However, the load applied was not the same for both as each volunteer's simulation results were compared with its own experimental results and so the applied load was varied according to their weight.

5.2 Mimics Software

The primary 3D model of the foot of each volunteer was generated and edited in Mimics software that reads CT and MRI images in the DICOM **(**Digital Imaging and Communications in Medicine) format. DICOM is medical imaging density segmentation software which provides information about each slide of the image which may be of bone, soft tissue or skin (Abulkhair, 2012). The CT images of the two volunteers' feet were imported to the Mimics software with resolution of 512×512 pixels and pixel size of 0.5527 mm. After importing the images they were displayed in the three window views of the software which allowed the user to work on each image in the axial, sagittal and coronal views. Although in the CT images, it was possible to observe the cartilages and ligaments, for this project, only the anthropometrical characteristics of the bones were constructed for the right foot of each volunteer.

The CT image of the foot consists of multiple slides that form one complete image. For the non-HV individual, there were 323 slides and for the HV volunteer 275. The CT scan device used for this was the spiral multi detector, set at 1 mm distance between image slices. When the distance between individual slides is decreased in high quality devices, the quality of the images becomes higher and the outline of each of the bones becomes more visible. Working with a reduced distance between slides the accuracy of the geometries of the bone is assured. In fact, assuring the quality of the CT image is very important so as to recognise the boarder of the ligaments and bones in the 2D slides and allow these to be treated as separate objects. This degree of accuracy depends on the CT scan device and its functional capacity regarding taking high quality images.

When the image of the foot is imported to the software, different parts of the foot that is, bone, soft tissue and cartilages presented in different levels of grey intensity. In this project the modelling of the 28 bones of the foot were constructed and soft tissue was not included. In order to achieve the 3D construction of each bone, a mask comprising a layer over the bone was created by using the thresholding command based on Hounsfield units (HU). This task was undertaken to fill the gaps in the three views (axial, sagittal and coronal) of the slides of the bones. This process was

carried out manually by applying the “editing density mask” operation and is shown in Figure 5.1.

To create one mask corresponding to one bone, the boarder of the bone is rendered visible according to the choice of the threshold value which is defined by the software default setting. The specified threshold value for bone was between 226 to 1693 (as shown in Figure5.1) which defines the limits. A custom option whereby the threshold range is changed manually for making the masks for the ligaments and cartilages, and for which the specific limits are set by the software.

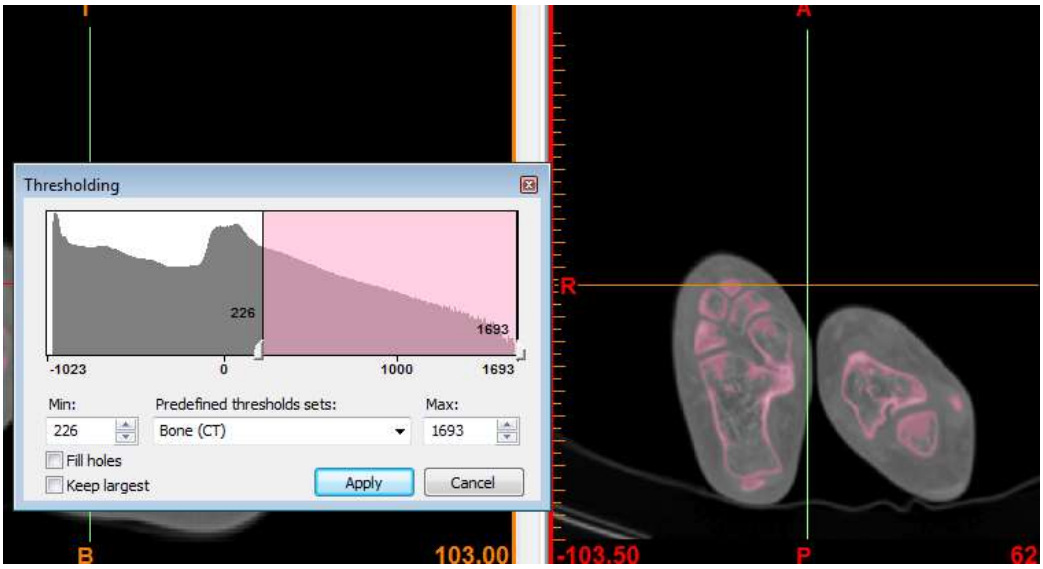

Figure5.1: The view of the mask creation over the bone with the bone related threshold value.

After creating masks for each bone, the holes in the image slides were filled in order to reduce the distances between slides. The “cavity fill” operation was applied to rule out voids in the density of the mask to get smoother bones. Each bone mask was defined by a separate colour so that 28 different colours were used to present the 28 bones. The process was repeated for all bones, for both foot models. After the 3D models of the 28 bones were obtained, to minimise voids around the bones, any voids and sharp edeges of the bones were removed in the 3D view of the assembled whole foot models.

In order to obtain smoother 3D models, all voids and sharp edges of all the bones were removed by using the smoothness and iterations icons in the Mimics package because smoother surfaces reduce simulation errors in the Abaqus software.

Furthermore, “Triangle reduction” was another option for reducing triangles in which it could help to reduce the simulation time in Abaqus. The assembled foot model and the filled masks over the bones are presented in Figure 5.2.

After clicking on the “3D calculation” of the bones, each could be transferred to the 3Matic software to allow the researcher to work on the quality of the meshes.

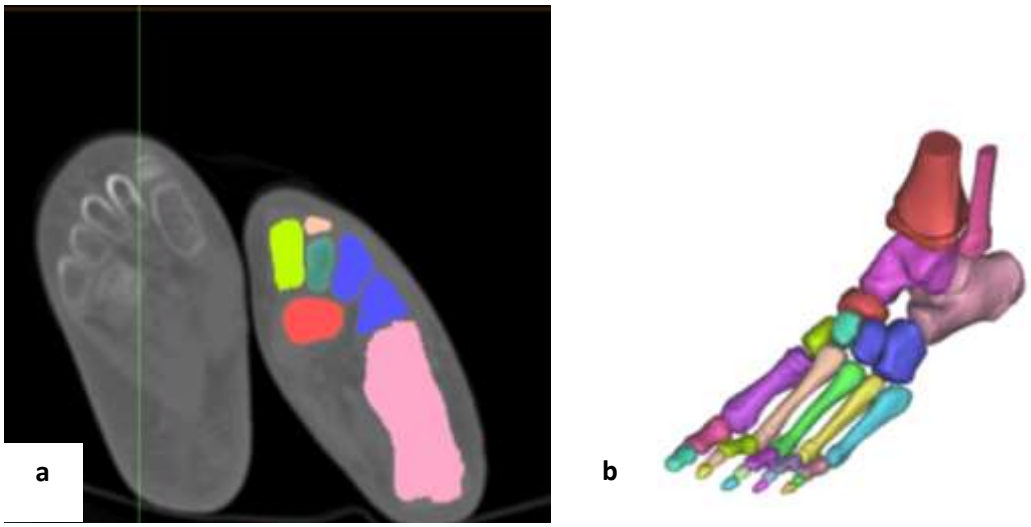

Figure5.2: (a), Mask creation, (b) 3D reconstruction out of the 2D masks

The geometrical complexity of the foot does not allow for the use of hexahedral elements that usually provide high accuracy with less computational costs. For this reason tetrahedral elements that are more versatile when capturing irregular shapes of bone structures were used to mesh the model (Antunes et al., 2008).

5.3 3Matic software

3Matic software reads the segmented images generated for the Mimics 3D models and it applies meshing capabilities. In addition it offers the following functions:

- Performing 3D measurements and engineering analyses
- Designing patient-specific implants or surgical guides
- Preparing anatomical data for finite element simulations (Materialise, 2014).

For this current investigation, 3Matic software was used to create the mesh over the bones and to improve the quality of the meshes for the bones so as to increase the accuracy of the analysis. If bones were imported with any voids and pixel noise surrounding them, this could also be removed by applying the software. All bones imported in to 3Matic form structured groups of triangles that make up the bone surfaces. After importing each bone from the Mimics to the 3Matic software, one by one, the "Auto remesh" option was applied to each bone for both foot models and with this command all the surfaces of the bones became meshed. Some of the bones that presented with sharp edges were smoothed in this software by applying different iteration rates that varied according to their severity.

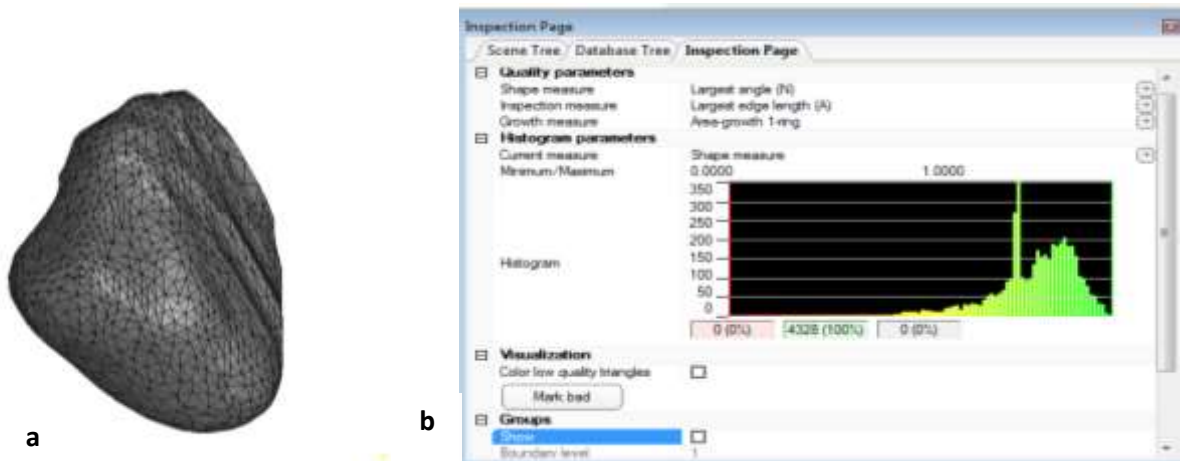

Figure5.3: (a) the re-meshed bone imported to 3Matic, (b) the histogram shows the quality of the mesh.

The re-meshing was carried out to reduce the number of triangles and decrease the details in the object as well as the simulation processing undertaken with the Abaqus package.

In this particular software, there is a "Mark Bad" option under the "Visualization" icon. When this is selected, all the low quality triangles are shown on the surface of each bone, and by clicking on these, they can be deleted and re-created. when most of the bone surface records bad mark triangles, the whole remeshing process has to be re-done. However, if after repeating this stage and the low quality meshes appear over the surface of the bone, the Mimics software can be used to resolve the problem

by working on the three views of each bone, slide by slide. When this process has been repeated in the Mimics package, a smoother surface with the least possible number of voids for each bone is subjected to the 3Matic software for remeshing. This process was followed to eliminate all the "mark bad" triangles on the surface of some bones until the histogram presented in Figure 5.3(b) was achieved with good quality meshes.

The limits of histogram lay between 0 and 1. When the numbers are close to 1, the quality of the mesh is acceptable and the mesh quality for each separate bone is within the histogram parameters. For this study the "Quality parameter" were chosen according to the programme default and for meshing the bone in this menu, the "Largest angle" option was chosen. This decision was made because in this option, the simulation processing time decreases considerably, which in this case is noticabely helpful as with 28 bones the model with more than 100,000 elements. Moreover, the "Inspection measure" was chosen as the "Largest edge length" according to the software default. All of these options were selected for all bones and for both foot models; firstly, to improve the quality of the meshes obtained and secondly, to reduce the time needed for the simulation process by reducing the number of elements (triangles).

5.4 Abaqus Software (6.11-1)

Abaqus Explicit is a special purpose software that uses an explicit dynamic finite element formulation. It is suitable for modelling brief, transient dynamic events, for highly nonlinear problems involving changing contact conditions (Berkey, 2002; 2014). In this study, to see the stress distribution under the right foot of the HV and non-HV volunteer, both models were imported to the Abaqus software as separate instances and then assembled in this software with the same geometry. The meshed bones in 3Matic are saved as "inp" files and then imported from the 3Matic software to Abaqus Explicit v6.11-1, with each bone having a separate file.

5.4.1 Modules

Eight step by step stages are required to obtain the plantar stress distribution results. These stages are: part, property, assembly, step, interaction, load, mesh and job. These are discussed next.

5.4.2 Part

When each part is imported to the Abaqus, the first thing to do is change the mesh shapes from "Tri to Tet" under the mesh module which converts the shape of the meshes from triangular (surface) to tetrahedral (solid). This was carried out for each imported bone separately because the meshes were defined as surface ones.

In addition, the task of making a plate was completed. This was located under the foot and the "Encaster" option was used to fix this plate as ground support.

5.4.3 Property

The material properties of the bone were elicited from previous literature. Furthermore, the units of measurement for all the materials were recorded according to the SI. The density of the bones was chosen as 1.5×10^{-9} tonne/mm^3. The mechanical property is chosen to be "elastic", with the Young modulus of 7300 Mpa and Poisson ratios of 0.3 were selected (Cheung et al., 2005). All materials were considered as isotropic and linearly elastic, solid and homogenous (Qiu et al., 2011).

The properties of the bone can be defined through the "Section" option, the whole bone should be selected and then the required property can be assigned.

5.4.4 Assembly

In this section by clicking on the "Calling the Instances", all the bones appeared and then assembled together. As the bones that were modelled in Mimics kept their geometries, when assembled in the Abaqus, they were gathered by their geometries. Figure 5.4 shows the assembled and mesh foot model in Abaqus for the HV patient.

Figure5.4: Assembled foot model of an HV patient

5.4.5 Step

In this section, the option "Dynamic-Explicit" was chosen in order to carry out the simulation speedily for each bone.

5.4.6 Interaction

When applying body weight force, the bones should be connected to each other so as not to become separated while the force is applying and transferring through the bones. In order to obtain this, the "Coupling" command was used. The interactions between the surfaces of the bones relative to each other were defined by the "Coupling" command and in the main tool bar under the "Tool" icon, the reference points were made.

In order to keep the bones together, one reference point was defined on each bone and then the whole bone was selected and coupled to the defined reference point on the same bone. For instance, one reference point was defined on the tibia and then the whole tibia selected and coupled to that reference point. In this way 28 reference points were defined for the 28 bones.

In the next step, the defined reference points over each bone can be coupled to the reference point located on the next bone with which it makes contact. Figure 5.5(a), shows all the bones are coupled to the reference point placed on each individually and the reference points coupled to each other. The method of coupling the bones to

each other in order to transfer the load was obtained according to the work of Antunes et al., (2008).

The contact between the bones was defined as frictionless contacting bodies (Yu et al., 2008). In order to achieve this, the "kinematic Coupling" option was used to define constraint for the bones so as to keep them together. The attachment of the bones was carefully done in keeping with the way that real bones are placed beside each other in the human foot as shown in Figure 5.5(a).

As explained previously, the bones were attached to each other by reference points placed over them. In this way the bones could have movements related to each other and each attached bone could move within six degree of freedom related to the bone to which it was attached.

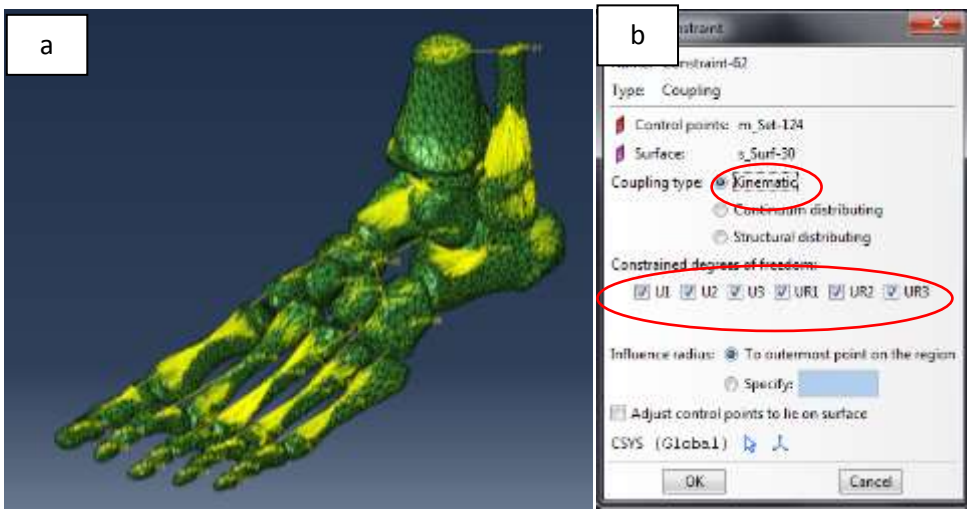

Figure5.5(a) Bone connected to each other by coupling command (b) shows that when the Kinematic coupling was chosen the sign of six degrees of freedom were ticked

5.4.7 Load

The force applied to the foot was obtained from experimental procedure during which the volunteer stood on the pressure mat in the balance position while the whole right foot had contact with it. The pressure distribution under the foot was measured with half of the body weight applying to the right foot of both volunteers (HV and non-HV) (Antunes et al., 2008). The total body weight of the HV volunteer was 63kg and for the non-HV one was 58kg.

The aim of conducting the FEA was to validate the plantar stress distribution pattern (but not the actual values) in 3D the model with experiment results obtained for each individual. That is, the 3D model of the HV patient was validated with her own experimental outcomes. The amount of 315 Newton equal to the half of the body weight for the HV individual and 290 Newton for the non-HV individual were considered to be applied to the centre of the tibia, in line with the scholarship of Antunes et al., (2008).

Recall that the frictionless plate was created under the foot as ground support.

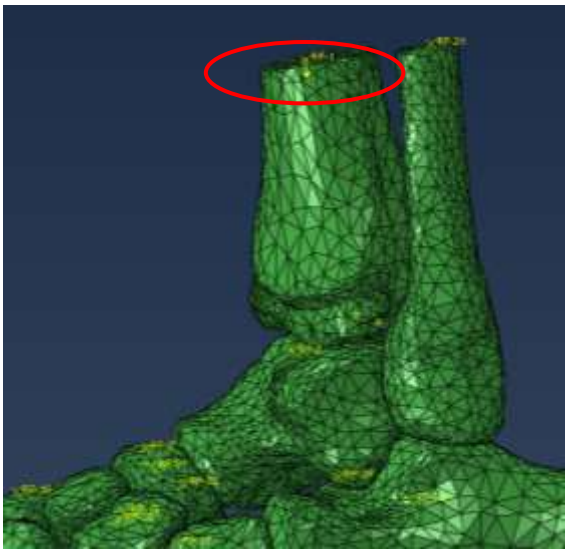

Figure5.6: The body force applied to the centre of tibia

The "Concentrated Body Force" was applied at a rate equal to half of the volunteer's body weight to the geometric reference point defined as being at the centre of the tibia. The direction of the applied force was in the –z direction as shown in Figure 5.6.

5.4.8 Mesh

As any necessary re-meshing and editing had been carried out in the 3Matic program, no more work was needed except for the converting of the mesh from having a triangular to tetrahedral shape which is recommended for it is a more accurate approach for carrying out the stress analysis.

5.4.9 Job

After defining the load for running the simulation for each model, a separate job was created for the HV and non-HV cases. These two jobs were "Submitted" for the software to carry out the "data check" stage and then each job started running. After the jobs were completed for each foot model, by clicking on the "Result" button, the outcomes appeared in the module section "Visualization". The Von Mises stress distribution pattern for the HV and non-HV are shown in Figures 5.8 and 5.9.

5.5 Results and Discussions

When using FEA there are some issues that need to be taken in to consideration regarding modelling human body segments. In particular, the input parameters such as bone materials and Young modulus are crucial.

In this project different boundary conditions were applied in order to obtain accurate stress distribution when comparing the two models with the experimental method results. As explained in chapter three, the experimental static results were obtained while the two volunteers were standing in the balance position on the pressure mat. In the Abaqus modelling, the Von Mises stress results were recorded and validated with the experimental graphs, as shown in Figure 5.7.

The Von Mises stress is not directly comparable with pressure, therefore to make comparison modelling with the experimental results, this comparison was made according to higher loaded areas in experiments and in simulation. That is, in the 3D models the higher loaded areas can be compared with the higher loaded areas obtained during experimental procedure because the comparison of pressure magnitude and Von Mises stress magnitude is not possible even though the way that the metatarsals bear the load is comparable. Figure 5.7, shows the pressure distribution graphs under the right foot of the HV and non-HV individuals. The x axis presents the number of frames and the y axis shows the pressure magnitude (Mpa) in ten anatomical regions of the foot.

The pressure graphs shown in Figure 5.7, indicate that the pressure on 2^{nd}, 3^{rd} and 1^{st} metatarsal heads regions are higher in the HV patient as compared to those of the

non-HV volunteer. As can be seen in Figure 5.7(a), regarding the non-HV individual, the highest pressure excluding the heel region is presented under the 2nd, 3rd followed by the 4th metatarsal heads. The heel bears the highest pressure in both models. The validation of the 3D foot model is carried out according to each individual's pressure graphs.

The pressure pattern under the feet in HV and non-HV individuals confirms previous the findings in extant published papers that the higher pressure level is recorded under the 2nd and the 3rd metatarsals for both groups, but the peak pressure for the HV patient is higher when compared to the non-HV individual (Hughes et al., 1991). Further, it can be seen from Figure 5.7(b), that the highest pressure area, excluding the heel, is under the 2nd and the 3rd followed by the 1st metatarsal heads. Subsequently, in order to make the comparison and validate the modelling results with the experimental ones, all the boundary conditions that were defined for both the models were based on the volunteer in a standing condition, with a plate created under the foot. The reference point was defined in the middle of the plate and Encaster option was used to fix the plate which means that when applying the force to the foot, the plate could not move in any direction. The concentrated force was applied from the top of the tibia to see how it was converted to stress and transferred through the whole foot.

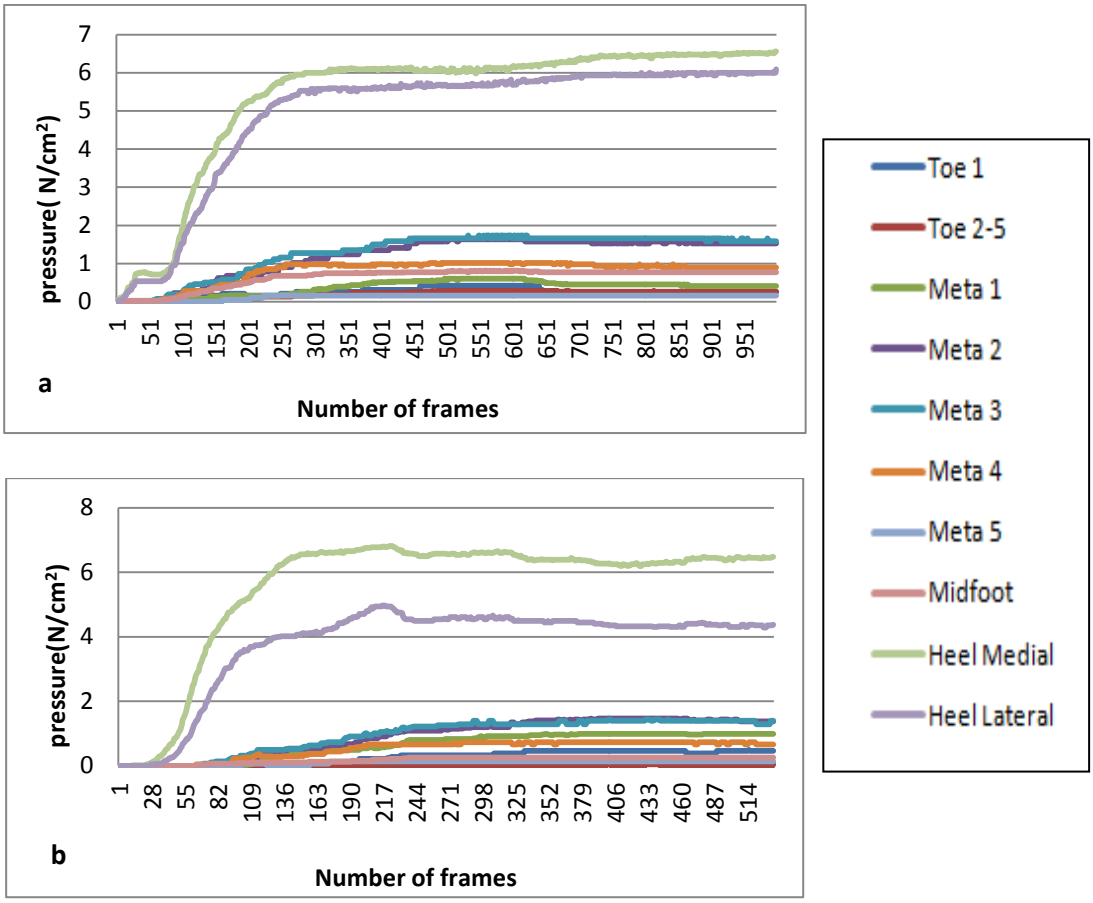

Figure5.7: (a) The pressure distribution under the foot without HV and (b) with HV in ten anatomical regions

With regards to Figure 5.7, the number of frames is different in both graphs. Hence, the pressure could not be normalised by the individuals' body weight because each 3D foot model was validated with its respective experimental graphs, which were obtained for the static condition.

Figure 5.8, presents the stress distribution under the foot in the non-HV volunteer from different views. As the concentrated force was applied, the most stress is shown as being on the tibia and the heel region. In the experimental results the heel is also shown to bear the highest pressure, which is consistent with the outcomes of previously published papers such as Bryant et al., (1999).

Moreover, referring to Figure 5.8, most stress is applied on the calcaneus (heel) and then is transferred to the fore-foot of the individual. The stress on the 2nd and the 3rd metatarsal heads followed by the 4th are higher compared to the other regions in the fore-foot area of the non-HV volunteer. In the standing position, the heel bears the most stress which is about half of the body weight. The legend in Figure 5.8,

confirms that the highest stresses applied to the calcaneus and the lowest to the middle phalanx of toe 3.

5.6 Non-HV volunteers' results

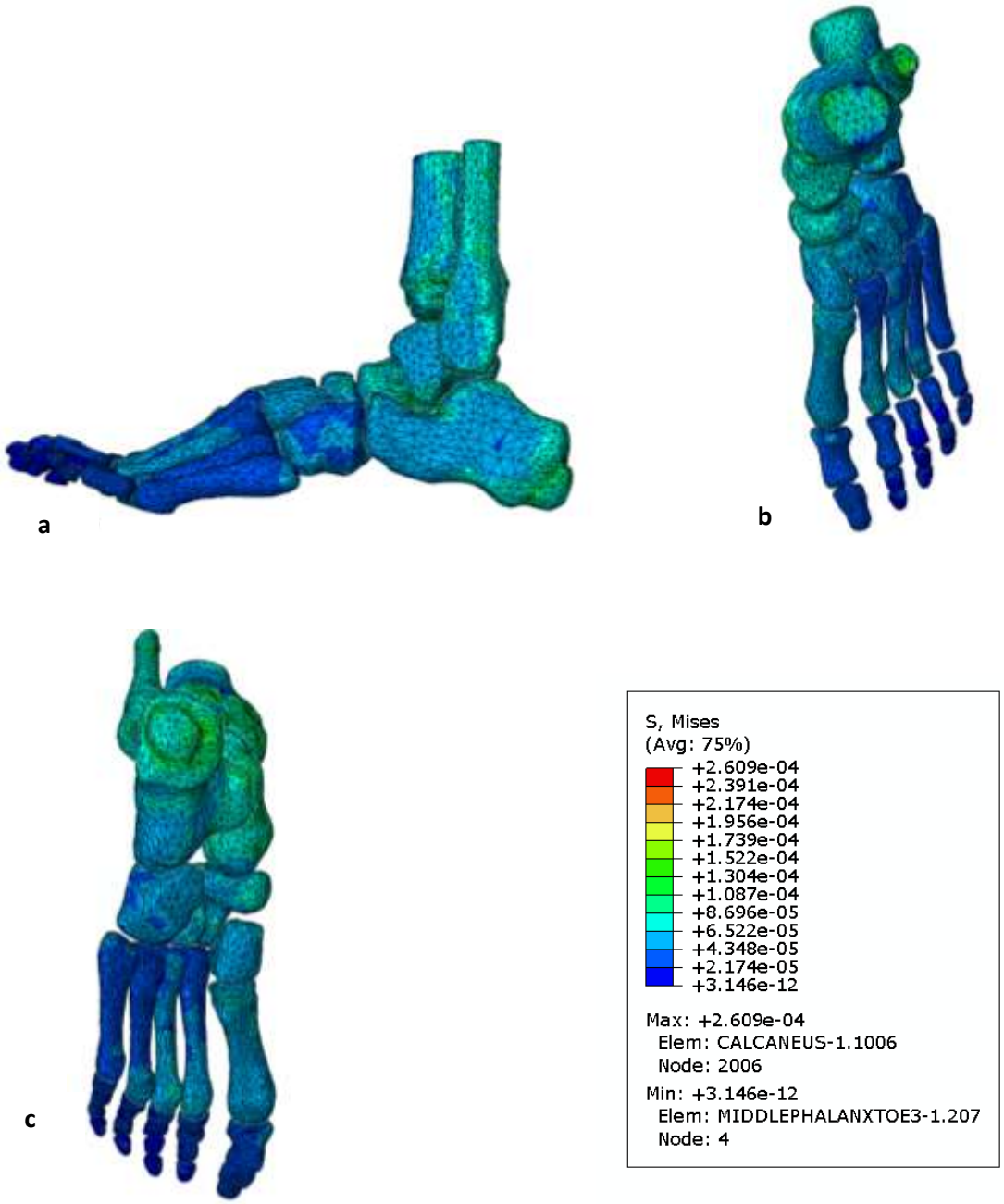

Figure5.8: (a, b and c) three different views of Von Mises stress distribution in a non-HV volunteer's right foot, the legend shows the Von Mises stress magnitude in different regions

Regarding previous foot scan experiments held by different authors, they found that the most pressure in the standing condition applied to the 2nd, 3rd and 1st metatarsal heads and 50% of the body weight applies to the heel. The pressure distribution

under the foot depends on the standing posture and whether the centre of the pressure moves forward or is in a balance position can affect the way that the pressure applies to the foot.

If the centre of pressure moves forward in the standing position, the pressure tends to apply to the fore-foot whereas when the centre of the body mass is in the balance position, half of the body weight applies to the heel. According to Bruening et al., (2010), forces on the lesser toes are smaller in amount than those applied to the hallux. In line with this, Figures 5.7 and 5.8, demonstrate that the lesser toes bear lower stress as compared to the hallux.

As shown in Figure 5.9, the most stress applied to the heel region, then transferred to the fore-foot area, and metatarsal 2^{nd} and 3^{rd} and then the 1^{st} metatarsal bear the most stress, excluding the heel, It was elicited from the experimental method data that the highest pressure after the heel region transfers towards the 2^{nd}, 3^{rd} and the 1^{st} metatarsals, as shown in Figure 5.7(b).

5.7 HV volunteers' results

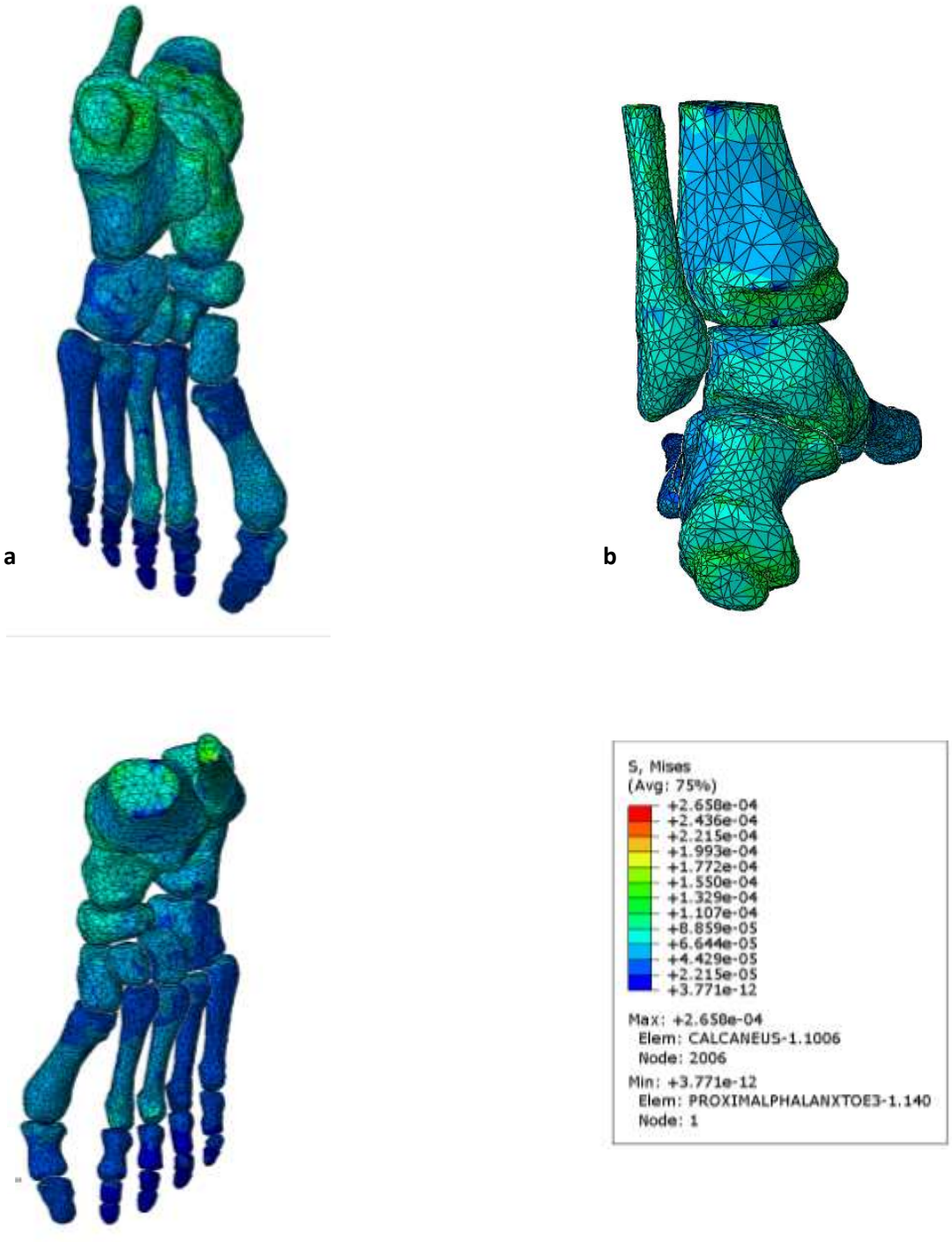

Figure5.9: (a, b and c) three different views of Von Mises stress distribution in the HV volunteer's right foot, the legend shows the Von Mises stress magnitude in different regions

As shown in legends of Figures 5.8 and 5.9, in both the HV and non-HV volunteers, the stress magnitude is similar because the weights of the two volunteers were similar. In both models, the highest stress levels were on the heel regions as was confirmed from the experimental procedure. Moreover, as happens naturally while in the standing position, the stress transfers through the whole of the foot and reduces from the heel area towards the fore-foot region. In both the models low stress was distributed under the 5^{th} metatarsal as compared to the other metatarsal heads and the lesser toes bear the lowest stress. In both models the foot was in the rest condition, and simulating them in the standing position was difficult.

In the non-HV individual the stress appeared more distributed along the foot as compared to the HV patient. However, the load is more widely distributed over the foot, particularly the fore-foot area, but overall, the load is more in the HV foot in comparison to the normal foot. Cheung et al., (2005) found that the most pressure in the standing position of a person without any foot deformity was, in this order, on the 2^{nd}, 3^{rd} and 1^{st} metatarsals in the fore-foot region.

In HV patients as there is a subluxation (joint dislocation) of the 1^{st} metatarsal bone, sesamoid bones underneath the 1^{st} metatarsal head joint have an inversion movement towards the Lesser toes, and as a result, the function of the sesamoids is eliminated. The pressure under the 1^{st} metatarsal head is higher in HV individuals because the function of these two bones, i.e. shock absorption, is disrupted. When they are dislocated from their true place, their abilities regarding absorbing shock applying from the ground are reduced.

5.8 Limitations of FEA

With respect to limitations in the use of FEA, there is lack of detail regarding how scholars who have published papers have connected the bones together and little information regarding defining materials.

In some previously published works such as study done by Cheung et al., (2005) the Young modulus of the ligaments is defined as 260 or 145 (Mpa) but in the real foot, the this would differ due to age, injuries or the location and the function of that specific ligament. Also ligament stiffness varies from one person to another.

Furthermore, the bone consists of two parts, cancellous and cortical. Distinguishing these two parts of the bone in the CT scan image produced in Mimics is very difficult. Treating these two parts of the bone as separate objects is an issue that may be overcome in future with the development of better quality CT imaging systems.

Another issue is defining boundary conditions and connecting the bone together. The foot contains 109 ligaments and in none of the previously published work have they all been included because the sizes of the ligaments are different, their locations are so close together and they vary in thicknesses. Overlapping the ligaments can cause errors in the simulation process.

A limitation of this current study was producing a CT scan image of the foot in the standing position. As the hospital did not have any facility with a CT device on which an individual could stand, this was not obtained.

5.9 Conclusion

In this chapter two feet models, one of an HV and one of a non-HV volunteer, were taken in the rest position and then simulated in the standing position. The comparison of stress distribution was made according to each volunteer's experimental results recorded in the standing condition. Experimental results for the HV person show that the highest pressure after the heel region was on the $2^{nd,}$ 3^{rd} and 1^{st} metatarsal heads. For the non-HV person the highest pressure, excluding the heel, was on the 2^{nd}, 3^{rd} and the 4^{th} metatarsal heads.

In the experimental investigation the plantar pressure distribution was achieved whereas in the FEA, the Von Mises stress was obtained. The comparison was made regarding the level of pressure bearing in experiments and the level of bearing stress in the simulation not based on the magnitude. The results achieved from the simulation for both volunteers were confirmed with the experimental results. It can be concluded that in FEA there are issues pertaining to the lack of inputs, but defining boundary conditions may have significant impact regarding achieving accurate results. In this study the results from the FEA were validated by the results obtained from the accompanying experimental procedure.

In sum, the FEA is a powerful tool that can help podiatrists recognise abnormal stress distribution under the foot in people presenting with foot and ankle disorders. Also it can be used for designing proper footwear for people with HV to redistribute the ground reaction force under the highly loaded area under the foot.

Conclusion and Future work

6.1 Summary

Hallux valgus is the most common deformity of the fore-foot. With its initiation and aggravation, the shape of the bone changes so that it becomes painful when the bone rubs against the inside of the shoe. Moreover, the force pattern under the patient's foot changes as a result of the onset of the deformity and foot function is impaired when the condition worsens. To identify people with HV, in this study the force pattern under the foot of volunteers was analysed while they walked over a pressure mat at two different speeds: a self-selected and a fast speed. More specifically, in order to study plantar force patterns, two groups of volunteers were recruited to the experiments comprising ten individuals with HV and ten without any foot disorders.

In this project, three methods were used to identify the HV condition, including experiments and a simulation. The experiments were carried out to identify the specific plantar force pattern to distinguish patients with HV condition from non-HV individuals. Volunteers' plantar force distributions were obtained for their walking at a self-selected and fast speed.

The methods were as follows:

1) Foot scan (RSscan) and

2) Motion Capture

3) Finite element analysis

Method 1: Foot scan (plantar force measurement). Under this method first the averages of the maximum force that applied under the fore-foot in HV patients was compared to the averages of the maximum force applied under the fore-foot in non-HV patients. This analysis was conducted for both speeds, the force was normalised to the individual's body weight and the time was normalised to 100 frames. Second**,** it was necessary to investigate the transfer changes from one metatarsal to the other metatarsals by using the Markovian chain transfer matrices. The matrix shows how much each metatarsal has a contribution to another one. To achieve this, the

appropriate code was developed in the Matlab software. The generated matrix shows how the data changed from one step to the next step, with regards to time, so the changes of the force in one location of the foot for different time steps is achieved. The matrices were produced for two speeds and capture the force transfer from one metatarsal to the others. Minus numbers in the transfer matrix show that at that particular position there is a negative contribution from one region to another. Third, an independent sample T-test was generated with SPSS software in order to see whether the force distribution under the feet of HV volunteers is significantly different to that of non-HV individuals, for both speeds.

Method 2: The Motion Capture system was used to measure the lateral flexibility of the 1st metatarsal joint. The relative fluctuations between the 1st and 2nd metatarsal joints was measured to see if the higher flexibility in the joint can be used as an indicator of the existence of HV or whether this could even be used as an early recognition signal of the presence of the disease. The ratio of changes in both groups was compared through applying the SPSS software and it confirmed that significant difference existed between the two groups.

Method 3: In Mimics software, two 3D models including 28 bones of the foot were generated using CT scan images of the right foot of two volunteers; one with HV and one without. Subsequently, 3Matic software was used to generate the meshed models and these were imported to Abaqus software for stress analysis. The simulation was carried out and validated with the experimental results of these two volunteers for their feet in the static position.

6.2 Conclusion

The force pattern analysis may have potential for diagnostics for HV this can help surgeons and clinicians to recognise gait problems. All analyses in this study were performed on individuals who were already suffering from the deformity or had been clinically diagnosed with this condition.

According to Milner (2010), HV is recognised as the angulation of the 1st metatarsal to more than 15 degrees. That is to say, every person for whom her/his big toe has an angle of more than 15 degrees is classified as an HV patient. In this project the ten

HV volunteers who were chosen as having this condition had an angle for their 1st metatarsal of at least 15 degrees.

One of the objectives of this study was to investigate the plantar force pattern. The results of the study show that people with this condition had an altered plantar force distribution, more specifically, individuals with the HV condition had a higher force under the hallux than the non-HV volunteers in fast speed. Furthermore, the forces under the 2nd and 3rd metatarsals heads were higher in HV patients than their counterparts, for both walking speeds.

The differences between the two groups of volunteers indicated that they were significantly different from each other in the plantar force distribution. This can assist technicians seeking to design appropriate insoles or footwear for people with HV deformity so as to correct their gait or to reduce the local forces applying to the highly stressed area under the foot. However, once the deformity has occurred, it cannot be reversed so in order to decrease its progression, offering suitable footwear with a roomy toe box may be an option.

Early recognition of the disease is a major issue. HV can be treated or possibly prevented if recognised in the early stages of initiation. The salient aspect of the two main methods proposed in this study is that these have investigated the force transfers among the metatarsals bones. This is a novel approach that has not been undertaken in previous scholarship. Moreover, no previous investigations measured the lateral flexibility of the 1st metatarsal head related to the 2nd metatarsal head, as an indicator of HV condition.

The Motion Capture method used for quantifying the laxity in the 1st metatarsal joint and lateral motion of the 1st and 2nd ones during the walking cycle, is thought to be related to the potential for developing the HV condition and thus may be suitable for application in early diagnostics.

6.3 Research findings

- The average of maximum normalised force for the fore-foot region was compared in HV and non-HV volunteers, for both speeds. The forces under the 2nd, 3rd and 1st metatarsal heads were higher in the HV patients compared to those individuals without HV, for the self-selected speed. However, for the fast speed, the applied force was significantly different compared to the self-selected speed. Although the same locations of the foot showed the highest force, the magnitude of applying force was significantly different from the self-selected speed. That is, by increasing the speed, the applied load increases.
- Force transformation among the five metatarsal regions was investigated by using Markovian chain transfer matrices. It was elicited that the applied force under the foot emerging as a result of ground reaction force was transferred among the metatarsals with different effects and contributions. Some of the metatarsals' contributions to other regions were higher when compared to other regions. That is, some of the metatarsals' effects on other regions were more considerable, in particular regarding the 3rd and 2nd metatarsal regions, for which more contribution was observed.
- The relative movements among the 1st and 2nd metatarsal joints were captured by Motion Capture cameras. It was discovered that the ratio of fluctuations that happened among these regions was significantly higher in HV individuals as compared to non-HV participants. As a result, the joint lateral laxity was higher in HV patients.
- 3D modelling of feet of two different volunteers, with and without HV, were conducted with the boundary condition implemented in the static condition.

The results gave the Von Mises stress distribution under the foot and this data was compared with the individuals' related experiment results that were similarly obtained in the static position.

These experiment results validated the FEA results obtained for both individuals. Specifically, in the HV patient the highest stress, excluding the heel, was reported as under the 2nd, 3rd and 1st metatarsals heads and in her experimental data the highest pressure was discovered under the same region. In the non-HV volunteer the highest

Von Mises stress levels were under the 2nd, 3rd and 4th metatarsal heads and this is similarly seen in her related experiment results.

6.4 Specific contributions of this work

The contribution of this research to science is as follows.

1. Investigating the force transfer contributions among five metatarsals with the Markovian chain transformation matrices is a novel method to figure out the effect of each metatarsal on another. This can be a creative tool for designing an orthopaedic shoe with potential for reducing the plantar force in specific regions of the foot.
2. The measurement of the 1st metatarsal head motion with respect to the 2nd in individuals, with and without the HV condition, is a new contribution to the biomechanical understanding of joint motion when this disease is already developing or is going to be developed. It is a good indicator for early stage diagnosis of the condition.
3. Generating the 3D feet models indicates that in order for the correct stress distribution under the foot to be obtained and made comparable with experimental results, clear definition of the boundary condition is crucial.

6.5 Future work

- Early diagnosis of the HV condition is very important for clinicians so that they can prevent this disease from progressing. Utilising the pressure mat technology is easy, but interpretation and analysing the results from this device can be time consuming. Therefore investigating a new method for analysing force data would appear to be a very pressing need.
- Investigating whether the pressure distribution under the foot changes as a result of deformity initiation or after the deformity has happened is not yet established. To date, there appears to have been no work produced on this matter.
- Defining and implementing the boundary condition in foot 3D modelling plays a fundamental role in the output of the program. To obtain more accurate results than

possible at present, modelling all the ligaments, cartilages as well as connecting these to each other, is an important development that should be considered.

- Applying the Markov chain is a new method for distinguishing the effect of one region of the foot on another, but the interpretation of the matrix elements is difficult due to the dynamic condition of the foot. Achieving a fixed pattern out of the transition matrix which can be used as an indicator of HV is a worthwhile future research undertaking.
- To know whether which people are prone to get this disease, the longitudinal studies in people with genetic inheritance is necessary.
- To study FEA in more appropriate way, the force distribution under the foot should be analysed in dynamic condition.

Appendices

7.1 Appendix A

The Graphs regarding to the transfer force among metatarsals. The effects of all five metatarsals on each other. There were five metatarsal heads regions in which the effect of the transfer coefficient are presented as a sample, the graphs are made from the self-selected speed.

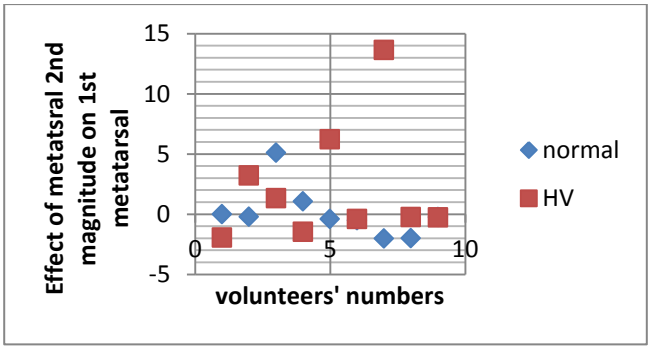

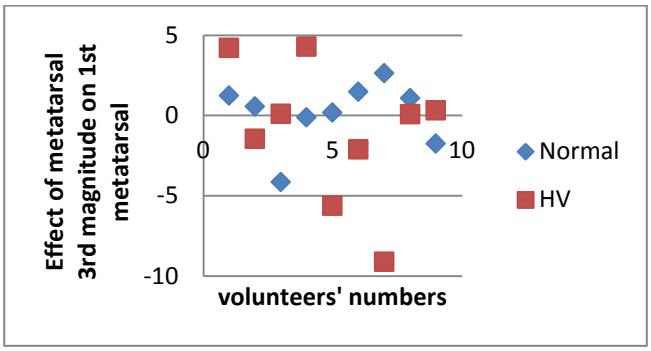

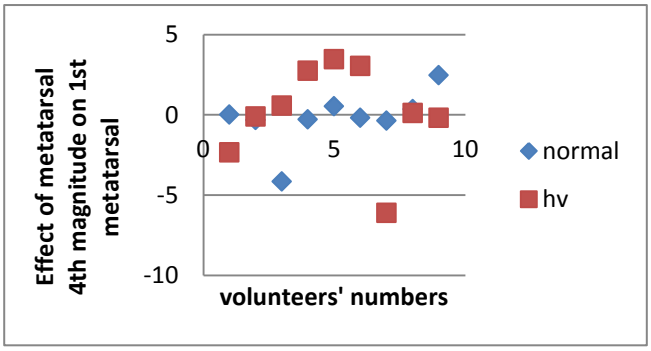

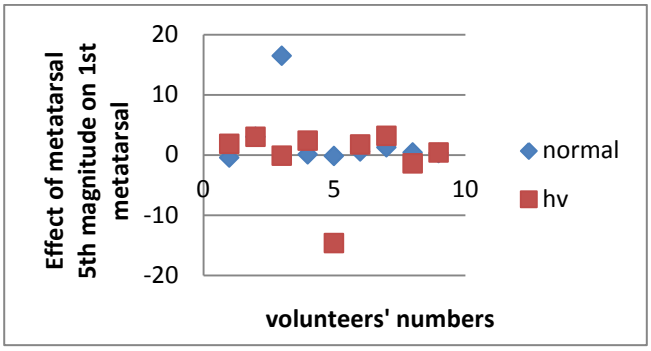

FigureA.1: Four samples of the transfer force pattern in all volunteers which shows the effect of metatarsal 5 on metatarsal 4, 10 with HV and 10 without in self-selected speed.

7.1.1 Fast speed transfer graphs

The four samples graphs are presented in Figure A.2 were obtained to the fast speed of volunteers, which show the dispersion of the data regarding the effect of metatarsal 3 on metatarsal 4. Bigger numbers show higher dispersion of data.

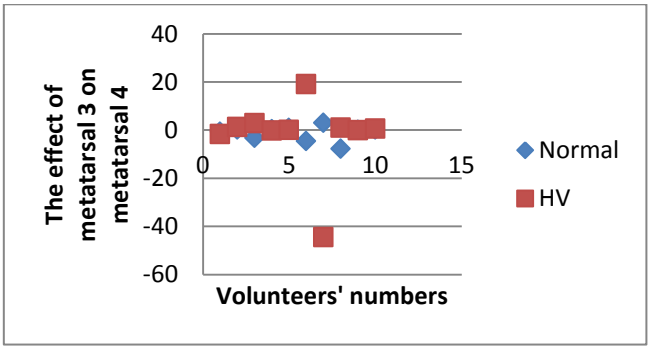

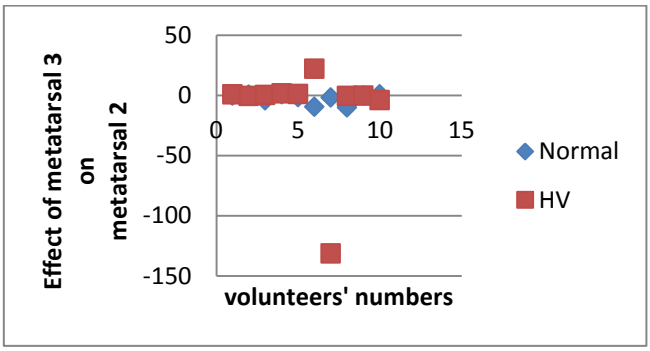

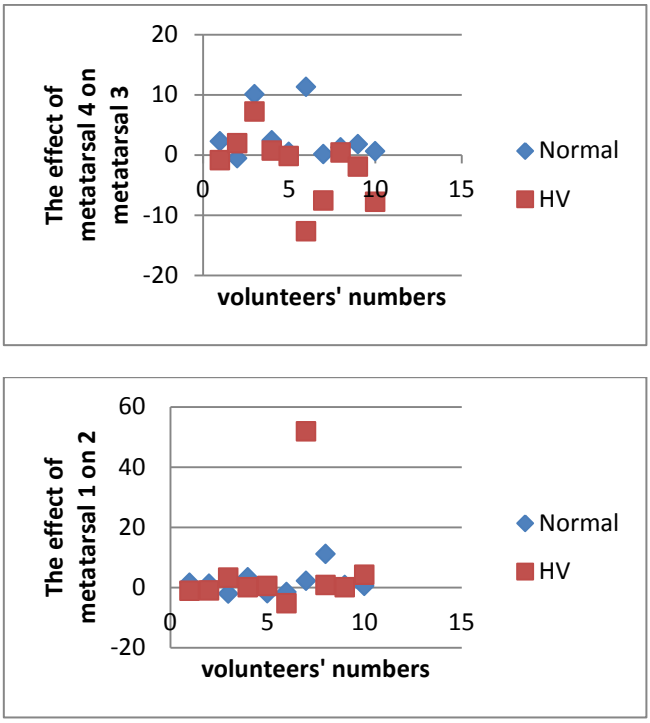

FigureA.2: The transfer force pattern in all volunteers obtained from fast speed data and shows the effect of metatarsal 3 on metatarsal 4, 3 on 2, 4 on 3 and 1 on 2.

7.2 Force raw data obtained with RSscan device in 10 foot anatomical regions

Figure A.3, presents the force raw data that was obtained from the stepping the volunteer's right foot on the pressure mat. The first column shows the number of frames, second column shows the time of stepping the foot on the pressure mat and the rest columns present applied forces under ten anatomical regions of the foot.

frames	time	Toe 1	Toe 2-5	Meta 1	Meta 2	Meta 3	Meta 4	Meta 5	Mid-foot	Heel Medial	Heel Lateral
1	0.269542	0	0	0	0	0	0	0	0	4.190314	6.704503
2	0.539084	0	0	0	0	0	0	0	0	9.218691	15.92319
3	0.808625	0	0	0	0	0	0	0	0	19.27545	31.84639
4	1.078167	0	0	0	0	0	0	0	0	36.45573	56.56924
5	1.347709	0	0	0	0	0	0	0	0	59.50246	84.22532
6	1.617251	0	0	0	0	0	0	0	0	86.7395	116.0717
7	1.886792	0	0	0	0	0	0	0	0	109.3672	137.8613
8	2.156334	0	0	0	0	0	0	0	0	126.9665	152.9465
9	2.425876	0	0	0	0	0	0	0	0	139.1184	159.2319

10	2.695418	0	0	0	0	0	0	0	0	145.4039	162.1652
11	2.96496	0	0	0	0	0	0	0	0	152.1084	162.5842
12	3.234501	0	0	0	0	0	0	0	0	155.8797	163.4223
13	3.504043	0	0	0	0	0	0	0	0	162.5842	164.6793
14	3.773585	0	0	0	0	0	0	0	0.419031	174.7361	170.9648
15	4.043127	0	0	0	0	0	0	0	0.419031	185.2119	178.5074
16	4.312668	0	0	0	0	0	0	0	0.838063	203.2302	188.5641
17	4.58221	0	0	0	0	0	0	0	1.676126	220.8296	196.9448
18	4.851752	0	0	0	0	0	0	0	4.190314	239.686	205.7444
19	5.121294	0	0	0	0	0	0	0	5.86644	253.095	214.9631
20	5.390836	0	0	0	0	0	0	0	7.123534	264.8279	225.0199
21	5.660377	0	0	0	0	0	0	0	10.89482	272.7895	235.0766
22	5.929919	0	0	0	0	0	0	0	16.34223	278.6559	244.2953
23	6.199461	0	0	0	0	0	0	0	21.78963	285.3604	251.8379
24	6.469003	0	0	0	0	0	0	0	30.58929	286.6175	258.9614
25	6.738544	0	0	0	0	0	0	0	40.22702	290.8078	266.085
26	7.008086	0	0	0	0	0	0	0	53.21699	293.322	271.1133
27	7.277628	0	0	0	0	0	0	0	68.30212	292.0649	276.1417
28	7.54717	0	0	0	0	0	1.257094	0	86.32047	291.6459	281.1701
29	7.816712	0	0	0	0	0	3.352251	0.419031	104.3388	292.4839	284.1033
30	8.086253	0	0	0	0	0.419031	5.028377	1.257094	123.1952	290.3888	286.1985
31	8.355795	0	0	0	0	0.419031	6.285471	1.676126	138.2804	290.3888	285.3604
32	8.625337	0	0	0	0	0.419031	7.123534	1.676126	152.9465	289.5507	285.3604
33	8.894879	0	0	0	0	1.257094	9.218691	2.93322	167.6126	291.2268	283.2652
34	9.16442	0	0	0	0	2.095157	10.47579	2.93322	179.7645	288.7126	281.1701
35	9.433962	0	0	0	0	2.095157	11.73288	4.190314	191.4974	289.9697	277.3988
36	9.703504	0	0	0	0	3.352251	12.57094	4.190314	203.6493	289.5507	273.2085
37	9.973046	0	0	0	0	4.190314	12.57094	4.190314	213.287	291.2268	271.1133
38	10.24259	0	0	0	0	4.609346	13.82804	4.609346	221.2486	289.9697	266.504
39	10.51213	0	0	0	0	5.028377	13.82804	4.609346	225.8579	292.4839	264.8279
40	10.78167	0	0	0	0	5.86644	14.6661	4.609346	232.1434	292.0649	263.9898
41	11.05121	0	0	0	0	6.285471	15.08513	4.609346	238.8479	292.903	262.7327
42	11.32075	0	0	0	0	6.285471	15.08513	4.609346	238.4289	294.9981	261.0566
43	11.5903	0	0	0	0.419031	6.285471	15.08513	4.609346	243.4573	297.5123	260.6375
44	11.85984	0	0	0	0.419031	6.285471	15.08513	4.190314	244.7143	299.1884	260.2185
45	12.12938	0	0	0	0.419031	7.542566	16.76126	4.190314	245.5524	298.3504	258.9614
46	12.39892	0	0	0	0.419031	9.637723	17.18029	4.190314	248.9047	297.5123	258.1234
47	12.66846	0	0	0	0.838063	9.637723	17.18029	4.190314	251.8379	297.9313	256.4472
48	12.93801	0	0	0	0.838063	10.05675	17.18029	4.190314	251.8379	297.5123	255.6092
49	13.20755	0	0	0	0.838063	10.89482	17.18029	4.190314	253.514	298.3504	255.6092
50	13.47709	0	0	0	0.838063	10.89482	17.18029	4.190314	255.6092	297.0933	253.095
51	13.74663	0	0	0	1.257094	11.31385	17.18029	4.190314	256.8663	292.903	251.8379
52	14.01617	0	0	0	1.676126	10.47579	17.18029	4.190314	258.9614	291.2268	249.3237
53	14.28571	0	0	0	2.095157	10.47579	17.18029	4.190314	262.7327	290.8078	247.6476

54	14.55526	0	0	0	2.095157	10.47579	17.18029	4.190314	262.7327	288.7126	246.3905
55	14.8248	0	0	0	2.095157	10.47579	17.18029	4.190314	266.085	284.1033	245.5524
56	15.09434	0	0	0	2.514189	10.47579	17.18029	4.190314	266.923	281.5891	245.1334
57	15.36388	0	0	0	2.514189	10.89482	17.18029	4.190314	267.7611	281.1701	243.0382
58	15.63342	0	0	0	2.514189	11.31385	18.43738	4.190314	269.0182	279.913	243.8763
59	15.90296	0	0	0	2.514189	11.31385	19.69448	4.190314	269.8562	279.494	243.4573
60	16.17251	0	0	0	2.514189	11.31385	19.69448	4.190314	274.0465	277.8178	242.6192
61	16.44205	0	0	0	2.514189	11.31385	18.85641	4.190314	278.2369	277.8178	243.8763
62	16.71159	0	0	0	2.514189	11.31385	18.85641	4.609346	282.0081	277.8178	243.0382
63	16.98113	0	0	0	2.93322	11.31385	18.85641	4.609346	280.7511	276.9798	243.0382
64	17.25067	0	0	0	2.93322	11.73288	17.59932	4.609346	281.1701	276.5607	240.9431
65	17.52022	0	0	0	2.93322	11.73288	17.59932	4.609346	281.1701	276.9798	239.686
66	17.78976	0	0	0	2.93322	12.57094	17.59932	4.609346	279.494	276.5607	239.686
67	18.0593	0	0	0	2.93322	12.98997	17.59932	4.609346	279.913	276.1417	239.686
68	18.32884	0	0	0	3.352251	12.98997	17.59932	4.609346	279.494	275.7227	238.8479
69	18.59838	0	0	0	3.352251	12.98997	17.59932	4.190314	280.332	275.7227	238.4289
70	18.86792	0	0	0	3.352251	12.98997	17.59932	4.190314	281.1701	274.4656	235.9147
71	19.13747	0	0	0	3.352251	12.98997	17.59932	4.190314	282.0081	274.0465	235.0766
72	19.40701	0	0	0	4.190314	12.98997	17.59932	4.190314	282.0081	273.6275	235.0766
73	19.67655	0	0	0	4.190314	12.98997	17.59932	4.190314	282.0081	271.5324	235.4957
74	19.94609	0	0	0	4.190314	12.98997	17.59932	4.190314	280.7511	271.5324	234.2386
75	20.21563	0	0	0	4.190314	12.98997	17.59932	4.190314	280.7511	271.5324	233.4005
76	20.48518	0	0	0	4.190314	12.98997	17.59932	4.190314	282.0081	272.3704	233.4005
77	20.75472	0	0	0	4.190314	12.98997	17.59932	4.190314	281.5891	271.5324	233.8195
78	21.02426	0	0	0	4.609346	12.98997	17.59932	4.190314	282.8462	272.3704	234.6576
79	21.2938	0	0	0	4.609346	12.98997	17.59932	4.190314	282.0081	272.3704	233.8195
80	21.56334	0	0	0	4.609346	12.98997	17.59932	4.190314	282.4272	271.5324	232.5624
81	21.83288	0	0	0	4.609346	12.98997	18.01835	4.190314	282.4272	272.7895	232.1434
82	22.10243	0	0	0	4.609346	12.98997	17.59932	4.190314	283.2652	272.3704	231.3053
83	22.37197	0	0	0.419031	4.190314	12.98997	17.59932	4.190314	283.2652	272.3704	231.7244
84	22.64151	0	0	0.838063	4.190314	12.98997	17.59932	4.190314	283.6843	274.0465	230.8863
85	22.91105	0	0	0.838063	4.190314	13.40901	18.01835	4.190314	282.4272	273.6275	231.3053
86	23.18059	0	0	0.838063	5.447408	13.40901	18.01835	4.190314	282.0081	273.6275	230.8863
87	23.45013	0	0	0.838063	6.704503	13.40901	18.01835	4.190314	282.8462	273.6275	229.6292
88	23.71968	0	0	0.838063	7.123534	13.40901	18.01835	4.190314	284.1033	272.7895	228.7912
89	23.98922	0	0	0.838063	7.123534	13.40901	18.01835	4.190314	284.5223	273.6275	229.2102
90	24.25876	0	0	0.838063	7.123534	13.40901	18.01835	4.190314	283.6843	273.6275	228.3721
91	24.5283	0	0	0.838063	7.123534	13.40901	18.01835	4.190314	283.2652	275.7227	228.7912
92	24.79784	0	0	0.838063	7.123534	13.82804	18.01835	4.190314	284.5223	277.3988	228.3721
93	25.06739	0	0	0.838063	7.123534	13.82804	18.01835	4.190314	286.1985	276.9798	227.9531
94	25.33693	0	0	1.257094	7.542566	13.82804	18.01835	4.190314	285.7794	276.5607	225.8579
95	25.60647	0	0	2.095157	7.542566	13.82804	18.01835	4.190314	287.0365	275.7227	225.8579
96	25.87601	0	0	2.514189	7.961597	14.6661	18.01835	4.190314	286.1985	276.1417	225.4389
97	26.14555	0	0	2.514189	7.961597	14.6661	18.01835	4.190314	286.1985	276.1417	224.6008

98	26.41509	0	0	2.514189	7.961597	15.92319	18.43738	4.190314	286.1985	276.5607	224.6008
99	26.68464	0.419031	0	2.514189	8.79966	15.92319	18.43738	4.190314	286.1985	276.5607	223.7628
100	26.95418	0.419031	0	2.93322	8.79966	15.92319	18.43738	4.190314	288.2936	276.9798	224.1818
101	27.22372	0.419031	0	2.93322	9.218691	15.92319	18.43738	4.190314	289.1317	276.9798	224.1818
102	27.49326	0.419031	0	2.93322	9.218691	15.92319	18.43738	4.190314	290.8078	277.3988	225.0199
103	27.7628	0.419031	0	2.93322	9.218691	15.92319	18.43738	4.190314	291.6459	277.3988	224.6008
104	28.03235	0.419031	0	2.93322	9.218691	15.92319	18.43738	4.190314	291.6459	277.8178	224.6008
105	28.30189	0.419031	0	3.352251	9.637723	15.92319	18.01835	4.190314	289.5507	279.0749	223.7628
106	28.57143	0.419031	0	3.352251	9.637723	15.92319	18.01835	4.190314	289.9697	279.0749	223.3437
107	28.84097	0.419031	0	3.771283	9.637723	15.92319	18.01835	4.190314	291.6459	278.2369	223.3437
108	29.11051	0.419031	0	4.190314	9.637723	15.92319	18.01835	4.190314	291.6459	278.2369	222.0867
109	29.38005	0.419031	0	4.190314	9.637723	15.92319	18.01835	4.190314	291.6459	277.3988	222.0867
110	29.6496	0.419031	0	4.190314	10.05675	15.92319	18.01835	4.190314	292.4839	276.1417	221.2486
111	29.91914	0.419031	0	4.190314	10.05675	15.92319	18.01835	4.190314	292.4839	276.1417	219.9915
112	30.18868	0.419031	0	4.190314	10.05675	15.92319	18.01835	4.190314	292.4839	276.1417	219.9915
113	30.45822	0.419031	0	4.609346	10.05675	16.34223	18.01835	4.190314	293.322	276.1417	219.9915
114	30.72776	0.419031	0	4.609346	10.05675	16.34223	18.01835	4.190314	294.5791	275.7227	219.5725
115	30.9973	0.419031	0	4.609346	10.05675	16.34223	18.01835	4.190314	293.741	275.7227	218.3154
116	31.26685	0.419031	0	4.609346	10.05675	16.34223	18.01835	4.190314	293.741	274.4656	217.4773
117	31.53639	0.419031	0	5.028377	10.05675	16.76126	18.01835	4.190314	294.5791	274.0465	218.3154
118	31.80593	0.419031	0	5.86644	10.47579	17.18029	18.43738	4.190314	294.9981	272.7895	216.6392
119	32.07547	0.419031	0	5.86644	10.47579	17.18029	18.43738	4.190314	294.9981	272.7895	215.8012
120	32.34501	0.419031	0	5.86644	11.73288	17.18029	18.85641	4.190314	295.4172	272.7895	214.9631
121	32.61456	0.419031	0	5.86644	11.73288	17.18029	18.85641	4.190314	296.2552	271.9514	214.9631
122	32.8841	0.419031	0	5.86644	11.73288	17.18029	18.85641	4.190314	297.5123	271.1133	214.9631
123	33.15364	0.419031	0	6.285471	11.73288	17.18029	18.85641	4.190314	297.5123	268.5991	214.9631
124	33.42318	0.419031	0	6.704503	12.15191	17.59932	18.85641	4.190314	297.9313	268.5991	214.5441
125	33.69272	0	0	6.704503	12.15191	17.59932	18.85641	4.190314	298.3504	268.1801	214.5441
126	33.96226	0	0	6.704503	12.15191	17.59932	18.85641	4.190314	299.1884	266.504	214.1251
127	34.23181	0	0	6.704503	12.15191	17.59932	18.85641	4.190314	300.0265	265.6659	214.1251
128	34.50135	0	0	6.704503	12.15191	17.59932	18.85641	4.190314	301.2836	264.4088	211.6109
129	34.77089	0	0	6.704503	12.15191	17.59932	18.85641	4.190314	301.7026	263.9898	211.6109
130	35.04043	0	0	6.704503	12.15191	17.59932	18.85641	4.190314	302.5407	263.9898	210.7728
131	35.30997	0	0	6.704503	12.15191	17.59932	18.85641	4.190314	303.7978	260.6375	208.6776
132	35.57951	0	0	6.704503	13.40901	18.01835	18.85641	4.190314	304.6358	259.3804	206.5825
133	35.84906	0	0	7.123534	14.24707	18.43738	18.85641	4.190314	307.5691	255.1901	205.7444
134	36.1186	0	0	7.123534	14.24707	18.43738	18.85641	4.190314	306.731	252.6759	205.3254
135	36.38814	0	0	7.123534	14.24707	18.43738	19.27545	4.190314	306.312	250.1618	204.0683
136	36.65768	0	0	7.123534	14.24707	19.69448	19.27545	4.190314	305.4739	248.4856	201.9731
137	36.92722	0	0	7.123534	14.24707	19.69448	19.27545	4.190314	310.9213	247.6476	201.1351
138	37.19677	0	0	7.123534	15.92319	20.95157	19.27545	4.190314	311.7594	246.3905	200.297
139	37.46631	0	0	7.123534	16.34223	20.95157	19.69448	4.609346	312.1784	244.2953	199.878
140	37.73585	0	0	7.542566	16.76126	21.78963	20.95157	4.609346	313.4355	240.105	196.9448
141	38.00539	0	0	8.380628	16.76126	21.78963	20.95157	4.609346	314.6926	239.2669	196.1067

142	38.27493	0	0	8.79966	16.76126	22.6277	20.53254	4.609346	316.3687	237.1718	194.4306
143	38.54447	0	0	9.218691	18.01835	22.6277	20.53254	4.609346	319.721	235.0766	193.5925
144	38.81402	0	0	9.218691	18.43738	22.6277	20.53254	4.609346	318.0448	229.6292	188.9832
145	39.08356	0	0	9.218691	19.27545	23.46576	21.3706	5.028377	320.14	227.115	188.1451
146	39.3531	0	0	9.218691	19.27545	23.46576	21.3706	5.447408	320.9781	224.1818	186.469
147	39.62264	0	0	9.218691	20.53254	23.46576	21.3706	5.447408	323.4923	221.6676	185.6309
148	39.89218	0	0	9.218691	20.53254	24.30382	22.20867	5.447408	326.4255	219.9915	182.6977
149	40.16173	0	0	9.637723	21.3706	24.72285	23.46576	5.447408	327.6826	215.3822	180.1835
150	40.43127	0	0	9.637723	21.78963	25.14189	23.46576	5.86644	328.1016	214.9631	179.3454
151	40.70081	0	0	9.637723	21.78963	25.97995	23.46576	5.86644	330.1968	212.868	177.6693
152	40.97035	0	0	10.47579	23.46576	26.81801	23.46576	5.86644	332.2919	211.1918	174.7361
153	41.23989	0	0	10.89482	24.30382	26.81801	23.46576	5.86644	332.7109	206.1635	173.898
154	41.50943	0	0	10.89482	24.30382	28.49414	23.88479	5.86644	333.13	201.9731	170.1268
155	41.77898	0	0	10.89482	25.14189	29.3322	23.88479	5.86644	334.3871	200.297	168.4506
156	42.04852	0	0	11.73288	25.56092	30.58929	23.88479	5.86644	337.3203	199.459	164.6793
157	42.31806	0	0	11.73288	25.56092	31.00833	25.14189	5.86644	339.8345	198.2019	163.8413
158	42.5876	0	0	11.73288	27.65607	31.84639	25.56092	5.86644	343.6058	193.1735	162.1652
159	42.85714	0	0	11.73288	28.07511	33.52251	26.39898	5.86644	344.8629	191.0783	160.07
160	43.12668	0	0	12.15191	29.3322	33.52251	27.23704	5.86644	346.12	188.1451	158.8129
161	43.39623	0	0	12.15191	30.17026	33.94155	28.49414	5.86644	347.7961	184.7929	156.2987
162	43.66577	0	0	12.15191	30.58929	34.36058	28.49414	5.86644	347.7961	181.8596	153.7845
163	43.93531	0	0	12.98997	31.42736	34.77961	28.49414	5.86644	350.7293	178.9264	150.4323
164	44.20485	0	0	12.98997	32.68445	36.45573	29.3322	5.86644	353.6625	175.9932	148.7562
165	44.47439	0	0	12.98997	32.68445	37.71283	30.17026	5.86644	355.7577	173.06	146.661
166	44.74394	0	0	12.98997	36.0367	38.96992	30.17026	5.86644	359.529	169.7077	144.1468
167	45.01348	0	0	13.82804	36.87477	40.64605	30.17026	7.123534	358.6909	164.6793	142.8897
168	45.28302	0	0	13.82804	38.13186	41.90314	31.00833	7.123534	359.1099	161.3271	139.9565
169	45.55256	0	0	13.82804	38.96992	43.16024	31.84639	7.123534	359.529	160.9081	137.0233
170	45.8221	0	0	13.82804	40.22702	43.16024	32.26542	7.123534	359.948	155.4607	134.9281
171	46.09164	0	0	14.24707	41.90314	44.41733	33.10348	7.542566	358.2719	154.2036	132.833
172	46.36119	0	0	14.6661	42.32217	46.09346	33.10348	7.961597	361.6241	150.4323	131.1568
173	46.63073	0	0	14.6661	43.16024	46.93152	33.94155	7.961597	362.0431	145.4039	126.9665
174	46.90027	0	0	14.6661	44.41733	48.18861	33.94155	7.961597	362.8812	140.7946	126.1285
175	47.16981	0	0	14.6661	44.83636	48.18861	35.61767	8.79966	363.3002	138.2804	122.7762
176	47.43935	0	0	15.50416	46.09346	48.60765	35.61767	8.79966	363.7193	135.7662	119.0049
177	47.70889	0	0	16.34223	46.09346	48.60765	36.0367	8.79966	365.3954	132.4139	117.3288
178	47.97844	0.419031	0	16.76126	46.93152	50.28377	36.45573	10.05675	367.9096	129.4807	114.8146
179	48.24798	0.419031	0	16.76126	48.60765	51.9599	36.87477	10.05675	367.0715	127.3856	109.7862
180	48.51752	0.419031	0	17.18029	48.60765	52.37893	37.2938	10.05675	368.3286	121.9381	106.853
181	48.78706	0.419031	0	18.85641	51.12183	53.21699	38.55089	10.05675	368.7477	119.843	104.7579
182	49.0566	0.419031	0	19.27545	52.79796	54.89312	39.38895	10.47579	364.9764	115.2336	102.2437
183	49.32615	0.419031	0	19.27545	54.05505	56.56924	40.22702	10.47579	362.8812	111.8814	98.05335
184	49.59569	0.419031	0	19.69448	54.89312	56.56924	41.06508	10.47579	361.6241	108.9482	95.9582
185	49.86523	0.419031	0	20.11351	56.98827	57.82634	41.90314	10.47579	359.1099	103.5008	93.02498

186	50.13477	0.419031	0	20.11351	56.98827	60.34052	41.90314	10.89482	359.948	99.72948	90.09176
187	50.40431	0.419031	0	21.3706	60.75956	62.85471	43.16024	10.89482	361.6241	97.21529	85.48241
188	50.67385	0.838063	0	21.78963	60.75956	64.11181	43.16024	10.89482	360.7861	96.37723	82.96822
189	50.9434	0.838063	0	23.04673	60.75956	64.94987	45.25539	11.31385	359.948	92.18691	79.19694
190	51.21294	0.838063	0	25.56092	63.69278	66.626	47.35055	11.73288	360.7861	88.83466	77.52081
191	51.48248	0.838063	0	25.56092	64.53084	67.46406	47.76958	11.73288	358.6909	85.06338	74.58759
192	51.75202	0.838063	0	25.97995	65.78793	68.30212	48.60765	12.15191	358.6909	82.13016	70.39728
193	52.02156	1.257094	0	26.81801	67.46406	68.72115	48.60765	12.15191	354.9196	78.77791	68.72115
194	52.29111	1.257094	0	26.81801	68.30212	72.49244	50.28377	13.82804	351.5674	75.84469	66.626
195	52.56065	1.257094	0	27.65607	70.81631	72.91147	50.7028	14.6661	351.5674	71.65437	61.59762
196	52.83019	1.257094	0	28.07511	74.16856	74.58759	50.7028	15.08513	350.7293	67.04503	59.92149
197	53.09973	1.676126	0	28.49414	75.42566	75.84469	51.54087	15.08513	347.7961	64.11181	56.15021
198	53.36927	2.514189	0	28.91317	76.68275	76.26372	51.54087	15.08513	343.1867	62.01665	53.63602
199	53.63881	2.514189	0	29.75123	77.93984	76.68275	51.9599	15.08513	341.0916	59.50246	52.37893
200	53.90836	2.93322	0.419031	30.17026	81.71113	78.77791	53.63602	15.08513	337.7393	53.63602	50.28377
201	54.1779	2.93322	0.419031	31.42736	82.13016	79.19694	54.05505	15.08513	337.7393	52.37893	46.09346
202	54.44744	3.771283	0.838063	33.94155	82.96822	81.2921	55.31215	15.50416	335.2251	50.28377	43.57927
203	54.71698	3.771283	1.257094	35.19864	85.06338	84.22532	55.73118	15.50416	332.2919	47.35055	41.06508
204	54.98652	3.771283	1.257094	36.87477	86.32047	85.48241	58.24537	15.50416	328.1016	42.74121	38.96992
205	55.25606	3.771283	1.257094	37.71283	87.15854	87.15854	59.92149	15.92319	324.7494	39.80799	36.45573
206	55.52561	3.771283	1.257094	38.13186	90.51079	88.41563	60.34052	15.92319	322.2352	38.13186	33.52251
207	55.79515	4.190314	1.676126	38.13186	91.76788	88.83466	62.01665	15.92319	318.8829	33.94155	31.84639
208	56.06469	4.190314	1.676126	38.13186	94.28207	91.76788	62.01665	15.92319	316.7878	31.00833	30.17026
209	56.33423	5.028377	1.676126	38.13186	94.28207	93.44401	62.85471	17.59932	315.1116	30.17026	28.07511
210	56.60377	5.447408	1.676126	38.96992	96.37723	94.7011	63.69278	17.59932	315.1116	28.07511	24.72285
211	56.87332	5.447408	1.676126	39.38895	98.05335	96.79626	63.69278	17.59932	310.0833	27.65607	23.46576
212	57.14286	6.704503	1.676126	40.22702	100.9866	98.05335	64.11181	18.01835	306.731	24.72285	23.04673
213	57.4124	6.704503	1.676126	41.48411	103.0817	98.47238	64.11181	18.01835	302.9597	23.04673	19.69448
214	57.68194	7.123534	1.676126	43.16024	104.3388	101.8246	66.20696	18.43738	300.8646	22.20867	18.85641
215	57.95148	7.123534	2.095157	44.41733	106.853	102.6627	66.20696	18.43738	298.7694	20.11351	16.34223
216	58.22102	7.961597	2.095157	46.51249	108.5291	102.6627	67.46406	18.43738	296.6742	16.76126	15.50416
217	58.49057	7.961597	2.514189	47.35055	109.3672	105.5959	68.72115	18.43738	292.903	16.34223	15.50416
218	58.76011	8.380628	2.514189	48.60765	111.0433	108.1101	68.72115	18.43738	291.2268	15.08513	13.82804
219	59.02965	8.380628	2.514189	49.02668	111.8814	109.7862	71.65437	18.43738	286.6175	13.40901	13.40901
220	59.29919	9.637723	2.514189	49.02668	114.3956	109.7862	72.49244	18.43738	284.9414	12.98997	11.31385
221	59.56873	9.637723	2.514189	49.02668	115.6527	111.0433	75.00662	18.43738	284.1033	11.73288	10.47579
222	59.83827	10.89482	2.514189	49.44571	117.7478	112.7195	75.42566	18.85641	279.494	11.73288	8.79966
223	60.10782	11.31385	2.514189	51.9599	119.843	115.2336	76.26372	18.85641	275.7227	10.05675	8.380628
224	60.37736	11.31385	2.514189	51.9599	120.681	117.7478	76.68275	18.85641	274.0465	7.542566	7.123534
225	60.6469	11.73288	2.514189	52.37893	124.4523	121.5191	76.68275	19.27545	272.3704	6.704503	5.028377
226	60.91644	12.57094	2.514189	53.63602	127.8046	122.7762	77.93984	19.27545	272.3704	6.704503	5.028377
227	61.18598	12.57094	2.514189	54.47409	129.0617	124.0333	77.93984	19.27545	268.5991	6.285471	5.028377
228	61.45553	12.98997	2.514189	54.89312	131.1568	126.1285	79.19694	19.69448	263.9898	4.609346	4.609346
229	61.72507	12.98997	2.514189	55.31215	134.0901	127.8046	79.61597	19.69448	263.1517	3.352251	2.095157

230	61.99461	15.08513	2.93322	55.73118	134.9281	129.8997	80.035	20.11351	256.8663	3.352251	2.095157
231	62.26415	15.50416	3.771283	57.40731	137.4423	131.1568	81.71113	20.11351	254.7711	2.93322	2.095157
232	62.53369	15.50416	3.771283	59.92149	140.7946	132.833	82.54919	20.11351	250.9998	2.514189	1.676126
233	62.80323	16.76126	3.771283	62.01665	145.4039	135.3471	83.80628	21.3706	250.5808	1.676126	1.257094
234	63.07278	16.76126	3.771283	62.01665	147.4991	137.0233	85.90144	21.3706	250.9998	1.257094	0.838063
235	63.34232	17.59932	4.190314	63.27374	148.3371	141.6326	85.90144	21.3706	250.1618	0.419031	0.419031
236	63.61186	18.85641	4.190314	63.27374	151.2703	141.6326	85.90144	21.78963	246.3905	0.419031	0.419031
237	63.8814	20.11351	4.190314	64.11181	155.0416	142.0517	87.57757	21.78963	244.2953	0	0
238	64.15094	21.3706	4.609346	65.3689	156.7178	144.5658	87.9966	21.78963	241.3621	0	0
239	64.42049	21.3706	5.447408	67.04503	157.5558	150.0132	90.09176	21.78963	238.4289	0	0
240	64.69003	22.20867	5.447408	67.88309	160.07	152.1084	90.92982	21.78963	235.4957	0	0
241	64.95957	23.04673	5.86644	70.81631	165.0984	153.7845	90.92982	21.78963	233.4005	0	0
242	65.22911	22.6277	5.86644	71.23534	168.4506	154.6226	91.76788	21.78963	228.7912	0	0
243	65.49865	24.72285	6.285471	72.0734	169.7077	160.07	93.44401	22.6277	225.4389	0	0
244	65.76819	25.56092	6.704503	74.58759	172.6409	162.5842	95.53916	23.04673	222.9247	0	0
245	66.03774	25.97995	7.123534	75.42566	174.7361	164.6793	97.21529	24.30382	221.6676	0	0
246	66.30728	26.81801	7.123534	75.42566	177.6693	166.3555	98.05335	24.30382	217.8963	0	0
247	66.57682	27.23704	7.123534	77.93984	181.0216	169.7077	100.9866	24.30382	214.1251	0	0
248	66.84636	28.49414	7.123534	80.87306	184.7929	170.9648	101.4056	25.97995	209.9347	0	0
249	67.1159	30.17026	7.123534	80.87306	186.469	173.479	102.6627	25.97995	207.0015	0	0
250	67.38544	31.42736	7.123534	82.13016	189.8212	176.4122	104.3388	25.97995	201.5541	0	0
251	67.65499	31.84639	8.380628	83.80628	191.4974	180.6025	106.434	26.39898	196.9448	0	0
252	67.92453	34.36058	8.380628	84.64435	195.6877	183.1167	108.5291	26.39898	192.3354	0	0
253	68.19407	36.45573	8.380628	88.41563	198.6209	186.888	109.7862	26.39898	188.9832	0	0
254	68.46361	36.45573	8.79966	90.51079	201.9731	188.9832	110.6243	26.81801	180.1835	0	0
255	68.73315	38.55089	10.89482	90.51079	205.7444	190.2403	110.6243	27.23704	176.8313	0	0
256	69.0027	41.48411	10.89482	93.02498	208.2586	192.7545	113.1385	27.23704	174.7361	0	0
257	69.27224	42.32217	10.89482	93.44401	209.9347	196.1067	113.1385	27.23704	168.0316	0	0
258	69.54178	44.83636	10.89482	93.86304	215.8012	200.7161	114.8146	27.23704	163.0032	0	0
259	69.81132	46.51249	12.15191	95.12013	217.8963	204.0683	116.4907	28.07511	159.651	0	0
260	70.08086	46.93152	13.40901	95.12013	219.9915	204.9064	118.1669	28.07511	153.7845	0	0
261	70.3504	49.86474	13.40901	95.53916	222.5057	209.5157	118.5859	28.49414	149.1752	0	0
262	70.61995	51.54087	14.24707	98.05335	224.6008	212.4489	120.681	28.49414	145.4039	0	0
263	70.88949	54.05505	16.34223	99.72948	226.277	215.3822	122.3572	28.49414	140.3755	0	0
264	71.15903	56.56924	16.34223	100.1485	229.2102	219.9915	124.4523	28.49414	135.3471	0	0
265	71.42857	57.40731	17.18029	102.2437	234.2386	220.8296	126.9665	28.91317	125.7094	0	0
266	71.69811	58.24537	18.01835	102.2437	237.5908	222.9247	128.2236	28.91317	121.5191	0	0
267	71.96765	61.59762	19.27545	103.0817	240.105	226.277	129.0617	29.3322	116.4907	0	0
268	72.2372	62.85471	20.95157	104.3388	240.9431	227.9531	129.0617	29.3322	110.2053	0	0
269	72.50674	66.20696	22.6277	104.3388	243.0382	232.9815	132.833	28.91317	105.1769	0	0
270	72.77628	67.46406	22.6277	104.3388	246.3905	236.7528	134.5091	30.17026	101.4056	0	0
271	73.04582	70.81631	23.88479	104.3388	246.8095	238.8479	134.5091	30.17026	92.60594	0	0
272	73.31536	72.91147	24.30382	104.3388	250.1618	243.0382	136.6042	29.75123	87.57757	0	0
273	73.58491	75.84469	25.56092	105.1769	252.2569	243.8763	138.2804	30.17026	81.2921	0	0

274	73.85445	78.35888	25.56092	106.853	253.514	248.4856	139.5375	30.17026	75.00662	0	0
275	74.12399	80.45403	26.81801	106.853	255.6092	249.7427	140.7946	29.75123	70.81631	0	0
276	74.39353	82.54919	26.81801	107.272	258.5424	248.9047	142.8897	30.17026	65.78793	0	0
277	74.66307	85.90144	28.49414	106.853	262.7327	253.933	144.9849	30.17026	58.6644	0	0
278	74.93261	87.57757	29.3322	106.853	263.5708	256.8663	146.242	30.17026	54.47409	0	0
279	75.20216	89.67272	29.75123	107.272	263.9898	258.9614	148.3371	31.42736	48.60765	0	0
280	75.4717	90.92982	31.00833	107.6911	264.4088	261.4756	150.0132	31.00833	44.83636	0	0
281	75.74124	93.02498	32.26542	108.1101	266.923	261.8946	152.5274	31.00833	39.80799	0	0
282	76.01078	94.7011	33.94155	109.3672	269.8562	263.5708	152.1084	31.42736	36.87477	0	0
283	76.28032	96.37723	34.36058	109.3672	271.9514	266.085	152.5274	31.00833	33.10348	0	0
284	76.54987	98.05335	36.0367	109.3672	271.9514	269.0182	153.7845	32.26542	28.91317	0	0
285	76.81941	102.2437	36.45573	109.3672	271.5324	270.6943	155.8797	32.68445	24.30382	0	0
286	77.08895	105.1769	37.71283	105.5959	272.3704	271.9514	156.2987	31.84639	21.3706	0	0
287	77.35849	105.5959	37.71283	105.5959	271.9514	275.3036	158.8129	31.84639	19.27545	0	0
288	77.62803	110.2053	38.55089	105.1769	272.7895	275.7227	159.2319	31.84639	16.76126	0	0
289	77.89757	111.8814	40.22702	104.3388	272.7895	279.0749	161.3271	31.00833	13.82804	0	0
290	78.16712	113.9765	41.06508	103.0817	273.2085	279.913	162.1652	31.42736	12.15191	0	0
291	78.43666	116.9098	42.74121	102.6627	273.6275	279.494	162.5842	31.42736	8.79966	0	0
292	78.7062	118.1669	42.74121	101.8246	273.6275	280.332	163.0032	29.3322	7.961597	0	0
293	78.97574	121.9381	43.9983	99.31045	275.3036	282.4272	163.0032	29.3322	4.609346	0	0
294	79.24528	123.6143	44.83636	99.31045	275.7227	283.2652	164.2603	29.3322	3.771283	0	0
295	79.51482	124.0333	45.67443	97.21529	274.8846	283.2652	165.0984	28.49414	3.352251	0	0
296	79.78437	126.9665	46.51249	96.37723	274.0465	284.5223	164.6793	27.65607	3.352251	0	0
297	80.05391	129.0617	46.51249	95.53916	272.7895	285.7794	163.4223	27.23704	1.257094	0	0
298	80.32345	131.9949	47.35055	95.53916	271.1133	284.1033	162.5842	25.97995	0.838063	0	0
299	80.59299	133.671	48.18861	95.12013	271.9514	284.1033	163.8413	25.56092	0.838063	0	0
300	80.86253	135.7662	49.44571	92.18691	271.9514	283.2652	161.7461	24.72285	0.838063	0	0
301	81.13208	137.8613	49.44571	90.92982	270.2753	282.4272	159.651	24.30382	0.419031	0	0
302	81.40162	139.9565	51.54087	89.25369	269.0182	282.8462	157.9748	21.78963	0	0	0
303	81.67116	141.2136	51.9599	86.7395	266.504	282.4272	157.1368	21.3706	0	0	0
304	81.9407	144.1468	52.79796	84.22532	267.7611	280.7511	156.7178	20.11351	0	0	0
305	82.21024	145.4039	52.79796	84.22532	267.342	280.7511	152.9465	19.27545	0	0	0
306	82.47978	148.7562	52.37893	80.87306	266.085	278.2369	150.8513	17.59932	0	0	0
307	82.74933	152.5274	53.63602	80.45403	264.4088	276.1417	147.4991	15.92319	0	0	0
308	83.01887	154.2036	54.47409	79.19694	262.7327	273.6275	143.7278	14.6661	0	0	0
309	83.28841	155.4607	54.47409	77.93984	259.7995	269.8562	138.6994	13.40901	0	0	0
310	83.55795	156.7178	54.47409	77.10178	257.7043	264.8279	134.9281	10.47579	0	0	0
311	83.82749	158.3939	55.31215	75.00662	253.933	259.7995	130.3188	10.05675	0	0	0
312	84.09704	159.2319	55.31215	72.49244	248.9047	256.0282	126.1285	9.218691	0	0	0
313	84.36658	163.0032	55.73118	71.65437	248.0666	250.9998	120.681	7.542566	0	0	0
314	84.63612	163.4223	54.47409	71.65437	248.9047	246.8095	116.0717	6.704503	0	0	0
315	84.90566	165.0984	56.15021	69.55922	246.8095	241.7811	111.0433	5.86644	0	0	0
316	85.1752	166.7745	56.15021	67.46406	245.1334	232.9815	104.7579	4.190314	0	0	0
317	85.44474	169.2887	56.15021	65.78793	240.9431	228.7912	100.5675	3.771283	0	0	0

318	85.71429	170.1268	56.15021	65.3689	235.9147	221.2486	94.7011	3.771283	0	0	0
319	85.98383	170.9648	56.15021	65.3689	232.1434	215.8012	89.67272	2.93322	0	0	0
320	86.25337	174.3171	56.15021	64.11181	227.5341	207.8396	82.13016	2.514189	0	0	0
321	86.52291	174.7361	55.31215	62.43568	224.1818	199.0399	78.35888	1.676126	0	0	0
322	86.79245	175.5742	54.89312	61.59762	217.4773	191.0783	71.23534	1.257094	0	0	0
323	87.06199	175.5742	53.63602	61.17859	212.868	181.4406	65.78793	0.419031	0	0	0
324	87.33154	171.8029	52.79796	61.17859	206.5825	175.1551	59.50246	0.419031	0	0	0
325	87.60108	172.2219	52.79796	60.34052	201.9731	165.0984	54.47409	0.419031	0	0	0
326	87.87062	165.5174	51.9599	60.34052	195.2686	156.7178	47.76958	0	0	0	0
327	88.14016	161.3271	51.9599	59.50246	191.4974	147.4991	43.16024	0	0	0	0
328	88.4097	157.1368	51.9599	56.56924	184.3738	137.4423	38.96992	0	0	0	0
329	88.67925	152.9465	51.12183	54.89312	176.4122	128.6426	32.68445	0	0	0	0
330	88.94879	150.0132	51.12183	54.47409	170.1268	121.1001	28.49414	0	0	0	0
331	89.21833	144.5658	49.44571	52.37893	163.0032	111.0433	24.30382	0	0	0	0
332	89.48787	138.2804	47.35055	49.86474	154.6226	100.5675	20.11351	0	0	0	0
333	89.75741	133.671	46.93152	49.44571	144.5658	88.41563	14.24707	0	0	0	0
334	90.02695	126.1285	46.09346	45.67443	136.1852	80.035	11.31385	0	0	0	0
335	90.2965	121.5191	43.16024	42.32217	124.8714	69.97825	7.542566	0	0	0	0
336	90.56604	116.9098	43.16024	36.45573	113.5575	59.08343	4.609346	0	0	0	0
337	90.83558	109.7862	38.55089	32.68445	102.6627	53.63602	2.93322	0	0	0	0
338	91.10512	104.7579	36.0367	26.81801	90.09176	43.57927	1.676126	0	0	0	0
339	91.37466	98.89142	33.94155	22.6277	79.19694	37.71283	1.257094	0	0	0	0
340	91.6442	94.28207	31.42736	17.59932	66.20696	29.75123	0.419031	0	0	0	0
341	91.91375	87.15854	29.75123	13.82804	56.56924	23.46576	0.419031	0	0	0	0
342	92.18329	83.38725	27.23704	9.218691	43.57927	16.76126	0	0	0	0	0
343	92.45283	78.35888	25.97995	6.704503	33.10348	11.31385	0	0	0	0	0
344	92.72237	73.3305	24.72285	3.771283	22.20867	6.285471	0	0	0	0	0
345	92.99191	71.65437	23.04673	2.514189	12.57094	3.771283	0	0	0	0	0
346	93.26146	68.30212	19.27545	1.257094	7.542566	0.838063	0	0	0	0	0
347	93.531	62.85471	17.59932	0	2.93322	0.419031	0	0	0	0	0
348	93.80054	59.08343	16.76126	0	1.676126	0	0	0	0	0	0
349	94.07008	54.05505	15.50416	0	0	0	0	0	0	0	0
350	94.33962	48.18861	13.40901	0	0	0	0	0	0	0	0
351	94.60916	42.32217	11.31385	0	0	0	0	0	0	0	0
352	94.87871	37.71283	8.380628	0	0	0	0	0	0	0	0
353	95.14825	31.00833	4.609346	0	0	0	0	0	0	0	0
354	95.41779	26.39898	3.771283	0	0	0	0	0	0	0	0
355	95.68733	22.20867	2.095157	0	0	0	0	0	0	0	0
356	95.95687	19.27545	2.095157	0	0	0	0	0	0	0	0
357	96.22642	13.82804	1.257094	0	0	0	0	0	0	0	0
358	96.49596	11.31385	1.676126	0	0	0	0	0	0	0	0
359	96.7655	8.79966	1.676126	0	0	0	0	0	0	0	0
360	97.03504	6.704503	1.676126	0	0	0	0	0	0	0	0
361	97.30458	4.609346	0.419031	0	0	0	0	0	0	0	0

362	97.57412	2.095157	0	0	0	0	0	0	0	0	0
363	97.84367	2.095157	0	0	0	0	0	0	0	0	0
364	98.11321	1.257094	0	0	0	0	0	0	0	0	0
365	98.38275	0.838063	0	0	0	0	0	0	0	0	0
366	98.65229	0.838063	0	0	0	0	0	0	0	0	0
367	98.92183	0.419031	0	0	0	0	0	0	0	0	0
368	99.19137	0	0	0	0	0	0	0	0	0	0
369	99.46092	0	0	0	0	0	0	0	0	0	0
370	99.73046	0	0	0	0	0	0	0	0	0	0
371	100	0	0	0	0	0	0	0	0	0	0

FigureA.3: The force raw data obtained for one trial of walking with self-selected speed.

7.2.1 Force distribution graphs in HV and non-HV volunteers

Figure A.4 presenting the normalised force graphs related to non-HV patients obtained from self-selected speed. The body force that applies to the foot has been normalised with the individuals' body weight and the total number of frames is normalised to the 100 frames. The Figure A.4, shows the three sample graphs of a non-HV volunteer.

Ten non-HV volunteers who took part in the experiment walked with self-selected speed and also with faster speed by 20%. So all participants in the foot scan test walked with two different speed and they had a full contact with the pressure mat while stepping on the mat and their plantar force was achieved and normalised to the body weight so the graphs related to the fast speed shows that the force applied under the foot was increased in different parts of the foot when compare it with the achieved graphs from the self-selected speed. The graphs in FigureA.5, presents that the force under the 1^{st}, 2^{nd} and 3^{rd} metatarsals is higher when the individual increased the speed of the walking.

The Figures A.4, and A.5 are belonged to the same non-HV individual.

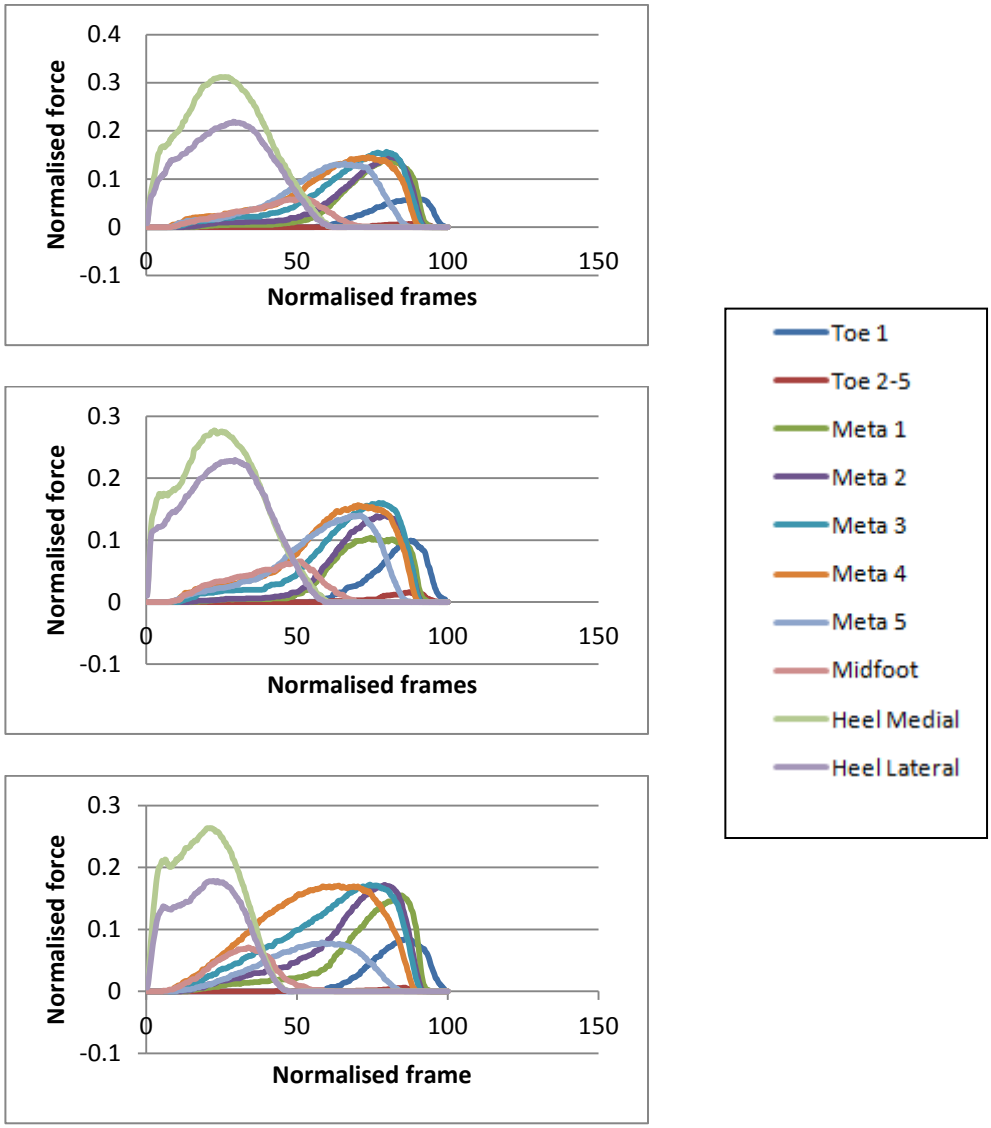

FigureA.4: Three samples of the same non-HV volunteer who walked with the self-selected speed. The X axis shows the normalised frame and Y axis shows the normalised force applied on different parts of the foot.

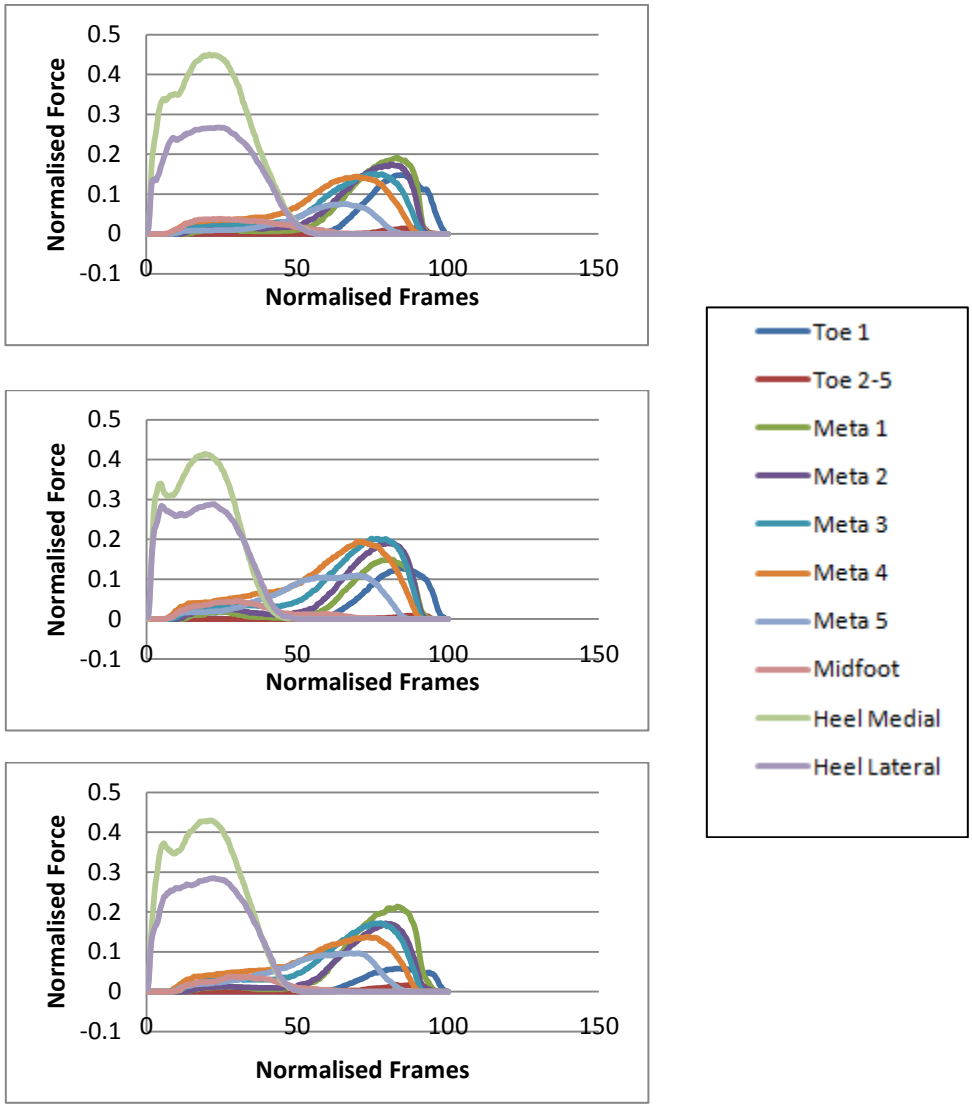

FigureA.5: Three samples of the fast speed graphs of a non- HV volunteer. The X axis shows the normalised frame and Y axis shows the normalised force applied on different parts of the foot.

In Figure A.6, the force distribution graphs are presented in self-selected speed of the HV volunteer which shows the higher force excluding the heel is under the toe1, metatarsals 3 and 2.

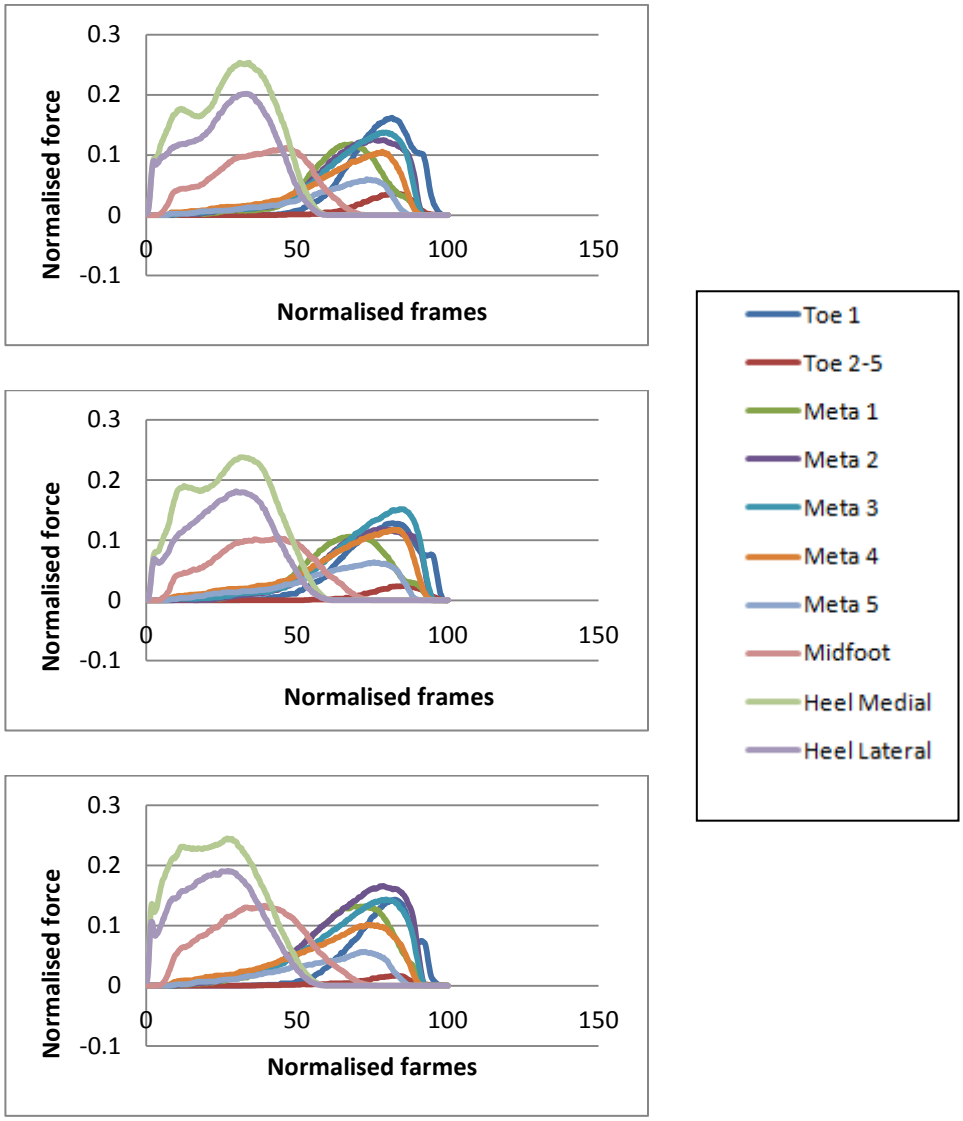

FigureA.6: Three samples of the self-selected speed graphs of a HV volunteer. The X axis shows the normalised frame and Y axis shows the normalised force applied on different parts of the foot

Figure A.7 shows the fast speed of the same volunteer (A.6) in which the heel and the mid-foot show the highest force and then metatarsal 2 and 3 bear the highest force compared to self-selected speeds' results.

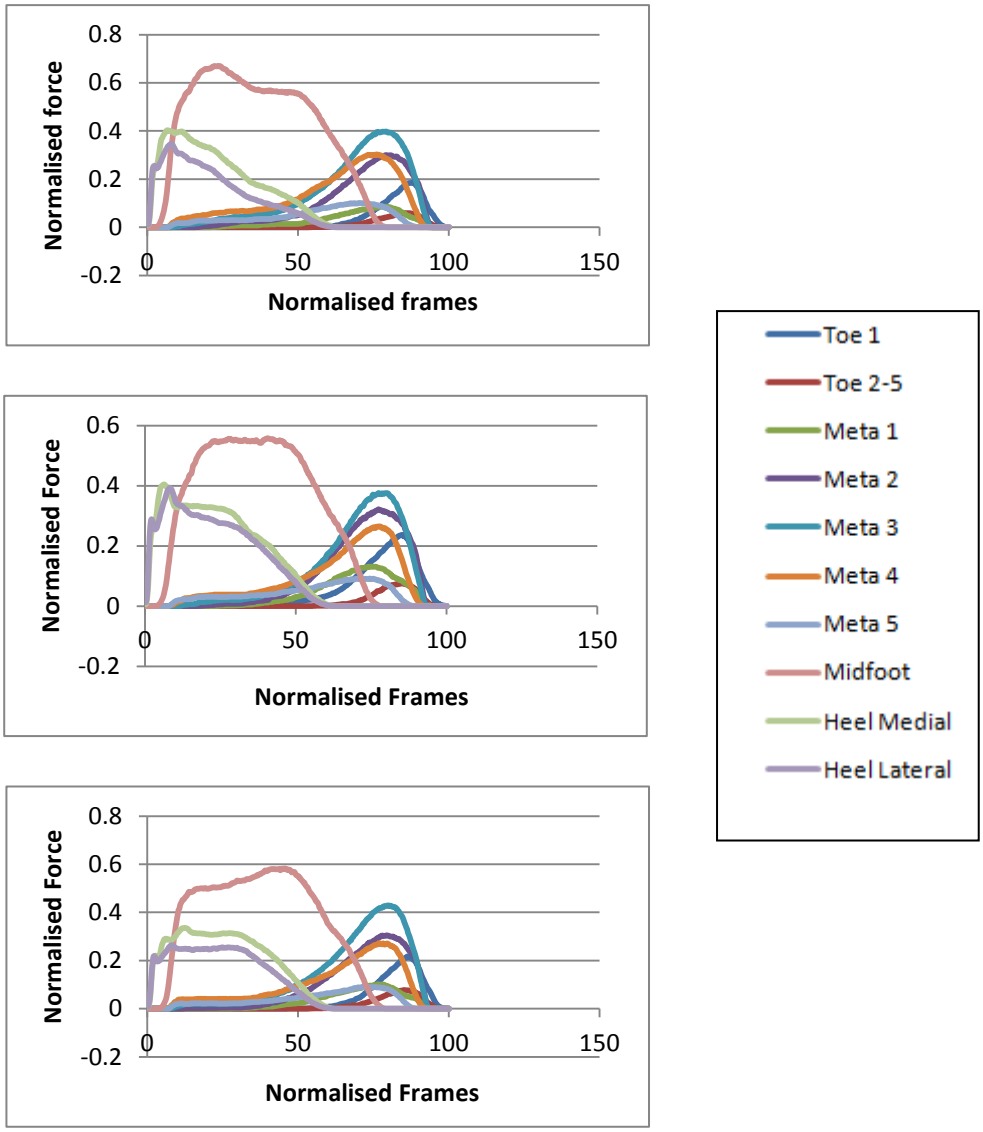

Figure A.7: Three samples of the fast speed graphs of an HV volunteer. The X axis shows the normalised frame and Y axis shows the normalised force applied on different parts of the foot.

7.3 Appendix B

7.3.1 Transfer matrices related to self-selected speed

A	Metatarsal 1	Metatarsal 2	Metatarsal 3	Metatarsal 4	Metatarsal 5
Time e	0.134039	0.207442	0.291057	0.264249	0.139784
Time e+1	0.13021	0.206803	0.292971	0.264887	0.136592
Time e+2	0.128933	0.207442	0.292971	0.26361	0.137869
Time e+3	0.128933	0.205527	0.294248	0.264249	0.137869
Time e+4	0.128933	0.20425	0.294886	0.264249	0.137231

B	Metatarsal 1	Metatarsal 2	Metatarsal 3	Metatarsal 4	Metatarsal 5
Time e+1	0.13021	0.206803	0.292971	0.264887	0.136592
Time e+2	0.128933	0.207442	0.292971	0.26361	0.137869
Time e+3	0.128933	0.205527	0.294248	0.264249	0.137869
Time e+4	0.128933	0.20425	0.294886	0.264249	0.137231
Time e+5	0.127018	0.20425	0.294886	0.268078	0.135954

T	Metatarsal 1	Metatarsal 2	Metatarsal 3	Metatarsal 4	Metatarsal 5
Metatarsal 1	-1.55378	-0.39906	-2.11651	3.035854	1.681607
Metatarsal 2	0.972166	0.910424	0.523025	-0.31478	-1.29782
Metatarsal 3	-0.08174	0.177874	0.906231	-0.27884	0.550482
Metatarsal 4	4.417211	1.509915	5.903945	-7.27815	-3.1159
Metatarsal 5	-1.04281	0.225463	-1.00941	1.695206	0.53967

FigureB.1: Matrix T obtained from Matrix A and B in HV patient.

Figure B.2: presented the relative matrices in non-HV participant in self-selected speed.

A	Metatarsal 1	Metatarsal 2	Metatarsal 3	Metatarsal 4	Metatarsal 5
Time e	0.036406	0.154599	0.152105	0.078795	0.002992
Time e+1	0.034909	0.154599	0.149612	0.077299	0.002992
Time e+2	0.033912	0.1541	0.148614	0.075803	0.002494
Time e+3	0.032416	0.153103	0.148116	0.075305	0.002494
Time e+4	0.032416	0.152604	0.146121	0.072312	0.002494

B	Metatarsal 1	Metatarsal 2	Metatarsal 3	Metatarsal 4	Metatarsal 5
Time e+1	0.034909	0.154599	0.149612	0.077299	0.002992
Time e+2	0.033912	0.1541	0.148614	0.075803	0.002494
Time e+3	0.032416	0.153103	0.148116	0.075305	0.002494
Time e+4	0.032416	0.152604	0.146121	0.072312	0.002494
Time e+5	0.032416	0.153103	0.144625	0.070318	0.002494

T	Metatarsal 1	Metatarsal 2	Metatarsal 3	Metatarsal 4	Metatarsal 5
Metatarsal 1	0.075919	-0.22483	0.553275	-0.33138	2.960583
Metatarsal 2	-0.09503	0.663566	0.705621	-0.74767	2.358274
Metatarsal 3	0.656086	0.897291	-0.33987	0.577031	-2.26082
Metatarsal 4	1.510364	0.63243	-1.07162	1.275676	-4.33695
Metatarsal 5	0.072331	-0.16094	0.234179	-0.1293	-0.06419

FigureB.2: Matrix T obtained from Matrix A and B in non-HV volunteer obtained from self-selected speed data.

7.3.2 Transfer matrices related to fast speed

A	Metatarsal 1	Metatarsal 2	Metatarsal 3	Metatarsal 4	Metatarsal 5
Time e	0.228431	0.231526	0.196859	0.162811	0.072429
Time e+1	0.230907	0.23524	0.201812	0.164668	0.073048
Time e+2	0.234002	0.23586	0.204907	0.165287	0.075525
Time e+3	0.237717	0.239574	0.207383	0.166526	0.076144
Time e+4	0.240812	0.24205	0.207383	0.167145	0.076144

B	Metatarsal 1	Metatarsal 2	Metatarsal 3	Metatarsal 4	Metatarsal 5
Time e+1	0.230907	0.23524	0.201812	0.164668	0.073048
Time e+2	0.234002	0.23586	0.204907	0.165287	0.075525
Time e+3	0.237717	0.239574	0.207383	0.166526	0.076144
Time e+4	0.240812	0.24205	0.207383	0.167145	0.076144
Time e+5	0.245145	0.245764	0.211716	0.172097	0.076144

T	Metatarsal 1	Metatarsal 2	Metatarsal 3	Metatarsal 4	Metatarsal 5
Metatarsal 1	5.341464	-5.51827	2.079292	2.36575	-6.98782
Metatarsal 2	3.14566	-2.91222	0.342681	1.920588	-2.61252
Metatarsal 3	11.11516	-13.9373	5.014202	7.173483	-17.4707
Metatarsal 4	8.479953	-9.9266	2.913314	5.306631	-12.5866
Metatarsal 5	2.197	-3.19003	1.65472	1.775113	-4.21092

FigureB.2: Matrix T obtained from Matrix A and B in HV volunteer obtained from self-selected speed data.

A	Metatarsal 1	Metatarsal 2	Metatarsal 3	Metatarsal 4	Metatarsal 5
Time e	0.092261	0.196989	0.203472	0.094255	0.001496
Time e+1	0.091263	0.197487	0.202973	0.093258	0.000997
Time e+2	0.089767	0.198984	0.201976	0.093258	0.000997
Time e+3	0.08877	0.194495	0.200978	0.092261	0.000499
Time e+4	0.090266	0.194495	0.199482	0.089268	0.000499

B	Metatarsal 1	Metatarsal 2	Metatarsal 3	Metatarsal 4	Metatarsal 5
Time e+1	0.091263	0.197487	0.202973	0.093258	0.000997
Time e+2	0.089767	0.198984	0.201976	0.093258	0.000997
Time e+3	0.08877	0.194495	0.200978	0.092261	0.000499
Time e+4	0.090266	0.194495	0.199482	0.089268	0.000499
Time e+5	0.090764	0.193498	0.196989	0.087273	0.000499

T	Metatarsal 1	Metatarsal 2	Metatarsal 3	Metatarsal 4	Metatarsal 5
Metatarsal 1	-4.84968	-1.24126	6.41263	-5.79782	16.64111
Metatarsal 2	11.02307	1.307349	-10.0736	10.88165	-35.4285
Metatarsal 3	0.751443	0.098014	0.019857	1.199126	-1.82298
Metatarsal 4	7.236965	1.378731	-7.78735	8.178818	-21.6655
Metatarsal 5	1.352594	0.132946	-1.32947	1.341032	-3.92483

FigureB.2: Matrix T obtained from Matrix A and B in non-HV volunteer obtained from self-selected speed data.

The code of transfer matrices has been written in Matlab software as it is presented below. Matrix B has been obtained with one gap of the force data from matrix A.

The Matlab code was written to achieve transfer matrices are as follows:

```
Matlab code
A = zeros(5,5);
Count = 266;
for k = 1 : 5
    A(k,:) = data(Count, 1:5);
    Count = Count + 1;
end
B = zeros(5,5);
Count = 267;
```

```
for k = 1 : 5
    B(k,:) = data(Count, 1:5);
    Count = Count + 1;
end

C=A';
E=B';
T=E*inv(C);
```

7.4 Appendix C

7.4.1 Motion capture raw data

The raw data that is achieved from Vicon cameras there were two markers and 3 columns are presenting each marker coordinates.

PathFileType	4	(X/Y/Z)	C:/saba-mahshid1october/3october/Project 2/Capture day 1/Session 1/Ibi right foot3.trc				
DataRate	CameraRate	NumFrames	NumMarkers	Units	OrigDataRate	OrigDataStartFrame	OrigNumFrames
120	120	318	0	mm	120	1	318
Frame#	Time						
1	0.008333	656.8973	10.201627	-468.301819	652.883362	2.638693	-418.342163
2	0.016667	656.9188	10.227149	-468.307648	652.870911	2.57111	-418.307434
3	0.025	656.8581	10.239536	-468.260223	652.866333	2.557005	-418.293976
4	0.033333	656.8879	10.326677	-468.20108	652.891846	2.594132	-418.297546
5	0.041667	656.8779	10.348563	-468.162262	652.932983	2.680354	-418.21463
6	0.05	656.8313	10.398465	-468.112793	652.949036	2.715551	-418.226776
7	0.058333	656.8331	10.495872	-468.094696	652.899231	2.638571	-418.208221
8	0.066667	656.7729	10.512563	-468.01828	652.894409	2.6427	-418.197968
9	0.075	656.7554	10.506477	-468.000305	652.895508	2.645341	-418.198456
10	0.083333	656.7318	10.59844	-467.994476	652.879028	2.620934	-418.194427
11	0.091667	656.7147	10.618715	-467.963409	652.878235	2.619224	-418.193909
12	0.1	656.7031	10.697414	-467.948151	652.878601	2.619918	-418.194122
13	0.108333	656.696	10.798524	-467.940399	652.901245	2.648482	-418.213654
14	0.116667	656.7272	10.982275	-467.992767	652.91925	2.808489	-418.266754
15	0.125	656.7596	11.138218	-468.009644	652.930847	2.942912	-418.39151
16	0.133333	656.7845	11.344223	-468.051239	652.971558	3.225086	-418.515594
17	0.141667	656.8713	11.592279	-468.138824	653.054321	3.506798	-418.759735

18	0.15	656.9668	11.823369	-468.146088	653.119446	3.835868	-418.951447
19	0.158333	657.0865	11.994375	-468.178741	653.20459	4.091129	-419.106873
20	0.166667	657.2	12.159394	-468.178192	653.171875	4.356336	-419.248077
21	0.175	657.1421	12.316205	-468.115265	653.140808	4.610587	-419.424377
22	0.183333	657.0992	12.533412	-468.102844	653.023499	4.78567	-419.472534
23	0.191667	656.9452	12.689478	-468.108643	652.919617	5.008207	-419.4888
24	0.2	656.7839	12.861166	-468.125549	652.643494	5.246861	-419.568573
25	0.208333	656.5266	13.072142	-468.231018	652.269958	5.514895	-419.712158
26	0.216667	656.2339	13.389676	-468.361908	651.963867	5.714472	-419.856354
27	0.225	655.9627	13.830771	-468.482208	651.739685	6.265411	-420.105133
28	0.233333	655.6362	14.166462	-468.541748	651.051636	6.504073	-420.307892
29	0.241667	655.2422	14.548364	-468.589111	650.330811	7.005737	-420.666931
30	0.25	654.7786	15.079645	-468.649536	649.398865	7.517438	-421.097076
31	0.258333	654.1942	15.576099	-468.816925	648.491333	8.053504	-421.532898
32	0.266667	653.3805	16.148815	-469.070831	647.551453	8.584774	-421.829529
33	0.275	652.3442	16.904108	-469.354706	646.122131	9.258864	-422.271973
34	0.283333	651.2803	17.682934	-469.540985	644.596924	9.871536	-422.624451
35	0.291667	649.7985	18.404604	-469.825256	642.743652	10.512031	-423.223969
36	0.3	647.9208	19.241562	-470.039124	640.52655	11.308604	-423.519135
37	0.308333	645.5286	20.268311	-470.463379	637.960144	11.955659	-423.86142
38	0.316667	642.9599	21.351267	-470.453918	634.866333	13.053878	-424.091736
39	0.325	639.8183	22.480247	-470.390045	631.543213	14.20444	-424.073639
40	0.333333	636.2592	23.386129	-470.051483	627.907654	15.163526	-423.893372
41	0.341667	632.2357	24.607622	-469.911591	623.942749	16.352875	-423.652985
42	0.35	628.0713	25.622614	-469.538116	619.528198	17.343025	-423.315247
43	0.358333	623.5353	26.696239	-469.061829	614.862183	18.222101	-422.907196
44	0.366667	618.7409	27.471018	-468.661774	609.814087	19.068975	-422.510834
45	0.375	613.5716	28.275826	-468.158966	604.749084	19.911491	-422.070099
46	0.383333	608.156	28.882977	-467.531586	599.314392	20.513733	-421.415833
47	0.391667	602.4811	29.484169	-466.932648	593.507935	21.107157	-420.77597
48	0.4	596.6345	29.869667	-466.097809	587.511597	21.73369	-419.975677
49	0.408333	590.4584	30.280577	-465.237213	581.504822	22.288601	-419.016815
50	0.416667	584.0467	30.747164	-464.258026	575.154114	22.788589	-418.116608
51	0.425	577.5727	31.076225	-463.135284	568.574585	23.392925	-417.046783
52	0.433333	570.961	31.7047	-462.235168	562.211426	23.993763	-415.816406
53	0.441667	564.1557	32.203274	-461.010498	555.307556	24.684803	-414.594299
54	0.45	557.0958	32.668163	-459.706543	548.54126	25.22443	-413.25885
55	0.458333	550.021	33.443779	-458.36673	541.681519	26.425318	-411.9505
56	0.466667	542.7359	34.179691	-456.996002	534.420532	26.758768	-410.5737
57	0.475	535.5079	34.960571	-455.758789	526.976868	27.570654	-409.222839
58	0.483333	527.9489	35.718658	-454.520721	519.703125	28.426607	-407.866943
59	0.491667	520.514	36.371857	-453.266693	512.150818	29.059389	-406.679016
60	0.5	512.9241	36.950478	-452.049255	504.65097	29.892591	-405.428864
61	0.508333	505.1389	37.710659	-450.934753	496.904144	30.449018	-404.315277

62	0.516667	497.4198	38.074463	-449.83725	489.224823	31.10845	-403.180939
63	0.525	489.7117	38.447578	-448.728882	481.48291	31.411657	-402.03656
64	0.533333	481.7017	38.574669	-447.691986	473.69693	31.753799	-400.951324
65	0.541667	473.8955	38.733437	-446.656036	465.76355	31.781307	-399.625244
66	0.55	465.9965	38.850578	-445.571136	458.049652	32.111542	-398.621521
67	0.558333	458.1202	38.960014	-444.541595	450.152222	32.361786	-397.643494
68	0.566667	450.1451	38.861763	-443.282318	442.349396	32.691002	-396.448059
69	0.575	442.4243	39.35638	-442.132172	434.678284	33.159691	-395.177124
70	0.583333	434.6901	39.82552	-440.988617	427.021942	33.905167	-394.082245
71	0.591667	427.0564	40.42942	-439.642426	419.348602	35.101089	-392.677368
72	0.6	419.291	41.655365	-438.447235	411.918732	36.662857	-391.489288
73	0.608333	411.9454	43.182667	-437.225769	404.60791	38.178852	-390.089386
74	0.616667	404.5893	44.383255	-435.774658	397.242249	39.765282	-388.747986
75	0.625	397.3188	46.093365	-434.364471	390.030029	41.480389	-387.157135
76	0.633333	390.1331	47.83453	-433.060516	382.970306	43.303928	-385.859711
77	0.641667	383.0017	49.374092	-431.66507	376.066925	45.067574	-384.522095
78	0.65	376.0774	50.987606	-430.371796	369.203979	46.707069	-382.941223
79	0.658333	369.1523	52.416695	-428.849792	362.409424	48.291462	-381.57251
80	0.666667	362.3486	53.744423	-427.419525	355.805786	49.775143	-380.20459
81	0.675	355.9025	55.337135	-426.156433	349.343231	51.531811	-378.90097
82	0.683333	349.4243	56.749702	-424.949005	343.15033	52.848835	-377.45047
83	0.691667	343.1776	57.94458	-423.565704	336.956116	54.457901	-376.096924
84	0.7	336.9047	59.106686	-422.253235	330.812195	55.450619	-374.888947
85	0.708333	330.8829	60.270039	-421.048004	324.827484	56.680115	-373.585938
86	0.716667	325.068	61.171459	-419.780182	319.018341	57.774208	-372.485291
87	0.725	319.4881	62.237099	-418.705872	313.573792	58.757164	-371.1763
88	0.733333	314.1122	63.414013	-417.54834	308.142334	59.852444	-370.069305
89	0.741667	308.9534	64.691277	-416.471893	302.994202	61.446209	-369.020538
90	0.75	303.9126	66.308456	-415.35849	298.043884	62.978291	-367.885071
91	0.758333	299.1055	67.788773	-414.239197	293.362305	64.39859	-366.789154
92	0.766667	294.1865	69.336555	-413.140381	288.648163	65.943863	-365.611725
93	0.775	289.5133	70.644592	-412.098236	284.095947	67.334435	-364.532715
94	0.783333	284.9715	71.984497	-410.947662	279.566376	68.570435	-363.536652
95	0.791667	280.4422	73.080795	-409.844818	275.092102	69.7061	-362.527985
96	0.8	275.9398	74.158844	-408.873383	270.708282	70.801468	-361.352173
97	0.808333	271.5509	75.121567	-407.80542	266.370056	71.560928	-360.245239
98	0.816667	267.2314	75.887375	-406.82724	262.194763	72.375877	-359.304626
99	0.825	263.0175	76.682777	-405.853882	258.095764	73.183319	-358.406372
100	0.833333	258.7508	77.390541	-405.020966	254.107956	73.964256	-357.482422
101	0.841667	254.6872	77.881027	-403.954254	250.260605	74.323227	-356.361145
102	0.85	250.6766	78.387131	-403.102356	246.233292	74.875992	-355.627197
103	0.858333	246.7396	78.907921	-402.299774	242.353104	75.339447	-354.795624
104	0.866667	242.8576	79.426147	-401.470947	238.605911	75.849335	-353.932861
105	0.875	239.2068	80.075371	-400.773376	234.99678	76.537109	-353.239685

106	0.883333	235.7289	80.850136	-400.218842	231.261353	77.256432	-352.812103
107	0.891667	232.177	81.552879	-399.764954	227.85701	77.828468	-352.337677
108	0.9	228.7877	82.190392	-399.487152	224.39888	78.379219	-352.013702
109	0.908333	225.4997	82.613014	-399.306458	220.845306	78.790939	-351.871918
110	0.916667	222.2044	82.756828	-399.0159	217.591629	78.995743	-351.787842
111	0.925	219.2264	82.933022	-398.952087	214.395004	79.045647	-351.528656
112	0.933333	216.3383	82.913048	-398.82019	211.45105	78.771378	-351.399384
113	0.941667	213.5246	82.716743	-398.625793	208.538666	78.388275	-351.240082
114	0.95	211.0195	82.389572	-398.343689	205.884354	77.905617	-351.046356
115	0.958333	208.4857	81.625816	-397.933746	203.41832	77.090073	-350.89209
116	0.966667	206.3186	81.294418	-397.776886	201.22966	76.24099	-350.653259
117	0.975	204.1601	80.438667	-397.439392	198.935791	75.25296	-350.423401
118	0.983333	202.1107	79.608208	-396.969482	196.891754	74.066566	-349.853943
119	0.991667	200.3086	78.677864	-396.429504	195.162094	73.111626	-349.413086
120	1	198.5681	77.872871	-395.959686	193.353638	71.971306	-348.930817
121	1.008333	197.1238	77.135841	-395.44693	191.945587	71.043358	-348.535889
122	1.016667	195.9209	76.169594	-395.115479	190.69754	69.919952	-348.003693
123	1.025	194.6991	75.168541	-394.663116	189.547165	69.11441	-347.715454
124	1.033333	193.5538	74.046806	-394.106598	188.493454	67.895676	-347.311096
125	1.041667	192.6009	72.831871	-393.692627	187.462463	66.48262	-346.77005
126	1.05	191.7724	71.389587	-393.287201	186.713135	64.960884	-346.328064
127	1.058333	191.1349	69.744667	-392.836548	186.050735	63.211494	-345.857635
128	1.066667	190.749	68.093117	-392.345245	185.664413	61.634365	-345.519409
129	1.075	190.5745	66.260956	-391.816467	185.439621	59.74308	-345.066254
130	1.083333	190.5839	64.349342	-391.101807	185.463913	57.640934	-344.410706
131	1.091667	190.8829	62.567482	-390.402069	185.522369	55.628647	-343.742828
132	1.1	191.1346	60.724735	-389.739105	185.627579	53.414967	-343.013977
133	1.108333	191.3179	58.788795	-389.098785	185.677979	51.336899	-342.508484
134	1.116667	191.0945	56.806068	-388.533417	185.260437	49.178246	-341.947693
135	1.125	190.483	54.92421	-388.037598	184.479019	47.333057	-341.604584
136	1.133333	189.6013	53.334469	-387.746124	183.197678	45.567734	-341.514099
137	1.141667	188.4787	51.934677	-387.917053	181.799515	44.132515	-341.748901
138	1.15	187.321	50.859318	-388.430969	180.483276	42.91489	-342.191345
139	1.158333	186.0491	49.464767	-389.0242	179.139526	41.677792	-342.830627
140	1.166667	185.0426	47.821064	-389.618744	178.101135	40.154896	-343.526611
141	1.175	184.1244	45.751293	-390.13562	177.356659	38.172844	-344.072723
142	1.183333	183.3383	43.639862	-390.412598	176.566544	36.077545	-344.316071
143	1.191667	182.589	41.484581	-390.362671	176.057312	33.777416	-344.230957
144	1.2	181.6673	39.05331	-389.895935	175.628342	31.283247	-343.878967
145	1.208333	180.6455	36.931667	-389.288666	175.047913	28.433241	-343.202698
146	1.216667	179.5143	34.05257	-387.989166	174.803879	25.180164	-341.992126
147	1.225	178.4812	30.94792	-386.654724	174.512131	21.538338	-340.543823
148	1.233333	177.1348	27.458776	-384.722961	174.381287	17.374296	-338.835724
149	1.241667	175.7156	24.064972	-382.540497	174.084396	12.20928	-336.725372

150	1.25	174.7428	21.26202	-380.560852	174.422638	8.127521	-334.82019
151	1.258333	173.4645	18.841963	-379.353455	174.29982	4.854951	-333.215546
152	1.266667	171.9395	17.637447	-379.404999	173.558044	3.731444	-332.602905
153	1.275	170.7194	17.129511	-380.248108	172.429871	3.496738	-332.974335
154	1.283333	169.5554	16.529402	-381.015747	171.496368	3.009424	-333.29538
155	1.291667	168.7937	15.769904	-381.292786	170.965363	2.541399	-333.255463
156	1.3	168.2698	15.238933	-381.231445	170.631317	2.151499	-333.074371
157	1.308333	167.6087	14.075585	-381.472504	170.331741	1.824713	-332.943237
158	1.316667	167.1072	13.714108	-381.624817	169.983246	1.631391	-332.958221
159	1.325	166.81	13.515995	-381.820923	170.051819	1.750516	-332.895752
160	1.333333	166.6238	13.24428	-381.831116	169.541412	1.420476	-333.03772
161	1.341667	166.8827	13.453731	-382.005646	170.086853	2.187987	-333.007294
162	1.35	166.7236	13.31407	-382.169891	169.438782	1.996136	-333.395752
163	1.358333	166.564	13.09494	-382.393158	169.173889	2.038427	-333.764038
164	1.366667	166.4719	12.896392	-382.610718	168.941437	2.103816	-334.133209
165	1.375	166.3896	12.857958	-382.872467	168.801682	2.060517	-334.462402
166	1.383333	165.8202	12.236797	-383.031708	168.056931	1.542249	-334.901245
167	1.391667	165.6717	12.040988	-383.080444	167.739532	1.505551	-335.389954
168	1.4	165.6539	11.964896	-383.19455	167.739197	1.296079	-335.628906
169	1.408333	165.6535	11.865974	-383.220795	167.566605	1.083428	-336.029572
170	1.416667	165.6059	11.867868	-383.26709	167.620087	0.799156	-336.281982
171	1.425	165.7885	12.122243	-383.229462	167.842651	0.303384	-336.404388
172	1.433333	165.795	12.259046	-383.231262	168.112244	-0.241382	-336.579254
173	1.441667	165.5389	11.723913	-383.282654	168.827835	-0.773761	-336.180359
174	1.45	165.7401	12.364983	-383.029205	168.810104	-0.964565	-336.189606
175	1.458333	165.7326	12.368952	-382.949463	168.659958	-1.111624	-336.266052
176	1.466667	165.6773	12.285639	-382.871277	168.612137	-1.187938	-336.322052
177	1.475	165.59	12.20869	-382.817474	168.527039	-1.360759	-336.362183
178	1.483333	165.5147	12.126355	-382.697174	168.376572	-1.498978	-336.297363
179	1.491667	165.3786	12.027907	-382.701385	168.335815	-1.590621	-336.297455
180	1.5	165.3449	11.98602	-382.665741	168.279343	-1.66205	-336.334656
181	1.508333	165.2111	11.79301	-382.716187	168.22522	-1.603181	-336.373169
182	1.516667	165.1825	11.822326	-382.768341	168.17572	-1.584299	-336.404816
183	1.525	165.1151	11.674167	-382.889771	168.070877	-1.465048	-336.489655
184	1.533333	165.0331	11.512435	-382.988342	168.047806	-1.472733	-336.647461
185	1.541667	165.0018	11.53023	-382.993866	167.981415	-1.461543	-336.664337
186	1.55	164.8921	11.405066	-383.053864	168.050308	-1.480722	-336.674927
187	1.558333	164.9448	11.501199	-383.026917	167.903366	-1.429034	-336.703583
188	1.566667	164.5916	10.83954	-383.235107	167.931854	-1.476442	-336.679077
189	1.575	164.5469	10.745339	-383.16684	167.896515	-1.547364	-336.71286
190	1.583333	164.5416	10.753166	-383.161469	167.860229	-1.557189	-336.630768
191	1.591667	164.5219	10.773053	-383.034851	167.87265	-1.581353	-336.588226
192	1.6	164.528	10.762046	-383.016846	167.834122	-1.686146	-336.607971
193	1.608333	164.5011	10.78123	-382.882599	167.814484	-1.787066	-336.507324

194	1.616667	164.9238	11.581188	-382.523773	167.820572	-1.822924	-336.396362
195	1.625	164.9247	11.658622	-382.446259	167.938873	-1.990837	-336.264008
196	1.633333	164.9301	11.67044	-382.313049	168.035919	-2.494726	-335.968079
197	1.641667	164.9897	11.697172	-382.260376	168.020248	-2.247672	-336.104309
198	1.65	164.974	11.66467	-382.089081	168.033112	-2.293165	-336.053925
199	1.658333	164.9713	11.659662	-382.082062	168.020004	-2.425548	-335.963959
200	1.666667	164.9386	11.648944	-382.088318	168.087845	-2.814758	-335.729675
201	1.675	164.9986	11.613134	-381.98822	168.050003	-2.908645	-335.597809
202	1.683333	164.973	11.5718	-381.939178	168.052963	-2.553022	-335.655304
203	1.691667	164.9988	11.551302	-381.873505	167.972504	-2.60874	-335.67749
204	1.7	164.9748	11.465557	-381.791748	168.004974	-2.69618	-335.551544
205	1.708333	164.9395	11.390067	-381.750519	167.93959	-2.79973	-335.429382
206	1.716667	164.9644	11.383417	-381.607758	167.996643	-2.896348	-335.285858
207	1.725	164.9634	11.361842	-381.490112	168.118134	-2.979538	-335.160004
208	1.733333	164.9728	11.354378	-381.338715	168.207535	-3.08531	-334.993622
209	1.741667	165.0098	11.334804	-381.130798	168.197006	-3.318458	-334.719086
210	1.75	165.1188	11.320692	-380.980042	168.25943	-3.405751	-334.558411
211	1.758333	165.1415	11.288471	-380.762878	168.285263	-3.622538	-334.300415
212	1.766667	165.136	11.303881	-380.61557	168.717743	-3.742989	-333.869232
213	1.775	165.1777	11.284853	-380.422455	168.42923	-3.891331	-333.771606
214	1.783333	165.1913	11.248083	-380.173401	168.445129	-4.134929	-333.645386
215	1.791667	165.2173	11.197133	-380.049957	168.43454	-4.21291	-333.399231
216	1.8	165.2221	11.129166	-379.792053	168.453918	-4.339406	-333.212646
217	1.808333	165.184	11.021022	-379.624725	168.452698	-4.440159	-333.027863
218	1.816667	165.1441	10.966728	-379.421875	168.430969	-4.526351	-332.76001
219	1.825	165.1112	10.857104	-379.235535	168.491577	-4.762564	-332.594513
220	1.833333	165.0463	10.805885	-379.098969	168.429398	-4.91343	-332.387634
221	1.841667	164.9429	10.752319	-378.902466	168.449905	-5.045376	-332.191315
222	1.85	164.8532	10.622402	-378.764435	168.34967	-5.123189	-331.944214
223	1.858333	164.793	10.519604	-378.629242	168.248337	-5.204229	-331.87146
224	1.866667	164.691	10.446321	-378.592957	168.185379	-5.236193	-331.673553
225	1.875	164.6259	10.358008	-378.614471	168.181488	-5.532608	-331.412598
226	1.883333	164.5073	10.28529	-378.626129	168.158234	-5.382221	-331.452942
227	1.891667	164.3021	10.174004	-378.763062	168.079437	-5.649689	-331.235809
228	1.9	164.1846	10.087044	-378.92865	167.968719	-5.325612	-331.306122
229	1.908333	163.8548	9.878406	-379.376923	167.863602	-5.328497	-331.289734
230	1.916667	163.5949	9.647511	-379.851593	167.830841	-5.340113	-331.269196
231	1.925	163.0406	9.326777	-380.34082	167.83522	-5.373328	-331.252411
232	1.933333	162.8295	9.548424	-380.385773	167.858765	-5.391083	-331.254425
233	1.941667	163.4846	10.133479	-379.025055	167.789078	-5.365687	-331.166595
234	1.95	163.5882	10.185338	-378.839325	167.799713	-5.3665	-331.156189
235	1.958333	163.4684	10.088557	-378.959778	167.623718	-5.346751	-331.219971
236	1.966667	163.4399	10.087202	-378.967804	167.622665	-5.338835	-331.23114
237	1.975	163.4094	10.046306	-378.987579	167.580719	-5.350039	-331.139984

238	1.983333	163.4258	10.005183	-378.964294	167.676804	-5.431665	-331.09494
239	1.991667	163.3848	10.020635	-378.868866	167.692047	-5.412494	-331.103821
240	2	162.3042	8.922093	-380.167969	167.6745	-5.441826	-331.093658
241	2.008333	162.2099	8.775147	-380.25769	167.526901	-5.471104	-331.038666
242	2.016667	162.2603	8.76442	-380.099609	167.589279	-5.502608	-331.025909
243	2.025	162.2041	8.691882	-380.115479	167.542206	-5.533788	-330.906647
244	2.033333	162.1448	8.66398	-380.107208	167.584778	-5.613582	-330.85907
245	2.041667	162.1387	8.605728	-380.163788	167.592529	-5.62084	-330.857605
246	2.05	162.0513	8.635784	-380.097473	167.565216	-5.604985	-330.794373
247	2.058333	162.0054	8.583892	-380.12854	167.523056	-5.625113	-330.832977
248	2.066667	162.0051	8.578396	-380.134308	167.526703	-5.639143	-330.832611
249	2.075	161.9502	8.509293	-380.167816	167.529724	-5.640305	-330.830078
250	2.083333	161.9199	8.486987	-380.142365	167.479675	-5.649243	-330.743469
251	2.091667	161.9124	8.428872	-380.042664	167.48439	-5.660998	-330.730774
252	2.1	161.8453	8.501678	-380.072845	167.480209	-5.6422	-330.745117
253	2.108333	161.8732	8.459916	-380.058014	167.442276	-5.638328	-330.730042
254	2.116667	161.8854	8.521246	-380.069244	167.485992	-5.695018	-330.697388
255	2.125	161.8417	8.510048	-380.078583	167.447983	-5.644855	-330.724548
256	2.133333	161.8543	8.532244	-380.078522	167.438889	-5.63623	-330.730774
257	2.141667	161.8288	8.549506	-380.001953	167.491577	-5.659078	-330.697693
258	2.15	161.8276	8.55074	-379.99588	167.497009	-5.69976	-330.588135
259	2.158333	161.828	8.549867	-379.998474	167.504654	-5.745351	-330.559418
260	2.166667	161.8302	8.499848	-379.955383	167.462799	-5.702972	-330.56488
261	2.175	161.8038	8.528022	-379.965851	167.46405	-5.764503	-330.620819
262	2.183333	161.8004	8.516442	-379.879425	167.461151	-5.791884	-330.594116
263	2.191667	161.7757	8.49542	-379.869171	167.466003	-5.856019	-330.561523
264	2.2	161.7341	8.436611	-379.910004	167.437378	-5.877204	-330.466522
265	2.208333	161.6968	8.434649	-379.894592	167.394318	-5.830904	-330.464325
266	2.216667	161.6956	8.437236	-379.891785	167.388657	-5.82492	-330.469635
267	2.225	161.6893	8.394217	-379.884674	167.439011	-5.853768	-330.451324
268	2.233333	161.6259	8.339991	-379.927399	167.40448	-5.843767	-330.458801
269	2.241667	161.5493	8.37368	-379.946503	167.393494	-5.797936	-330.4823
270	2.25	161.5394	8.295952	-379.969299	167.396561	-5.836481	-330.464142
271	2.258333	161.4654	8.321373	-380.000732	167.392441	-5.829498	-330.467834
272	2.266667	161.3677	8.318362	-380.081116	167.37381	-5.783986	-330.579865
273	2.275	161.3489	8.259241	-380.074554	167.437683	-5.814289	-330.56485
274	2.283333	161.3457	8.271553	-380.078217	167.414795	-5.787777	-330.598907
275	2.291667	161.2848	8.332429	-380.107147	167.407242	-5.78242	-330.604553
276	2.3	161.1409	8.298287	-380.080017	167.383163	-5.781219	-330.622223
277	2.308333	161.1103	8.301377	-380.084229	167.35672	-5.732467	-330.650391
278	2.316667	161.1054	8.319709	-380.09314	167.369934	-5.763113	-330.633881
279	2.325	160.989	8.282998	-380.146484	167.374878	-5.768754	-330.629974
280	2.333333	160.9565	8.287428	-380.158478	167.356888	-5.73958	-330.644135
281	2.341667	160.9184	8.31264	-380.171112	167.352448	-5.758172	-330.638733

282	2.35	160.8701	8.274374	-380.216888	167.353043	-5.754767	-330.728302
283	2.358333	160.7972	8.273192	-380.228943	167.389374	-5.724422	-330.767242
284	2.366667	160.7931	8.275571	-380.228943	167.404343	-5.709354	-330.858185
285	2.375	160.6834	8.258645	-380.314392	167.385223	-5.729788	-330.871429
286	2.383333	160.6363	8.310481	-380.346893	167.357178	-5.670128	-330.923676
287	2.391667	160.4748	8.290456	-380.397003	167.375519	-5.634787	-331.028412
288	2.4	160.5082	8.276241	-380.404266	167.383759	-5.655445	-331.021301
289	2.408333	160.4576	8.331382	-380.428925	167.380005	-5.616448	-331.03656
290	2.416667	160.3479	8.303373	-380.496857	167.472275	-5.571721	-331.070679
291	2.425	160.3851	8.288536	-380.506012	167.472107	-5.559056	-331.077606
292	2.433333	160.324	8.283098	-380.535065	167.409668	-5.51928	-331.218719
293	2.441667	160.1554	8.308547	-380.584167	167.416443	-5.528162	-331.236572
294	2.45	160.0985	8.332399	-380.626373	167.456665	-5.579285	-331.293518
295	2.458333	160.0472	8.26965	-380.699829	167.419067	-5.464483	-331.353424
296	2.466667	160.0736	8.239023	-380.794861	167.475281	-5.466751	-331.454834
297	2.475	160.0398	8.289758	-380.821747	167.490021	-5.473822	-331.453522
298	2.483333	159.9568	8.292593	-380.887756	167.465897	-5.42692	-331.552338
299	2.491667	159.9192	8.286489	-380.884918	167.44812	-5.372831	-331.66687
300	2.5	159.9035	8.28874	-381.006561	167.559723	-5.390727	-331.733154
301	2.508333	159.8441	8.344971	-381.031982	167.586761	-5.402474	-331.72525
302	2.516667	159.8009	8.292432	-381.066345	167.504181	-5.324831	-331.746124
303	2.525	159.757	8.304789	-381.10495	167.65741	-5.335004	-331.827209
304	2.533333	159.7539	8.308376	-381.107208	167.68602	-5.386618	-331.805084
305	2.541667	159.7769	8.302485	-381.113586	167.603928	-5.315445	-331.8591
306	2.55	159.7605	8.335217	-381.114502	167.55777	-5.265044	-331.878662
307	2.558333	159.6815	8.293748	-381.17868	167.61937	-5.295733	-331.955627
308	2.566667	159.6331	8.345191	-381.216705	167.627045	-5.302374	-331.958191
309	2.575	159.6282	8.322656	-381.20813	167.625717	-5.301301	-331.955872
310	2.583333	159.5738	8.318645	-381.20636	167.625214	-5.300807	-331.95578
311	2.591667	159.5693	8.320242	-381.207581	167.56134	-5.312644	-331.990387
312	2.6	159.4891	8.281235	-381.280731	167.58754	-5.285004	-331.985077
313	2.608333	159.4816	8.287683	-381.273773	167.572693	-5.237877	-332.09552
314	2.616667	159.4847	8.289211	-381.269318	167.535416	-5.219607	-332.026917
315	2.625	159.4635	8.292526	-381.329315	167.573914	-5.20173	-332.14389
316	2.633333	159.4068	8.381718	-381.361816	167.541107	-5.205084	-332.174164
317	2.641667	159.389	8.375026	-381.357971	167.585358	-5.205782	-332.149658
318	2.65	159.3297	8.320036	-381.397949	167.607773	-5.216606	-332.229095

FigureC.1: The raw motion data of two markers stuck on the 1st and 2nd metatarsal heads.

7.4.2 Motion capture results

The three sample graphs in Figure C.2 shows the distance between the two markers stack on the 1st and 2nd metatarsal heads on the right foot of the volunteer without HV. The fluctuations happening between these two markers in the non-HV volunteer is different from the HV individual when comparing with Figure C.3.

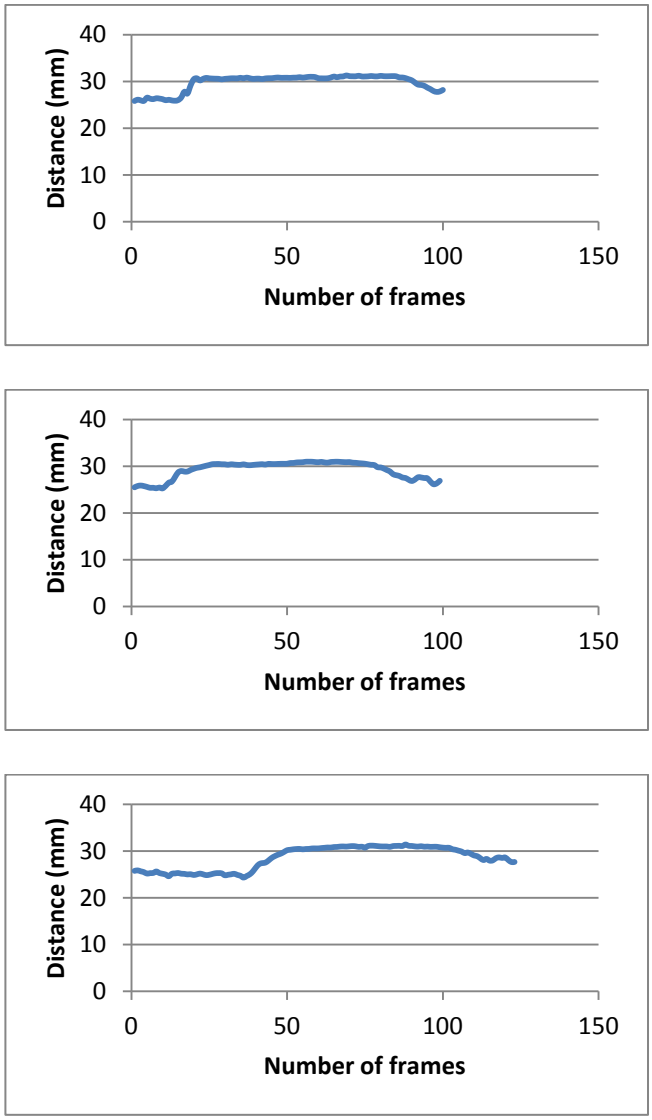

FigureC.2: The distance happening between the two markers in the non-HV volunteer, the X axis shows the number of frames and the Y axis presents the fluctuations between markers in millimeter.

In Figure C.3, the distance changes is shown to be different compared to non-HV volunteer, the higher fluctuations appeared in the three sample graphs in C.3.

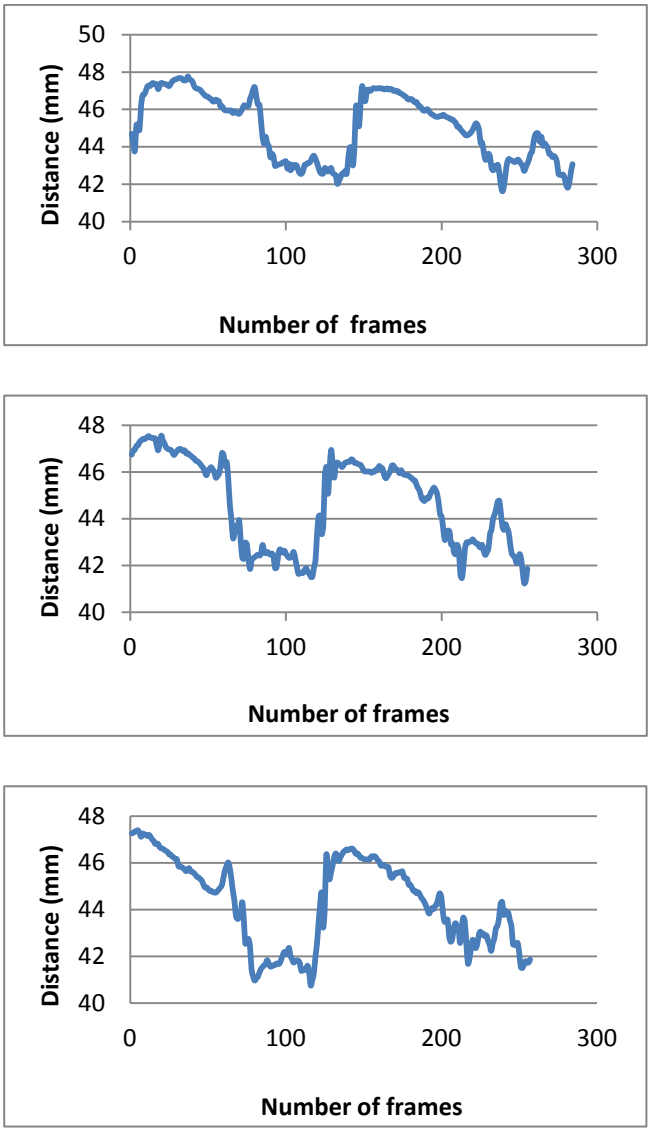

FigureC.3: Presents the distance changes between markers stuck on the right foot in HV patient.

7.5 Appendix D

7.5.1 Independent Sample T-test

Independent sample T-test has been done on all fore-foot regions, including toe1, toe2-5, and metatarsal 1st to 5th based on following algorithms:

$$t = \frac{\overline{X}_1 - \overline{X}_2}{s_{\overline{X}_1 - \overline{X}_2}}$$

Where

$$s_{\overline{X}_1 - \overline{X}_2} = \sqrt{\frac{s_1^2}{n_1} + \frac{s_2^2}{n_2}}.$$

When the variances of two groups of volunteers are different this algorithm is used. Furthermore, the number of force data related to each person was different from other volunteers so the size of data assumed to be unequal.

S^2 is the variance of two groups of data related to HV and non-HV individuals.

$\overline{X_1} - \overline{X_2}$ is the mean value of both groups of volunteers and n_1 represents group 1 which is HV and n_2 represents non-HV .

Figure D.1 presents the "Data View" of the SPSS soft ware that all forces data related to specific region (metatarsal 5th) have entered to this view and the comparison of the data has been conducted. So in order to find out whether there are significant differences among force data in HV and non-HV groups, by going to Analyze toolbar, then click on the "Compare means" and finally on the "Independent-Sample T test", the comparison has been achieved.

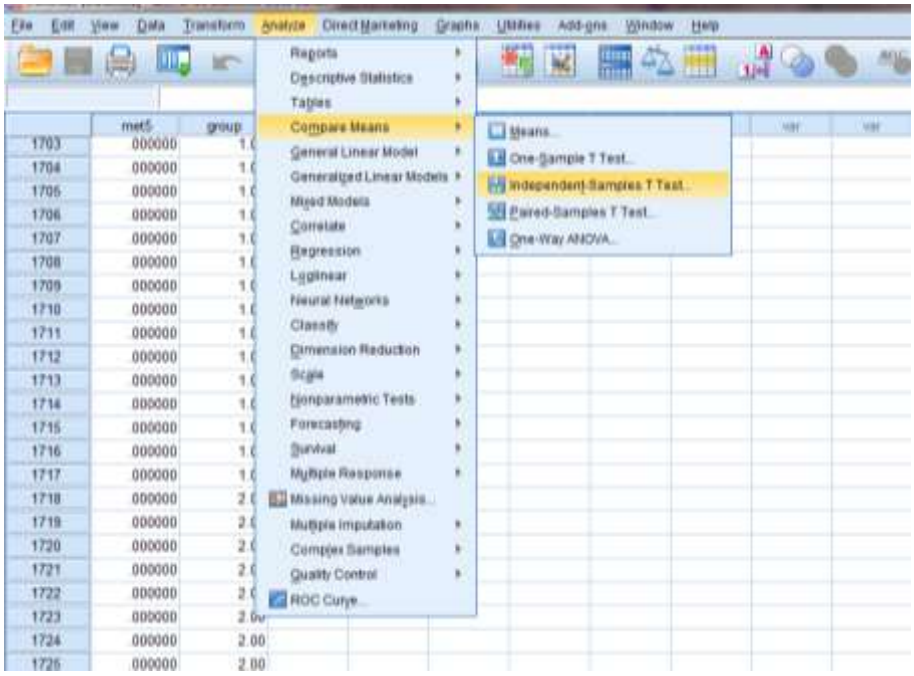

FigureD.1: the Data View of the SPSS software.

In order to have the comparison between means after entering force data in the "Data View", HV and Non-HV group should be defined as separate groups. So in "Variable View" the names of the groups have been defined. HV as group number 1 and non-HV as group number 2.

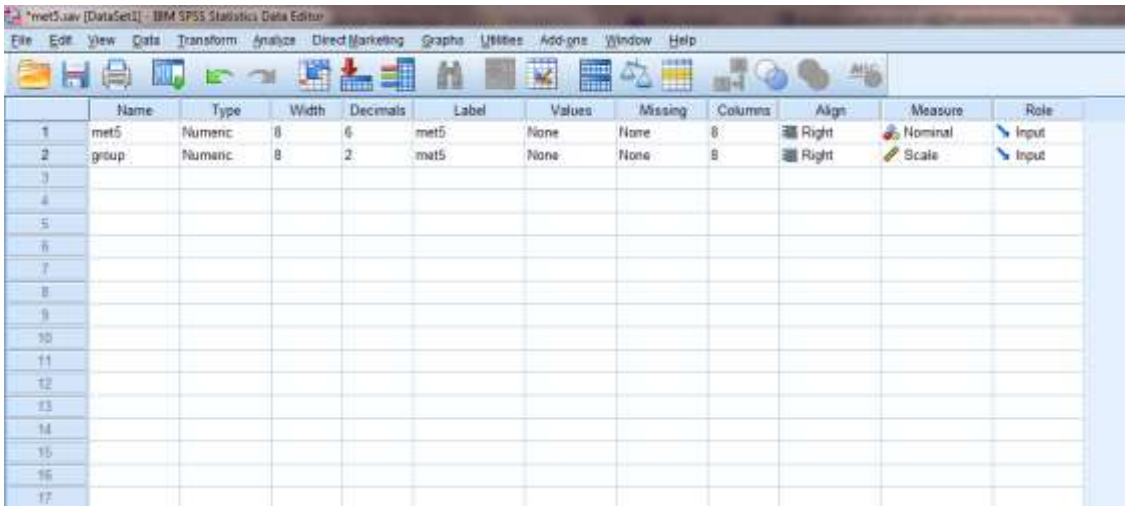

FigureD.2: The Variable View of Software.

After clicking on Independent Sample T test in shown in Figure D.1, the window appears as shown in Figure D.3. The specified number of each group should go in "Define Groups" window and then by clicking on the Continue button, final result will appear on new window as shown in Figure D.4.

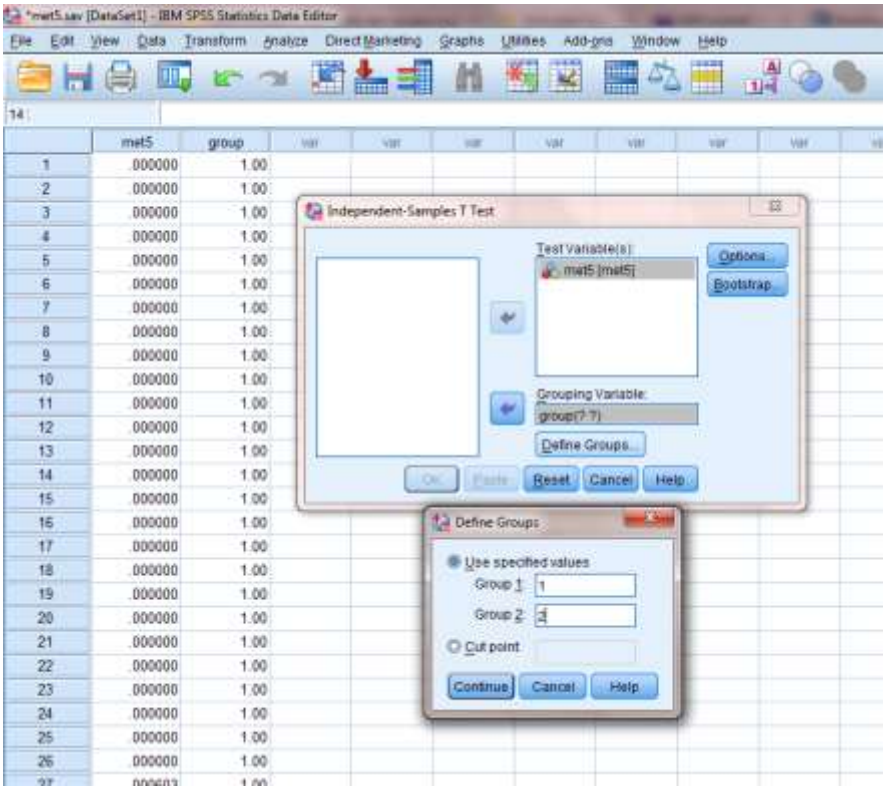

FigureD.3: The final stage of mean comparison

T-Test

[DataSet1] D:\spss\trial7\met5.sav

Group Statistics

	met5	N	Mean	Std. Deviation	Std. Error Mean
met5	1.00	1717	.02358609	.031439768	.000758742
	2.00	1770	.02867692	.035428124	.000842049

Independent Samples Test

		Levene's Test for Equality of Variances		t-test for Equality of Means						
									95% Confidence Interval of the Difference	
		F	Sig.	t	df	Sig. (2-tailed)	Mean Difference	Std. Error Difference	Lower	Upper
met5	Equal variances assumed	67.655	.000	-4.483	3485	.000	-.005090829	.001135511	-.007317162	-.002864495
	Equal variances not assumed			-4.491	3457.854	.000	-.005090829	.001133461	-.007313150	-.002868507

FigureD.4: Shows the differences which are existed among HV and non-HV groups

References

Abboud, R.J. (2002) ' Relevant foot biomechanics', *Current Orthopaedics,* 16(3), pp. 165-179.

Abdul Razak, A.H., Zayegh, A., Begg, R.K. and Wahab, Y. (2012) 'Foot Plantar Pressure Measurement System: A Review', *Sensors,* 12(7), pp. 9884-9912.

Abulkhair, N. (2012) *Investigating the Effect of Mechanical Loading in a Total Reversed Shoulder Implant* Doctor of philosophy. Brunel University.

Antunes, P.J., Dias, G.R., Coelho, A.T., Rebelo, F. and Pereira, T. (2008) 'Non-Linear Finite Element Modelling of Anatomically Detailed 3D Foot Model', , pp. 1-11.

Atiya, S., Quah, C. and Pillai, A. (2013) 'Sesamoiditis of the metatarsophalangeal joint', 1(2)(19), pp. 1-6.

Baker, M.K. (2008). Available at: http://www.livescience.com/4964-shoes-worn-40-000-years.html (Accessed: 06/09/ 2012).

Berkey, S. (2002-2014). Available at: http://www.3ds.com/products-services/simulia/overview/ (Accessed: 05/ 2011).

Boonpratatong, A. and Ren, L. (2010) 'The Human Ankle-Foot Complex as a Multi-Configurable Mechanism during the Stance Phase of Walking', *Journal of Bionic Engineering,* 7(3), pp. 211-218.

Brantingham, J.W. and Wood, T.G. (2002) 'Hallux rigidus', *Journal of Chiropractic Medicine,* 1(1), pp. 31-37.

Briggs, P.J. (2005) '(i) The structure and function of the foot in relation to injury', *Current Orthopaedics,* 19(2), pp. 85-93.

Bruening, D.A., Cooney, K.M., Buczek, F.L. and Richards, J.G. (2010) 'Measured and estimated ground reaction forces for multi-segment foot models', *Journal of Biomechanics,* 43(16), pp. 3222-3226.

Bryant, A., Tinley, P. and Singer, K. (2000) 'Radiographic measurements and plantar pressure distribution in normal, hallux valgus and hallux limitus feet', *The Foot*, 10(1), pp. 18-22.

Bryant, A., Tinley, P. and Singer, K. (1999) 'Plantar pressure distribution in normal, hallux valgus and hallux limitus feet', *The Foot*, 9(3), pp. 115-119.

Cavanagh, P.R., Morag, E., Boulton, A.J.M., Young, M.J., Deffner, K.T. and Pammer, S.E. (1997) 'The relationship of static foot structure to dynamic foot function', *Journal of Biomechanics*, 30(3), pp. 243-250.

Chen, W., Vee-Sin Lee, P., Park, S., Lee, S., Phyau Wui Shim, V. and Lee, T. (2010) 'A novel gait platform to measure isolated plantar metatarsal forces during walking', *Journal of Biomechanics*, 43(10), pp. 2017-2021.

Cheung, J.T., Zhang, M. and An, K. (2004) 'Effects of plantar fascia stiffness on the biomechanical responses of the ankle–foot complex', *Clinical Biomechanics*, 19(8), pp. 839-846.

Cheung, J.T., Zhang, M., Leung, A.K. and Fan, Y. (2005) 'Three-dimensional finite element analysis of the foot during standing—a material sensitivity study', *Journal of Biomechanics*, 38(5), pp. 1045-1054.

Chevalier, T.L., Hodgins, H. and Chockalingam, N. (2010) 'Plantar pressure measurements using an in-shoe system and a pressure platform: A comparison', *Gait & posture*, 31(3), pp. 397-399.

Coughlin, M.J. (2000) 'Common causes of pain in the forefoot in adults', *The Journal of bone and joint surgery.British volume*, 82(6), pp. 781-790.

Crates, J.M. (2013). Available at: http://texasanklemd.com/conditions-treat/foot/sesamoiditis/ (Accessed: 07/14/ 2014).

Dawe, E.J.C. and Davis, J. (2011) '(vi) Anatomy and biomechanics of the foot and ankle', *Orthopaedics and Trauma*, 25(4), pp. 279-286.

Dawson, J., Thorogood, M., Marks, S.A., Juszczak, E., Dodd, C., Lavis, G. and Fitzpatrick, R. (2002) 'The prevalence of foot problems in older women: a cause for concern', *Journal of public health medicine*, 24(2), pp. 77-84.

De Wit, B., De Clercq, D. and Aerts, P. (2000) 'Biomechanical analysis of the stance phase during barefoot and shod running', *Journal of Biomechanics*, 33(3), pp. 269-278.

Deschamps, K., Birch, I., Desloovere, K. and Matricali, G.A. (2010) 'The impact of hallux valgus on foot kinematics: A cross-sectional, comparative study', *Gait & posture*, 32(1), pp. 102-106.

Donatelli, R.A. (1985) 'Normal biomechanics of the foot and ankle', *The Journal of orthopaedic and sports physical therapy*, 7(3), pp. 91-95.

Drake,R.J,Vogl,W,Mitchell.A.W.M (2005) *Gray's anatomy for students.* Philadelphia: Elsevier Science Health Science Division.

Drake, R.L., Vogl, W. and Mitchell, A.W.M. (2010) *Gray's Anatomy For Students.* 2nd edn. Philadelphia: Churchill Livingstone.

Draper, R. (2013). Available at: http://www.patient.co.uk/doctor/Hallux-Valgus.htm (Accessed: 04/27/ 2013).

Eshraghi, S., Esat, I., Rahmanivahid, P., Yazdifar, M., Eshraghi, M., Mohaghegh, A. and Horne.S (2013) 'Study on relationship between foot pressure pattern and Hallux Valgus progression.', *Human-Computer Interaction. Applications and Services.* Las Vegas, 21/07/2013. Springer, 76-83.

Eslami, M., Begon, M., Farahpour, N. and Allard, P. (2007) 'Forefoot–rearfoot coupling patterns and tibial internal rotation during stance phase of barefoot versus shod running', *Clinical Biomechanics*, 22(1), pp. 74-80.

Fan, Y., Fan, Y., Li, Z., Lv, C. and Luo, D. (2011) 'Natural gaits of the non-pathological flat foot and high-arched foot', *PloS one*, 6(3), pp. e17749.

Fiedler, K.E., Stuijfzand, W.J.A., Harlaar, J., Dekker, J. and Beckerman, H. (2011) 'The effect of shoe lacing on plantar pressure distribution and in-shoe displacement of the foot in healthy participants', *Gait & posture*, 33(3), pp. 396-400.

Gefen, A. (2007) 'Pressure-Sensing Devices for Assessment of Soft Tissue Loading Under Bony Prominences: Technological Concepts and Clinical U', 19(12).

Gilheany, M.F., Landorf, K.B. and Robinson, P. (2008) 'Hallux valgus and hallux rigidus: a comparison of impact on health-related quality of life in patients presenting to foot surgeons in Australia', *Journal of foot and ankle research*, 1(1), pp. 14-1146-1-14.

Glasoe, W.M., Yack, H.J. and Saltzman, C.L. (1999) 'Anatomy and biomechanics of the first ray', *Physical Therapy*, 79(9), pp. 854-859.

Goryachev, Y., Debbi, E.M., Haim, A. and Wolf, A. (2011) 'The effect of manipulation of the center of pressure of the foot during gait on the activation patterns of the lower limb musculature', *Journal of Electromyography and Kinesiology*, 21(2), pp. 333-339.

Gregg, J., Silberstein, M., Clark, C. and Schneider, T. (2007) 'Plantar plate repair and Weil osteotomy for metatarsophalangeal joint instability', *Foot and Ankle Surgery*, 13(3), pp. 116-121.

Hamill, J.K.,K (1995) *Biomechanical basis of human movement.* USA: Williams and Wilkins.

Hughes, J., Clark, P., Jagoe, R.R., Gerber, C. and Klenerman, L. (1991) 'The pattern of pressure distribution under the weightbearing forefoot', *The Foot*, 1(3), pp. 117-124.

Hwang, S.J., Choi, H.S., Cha, S.D., Lee, K.T. and Kim, Y.H. (2005) 'Multi-Segment Foot Motion Analysis on Hallux Valgus Patients', *Engineering in Medicine and Biology Society, 2005. IEEE-EMBS 2005. 27th Annual International Conference of the.* , 6875-6877.

Imaizumi, K., Iwakami, Y. and Yamashita, K. (2011) 'Analysis of foot pressure distribution data for the evaluation of foot arch type', *Conference proceedings : ...Annual International Conference of the IEEE Engineering in Medicine and Biology*

Society.IEEE Engineering in Medicine and Biology Society.Conference, 2011, pp. 7388-7392.

Jenkyn, T.R. and Nicol, A.C. (2007) 'A multi-segment kinematic model of the foot with a novel definition of forefoot motion for use in clinical gait analysis during walking', *Journal of Biomechanics*, 40(14), pp. 3271-3278.

Kadambande, S., Khurana, A., Debnath, U., Bansal, M. and Hariharan, K. (2006) 'Comparative anthropometric analysis of shod and unshod feet', *The Foot*, 16(4), pp. 188-191.

Keijsers, N.L.W., Stolwijk, N.M., Nienhuis, B. and Duysens, J. (2009) 'A new method to normalize plantar pressure measurements for foot size and foot progression angle', *Journal of Biomechanics*, 42(1), pp. 87-90.

Kwan, R.L., Zheng, Y. and Cheing, G.L. (2010) 'The effect of aging on the biomechanical properties of plantar soft tissues', *Clinical Biomechanics*, 25(6), pp. 601-605.

Lam, W.K., Sterzing, T. and Cheung, J.T. (2011) 'Reliability of a basketball specific testing protocol for footwear fit and comfort perception', *Footwear Science*, 3(3), pp. 151-158.

LFAC (2014). Available at: http://www.londonfootandanklecentre.co.uk/conditions/bunions.php (Accessed: 07/18/ 2014).

Lowery, N.J. and Wukich, D.K. (2009) 'Adolescent Hallux Valgus: Evaluation and Treatment', *Operative Techniques in Orthopaedics*, 19(1), pp. 52-57.

Ly, Q.H., Alaoui, A., Erlicher, S. and Baly, L. (2010) 'Towards a footwear design tool: Influence of shoe midsole properties and ground stiffness on the impact force during running', *Journal of Biomechanics*, 43(2), pp. 310-317.

Mafart, B. (2007) 'Hallux valgus in a historical French population: Paleopathological study of 605 first metatarsal bones', *Joint Bone Spine*, 74(2), pp. 166-170.

Mann RR, C.M. (1993) *Adult hallux valgus.* USA: St Louis: Mosby;.

Martínez-Nova, A., Sánchez-Rodríguez, R., Pérez-Soriano, P., Llana-Belloch, S., Leal-Muro, A. and Pedrera-Zamorano, J.D. (2010) 'Plantar pressures determinants in mild Hallux Valgus', *Gait & posture,* 32(3), pp. 425-427.

Materialise (2014). Available at: http://biomedical.materialise.com/3-matic (Accessed: 05/26 2014).

Mc Lester, J. and Pierre, P.S. (2008) *Applied Biomechanics:Concepts and Conncetions.* Canada: Thomson Wadsworth.

McDonald, S.W. and Tavener, G. (1999) 'Pronation and supination of the foot: confused terminology', *The Foot,* 9(1), pp. 6-11.

MedicalExpo (2014). Available at: http://www.medicalexpo.com/prod/ella-legros/fluorescent-podoscopes-68340-418940.html (Accessed: 07/15 2014).

Menz, H.B. and Morris, M.E. (2005) 'Footwear characteristics and foot problems in older people', *Gerontology,* 51(5), pp. 346-351.

Mickle, K.J., Munro, B.J., Lord, S.R., Menz, H.B. and Steele, J.R. (2011) 'Gait, balance and plantar pressures in older people with toe deformities', *Gait & posture,* 34(3), pp. 347-351.

Milner, S. (2010) 'Common disorders of the foot and ankle', *Surgery (Oxford),* 28(10), pp. 514-517.

Nguyen, U.-.D.T., Hillstrom, H.J., Li, W., Dufour, A.B., Kiel, D.P., Procter-Gray, E., Gagnon, M.M. and Hannan, M.T. (2010) 'Factors associated with hallux valgus in a population-based study of older women and men: the MOBILIZE Boston Study', *Osteoarthritis and Cartilage,* 18(1), pp. 41-46.

Nix, S., Smith, M. and Vicenzino, B. (2010) 'Prevalence of hallux valgus in the general population: a systematic review and meta-analysis', *Journal of foot and ankle research,* 3, pp. 21-1146-3-21.

Nix, S.E., Vicenzino, B.T., Collins, N.J. and Smith, M.D. (2012) 'Characteristics of foot structure and footwear associated with hallux valgus: a systematic review', *Osteoarthritis and Cartilage,* 20(10), pp. 1059-1074.

Nyska, M., Liberson, A., McCabe, C., Linge, K. and Klenerman, L. (1998) 'Plantar foot pressure distribution in patients with Hallux valgus treated by distal soft tissue procedure and proximal metatarsal osteotomy', *Foot and Ankle Surgery,* 4(1), pp. 35-41.

Pallant, J. (2005) *SPSS Survival Manual.* 5th edn. England: McGraw-Hill.

Periyasamy, R., Mishra, A., Anand, S. and Ammini, A.C. (2011) 'Preliminary investigation of foot pressure distribution variation in men and women adults while standing', *The Foot,* 21(3), pp. 142-148.

Plank, M.J. (1995) 'The pattern of forefoot pressure distribution in hallux valgus', *The Foot,* 5(1), pp. 8-14.

Qian, Z., Ren, L. and Ren, L. (2010) 'A Coupling Analysis of the Biomechanical Functions of Human Foot Complex during Locomotion', *Journal of Bionic Engineering,* 7, Supplement(0), pp. S150-S157.

Qiu, T., Teo, E., Yan, Y. and Lei, W. (2011) 'Finite element modeling of a 3D coupled foot–boot model', *Medical engineering & physics,* 33(10), pp. 1228-1233.

Randolph, A.L., Nelson, M., Akkapeddi, S., Levin, A. and Alexandrescu, R. (2000) 'Reliability of measurements of pressures applied on the foot during walking by a computerized insole sensor system', *Archives of Physical Medicine and Rehabilitation,* 81(5), pp. 573-578.

Rao, S., Song, J., Kraszewski, A., Backus, S., Ellis, S.J., Md, J.T.D. and Hillstrom, H.J. (2011) 'The effect of foot structure on 1st metatarsophalangeal joint flexibility and hallucal loading', *Gait & posture,* 34(1), pp. 131-137.

Roddy, E., Zhang, W. and Doherty, M. (2008) 'Prevalence and associations of hallux valgus in a primary care population', *Arthritis Care & Research,* 59(6), pp. 857-862.

Rosenbaum, D., Hautmann, S., Gold, M. and Claes, L. (1994) 'Effects of walking speed on plantar pressure patterns and hindfoot angular motion', *Gait & posture*, 2(3), pp. 191-197.

RSscan (2014). Available at: http://www.rsscan.com/user-area/downloads/ (Accessed: 05/11 2014).

Rucosm (2012). Available at: http://www.rucosm.com/operations/hallux.php (Accessed: 05/23/ 2012).

Smith, B.W. and Coughlin, M.J. (2008) 'The first metatarsocuneiform joint, hypermobility, and hallux valgus: What does it all mean?', *Foot and Ankle Surgery*, 14(3), pp. 138-141.

Soames, R.W. (1985) 'Foot pressure patterns during gait', *Journal of Biomedical Engineering*, 7(2), pp. 120-126.

Speksnijder, C.M., vd Munckhof, R.J.H., Moonen, S.A.F.C.M. and Walenkamp, G.H.I.M. (2005) 'The higher the heel the higher the forefoot-pressure in ten healthy women', *The Foot*, 15(1), pp. 17-21.

Stainsby, G.D. (1997) 'Pathological anatomy and dynamic effect of the displaced plantar plate and the importance of the integrity of the plantar plate-deep transverse metatarsal ligament tie-bar', *Annals of the Royal College of Surgeons of England*, 79(1), pp. 58-68.

Stebbins, J., Harrington, M., Thompson, N., Zavatsky, A. and Theologis, T. (2006) 'Repeatability of a model for measuring multi-segment foot kinematics in children', *Gait & posture*, 23(4), pp. 401-410.

Suero, E.M., Meyers, K.N. and Bohne, W.H.O. (2012) 'Stability of the metatarsophalangeal joint of the lesser toes: A cadaveric study', *Journal of Orthopaedic Research*, 30(12), pp. 1995-1998.

van der Zwaard, B.C., Vanwanseele, B., Holtkamp, F., van der Horst, H.E., Elders, P.J. and Menz, H.B. (2014) 'Variation in the location of the shoe sole flexion point

influences plantar loading patterns during gait', *Journal of foot and ankle research,* 7(1), pp. 20-1146-7-20.

Vass, L. and Molnar, M. (1999) *Handmade shoes for men.* Illustrated edn. Germany: Könemann.

WebMD (2010). Available at: http://www.webmd.com/pain-management/picture-of-the-feet (Accessed: 10/25/ 2011).

Wen, J., Ding, Q., Yu, Z., Sun, W., Wang, Q. and Wei, K. (2012) 'Adaptive changes of foot pressure in hallux valgus patients', *Gait & posture,* 36(3), pp. 344-349.

Wong, D.W., Zhang, M., Yu, J. and Leung, A.K. 'Biomechanics of first ray hypermobility: An investigation on joint force during walking using finite element analysis', *Medical engineering & physics,* (0).

Yavuz, M., Hetherington, V.J., Botek, G., Hirschman, G.B., Bardsley, L. and Davis, B.L. (2009) 'Forefoot plantar shear stress distribution in hallux valgus patients', *Gait & posture,* 30(2), pp. 257-259.

Yu, J., Cheung, J.T., Fan, Y., Zhang, Y., Leung, A.K. and Zhang, M. (2008) 'Development of a finite element model of female foot for high-heeled shoe design', *Clinical Biomechanics,* 23, Supplement 1(0), pp. S31-S38.

Zander, T., Rohlmann, A. and Bergmann, G. (2004) 'Influence of ligament stiffness on the mechanical behavior of a functional spinal unit', *Journal of Biomechanics,* 37(7), pp. 1107-1111.